Kinetic And Mechanistic Studies on Aldehyde Dehydrogenases From Sheep Liver

A thesis presented in partial
fulfilment of the requirements
for the degree of

Master of Science in Chemistry

at

Massey University
New Zealand

ADRIAN FRANCIS BENNETT
1981

Abstract

The mechanisms of sheep liver aldehyde dehydrogenases have been further investigated by both steady-state and pre-steady-state kinetic methods.

By utilizing the acid/base indicator phenol red, a burst in the production of protons has been detected for both the cytoplasmic and mitochondrial isoenzymes. The rates and amplitudes of the two proton bursts were almost identical to those for the NADH bursts which both isoenzymes exhibit. After a consideration of the kinetic data, the electronic structure of various aldehydes and computer simulation studies, the proton burst process was postulated as arising from a conformational change on aldehyde binding to the enzyme-NAD^+ binary complex. The proton release arises from the perturbation of the pKa of a protonated functional group from about 8.5 to below 5.0

The effects of the Mg^{2+} ion on the cytoplasmic isoenzyme were also studied. The presence of millimolar concentrations of this ion resulted in marked inhibition of the enzyme activity, and a lowering of the dissociation constants for both the E.NAD^+ and E.NADH binary-enzyme complexes. Steady-state and pre-steady-state studies showed that the major effect of $MgCl_2$ on the enzyme mechanism was to slow the steady-state rate-limiting step, which was NADH dissociation at high propionaldehyde concentrations and an unidentified step, possibly involving deacylation, at low propionaldehyde concentrations.

Acknowledgements

I wish to thank my supervisors Dr Paul Buckley and Dr Len Blackwell for their advice and assistance during this study.

I would also like to thank Dr Kathryn Crow, Mrs Rose Motion, Dr Alastair MacGibbon and all the members of the Chemistry-Biochemistry Department for helpful advice and comments.

Thanks are also extended to Professor R. Hodges for allowing the use of his computer, Dr Neil Pinder for allowing the use of his light scattering apparatus, Mr J. Napier and Mr R. Poll for help in preparing aldehyde dehydrogenase samples and Mrs Trish Fleet for typing this thesis.

CONTENTS

Page No.

SECTION 3

Page No.

Page No.

SECTION 5

PRE-STEADY-STATE STUDIES ON THE EFFECTS OF $MgCl_2$ ON CYTOPLASMIC ALDEHYDE DEHYDROGENASE

Page No.

LIST OF FIGURES

SECTION 1

INTRODUCTION

The ingestion of excess ethanol by mammals results in symptoms such as flushing, sweating, respiratory difficulties and, in humans, a severe headache, these symptoms being collectively known as a hangover. These effects are believed to result mainly from a build up in the bloodstream of acetaldehyde, the primary product of ethanol metabolism. Acetaldehyde introduced into the bloodstream can reproduce the effects mentioned above, and is thought to exert its effect by a variety of means which include, the production of alcohols from biogenic amines by shifting their catabolism to a reductive pathway (Truitt and Walsh, 1971) and direct condensation with biogenic amines (Cohen and Collins, 1970). A further possible effect of acetaldehyde in mammals is the formation of tetrahydropapaveroline (Davis and Walsh, 1970), an alkaloid similar to morphine which is a possible link with the addiction to alcohol seen with alcoholics.

During normal metabolism, the level of acetaldehyde in the blood is kept to a relatively low level by three aldehyde oxidising systems, aldehyde oxidase, xanthine oxidase and aldehyde dehydrogenase. The first two enzymes have much lower affinities for aldehydes (Rajogopalan and Handler, 1964; Mackler *et al.*, 1954) than aldehyde dehydrogenase (Buttner, 1965; Feldman and Weiner, 1972a, Crow *et al.*, 1974) and as a result it has been assumed that aldehyde dehydrogenase is the most important enzyme involved in the removal of acetaldehyde in mammals. Further evidence to support this conclusion comes from the results of studies with the drug disulfiram (antabuse). The administration of this drug results in nausea, flushing, sweating and respiratory difficulties when the recipients ingest ethanol, and it has been shown by Kitson (1975) that the drug's presence causes inhibition of aldehyde

dehydrogenase activity, indicating that the hangover-like symptoms observed are due to a build up of acetaldehyde levels in the blood.

The existence of aldehyde dehydrogenase was first shown by Racker (1949) and has since been purified to homogeneity from a number of mammalian sources including horse liver (Feldman and Weiner, 1972a; Eckfeldt and Yonetani, 1976), bovine liver (Sugimoto et al., 1976), rat liver (Shum and Blair, 1972; Tottmar et al., 1973), sheep liver (Crow et al., 1974; MacGibbon et al., 1979; Hart and Dickinson, 1977) and human liver (Greenfield and Pietruszko, 1977; Kraemer and Deitrich, 1968). Sheep liver aldehyde dehydrogenase has been extensively studied since it was first isolated by Crow et al., (1974). The enzyme has been shown to be present in sheep liver as three distinct isoenzymes, one located in the mitochondria, one in the cytoplasm and the other in the microsomes. The majority of the enzyme being present in approximately equal proportions in the mitochondria and the cytoplasm.

The mechanism of oxidation of aldehydes by the cytoplasmic enzyme is believed to be an ordered Bi Bi mechanism with NAD^+ binding first (MacGibbon et al., 1977a), the rate-determining step in the steady-state being dissociation of NADH from the binary E.NADH complex. The rate determining step in the pre-steady-state was not identified by these workers although, due to the absence of a kinetic isotope effect on the hydride transfer step, they concluded that it occurred prior to this step. The mitochondrial isoenzyme has also been studied by these workers who have suggested that it operates by a mechanism similar to that found for the cytoplasmic enzyme. However a report has been published by Hart and Dickinson (1978) suggesting that the mitochondrial enzyme may operate by a group transfer mechanism rather than an ordered Bi Bi mechanism.

In view of the potential importance of aldehyde dehydrogenase in the metabolism of ethanol, it was decided to carry out further steady-state and pre-steady-state

studies using both the mitochondrial and cytoplasmic isoenzymes in an attempt to resolve some of the unanswered questions which remain about the mechanism of the cytoplasmic isoenzyme and determine which of the proposed mitochondrial mechanisms is the better approximation to the actual reaction mechanism. In particular, studies on proton release during the first enzyme turnover, which have not so far been carried out, may reveal information about the rate determining steps in both the steady-state and pre-steady-state. Also it has been recently reported (Venteicher et al., 1977) that both the mitochondrial and cytoplasmic horse liver isoenzymes are sensitive to the presence of $MgCl_2$, and since the cytoplasm of liver cells contains significant levels of this ion (20 meq/Kg, Soman et al, 1970) it was decided to investigate the effects of $MgCl_2$ on the cytoplasmic sheep liver enzyme. This thesis presents the results of such studies.

SECTION 2

PURIFICATION OF ALDEHYDE DEHYDROGENASES FROM SHEEP LIVER

2.1 INTRODUCTION

Studies carried out on aldehyde dehydrogenase (EC 1.2.1.3) prior to about 1970 utilized either crude enzyme preparations which resulted in purifications of less than about 60-fold, or homogenates of whole cells. The introduction of column chromatography to the isolation and purification of aldehyde dehydrogenases, first reported by Shum and Blair (1972), resulted in dramatic improvements to both the yields and purity of the enzyme preparations. Typical preparations involved homogenisation of the tissue from which the enzyme is to be extracted followed by, centrifugation to remove insoluble cell debris, then ammonium sulphate precipitations followed by a variety of chromatographic columns. Columns used included CM cellulose, DEA cellulose and gel filtration columns such as Sephadex G-200 or Biogel A 0.5 M.

The use of these techniques led to the discovery that most mammalian livers possess at least two isoenzymes of aldehyde dehydrogenase, one located in the cytoplasm and the other in the mitochondria. The two isoenzymes usually show different affinities for DEA-cellulose resins enabling the enzyme activity to be resolved into the two isoenzymes, as for example horse liver aldehyde dehydrogenase (Feldman and Weiner, 1972a; Eckfeldt *et al.*, 1976a). Other methods of separating mitochondrial and cytoplasmic aldehyde dehydrogenases include differential centrifugation which has been used to separate isoenzymes of beef liver (Sugimoto *et al.*, 1976) and affinity chromatography which has been used to separate isoenzymes of human liver aldehyde dehydrogenase (Greenfield and Pietruszko, 1977).

Two isoenzymes from sheep liver have also been isolated utilising these procedures, firstly by Crow et al., (1974) then more recently by MacGibbon et al., (1979) and Hart and Dickinson (1977) using improved column procedures.

Both sheep liver isoenzymes were prepared for use in this study by methods similar to those of MacGibbon et al., (1979).

2.2 METHODS

2.2.1 Buffers

Phosphate buffers were prepared from AR grade potassium dihydrogen phosphate and adjusted to the appropriate pH with NaOH as described by Dawson et al., (1969). Buffer strengths were expressed in terms of phosphate concentrations and all buffers used in the enzyme preparation procedures contained 0.1% vol/vol β-mercaptoethanol.

2.2.2 Enzyme Assays

(1) Assays for aldehyde dehydrogenase activity were as follows:

2.15 cm^3 of 35 mM pH 7.6 phosphate buffer
0.5 cm^3 of 14 mM NAD^+ solution
0.25 cm^3 of 240 mM propionaldehyde solution
0.1 cm^3 of enzyme solution

The reaction was initiated by the addition of the aldehyde to a cell containing the other components equilibrated at 25°C, and the reaction progress followed by monitoring the production of NADH at 340 nm. Pyrazole (0.5 mM), a potent inhibitor of alcohol dehydrogenase activity, was added to assays where the sample was suspected to contain this enzyme.

(2) Assays for lactate dehydrogenase activity were as follows:

0.5 cm^3 of 500 μM NADH solution
0.5 cm^3 of 5 mM sodium pyruvate solution

1.9 cm^3 of 35 mM pH 7.6 phosphate buffer
0.1 cm^3 of enzyme solution

The NADH solution was prepared in pH 7.6 phosphate buffer, and the reaction was initiated by the addition of the pyruvate solution. The reaction progress was followed by monitoring the disappearance of NADH at 340 nm.

(3) Assays for alcohol dehydrogenase were as follows:

0.5 cm^3 of 800 μM NADH solution
0.25 cm^3 of 240 mM propionaldehyde solution
2.15 cm^3 of 35 mM pH 7.6 phosphate buffer
0.1 cm^3 of enzyme solution

The reaction was initiated by the addition of aldehyde and the reaction followed by monitoring the disappearance of NADH at 340 nm.

2.2.3 Enzyme Isolation and Purification

2.2.3.1 Cytoplasmic Aldehyde Dehydrogenase

Two methods were used to prepare the cytoplasmic isoenzyme, the first is essentially that of MacGibbon *et al.*, (1979) while the second is a modification of the MacGibbon method used by R.L. Motion (personal communication).

Method 1

Sheep livers were obtained from freshly slaughtered sheep and placed directly in ice, all subsequent work was carried out at 4°C. 500 g of sliced sheep liver was homogenised for 30 seconds in 1 litre of 0.005 M pH 7.3 phosphate buffer containing 0.25 M sucrose using a Janke and Kunkel ultra-turrax T45. The homogenate was centrifuged at 12 500 g for 10 minutes, strained through glass wool to remove cell wall debris and excess fat, then recentrifuged for 1 hour at 20 000 g to sediment the mitochondria. The precipitate was discarded and finely powdered ammonium sulphate was added to the supernatant over 30 minutes with stirring to give 45% saturation (258 g/l at 0°C). The

mixture was equilibrated for 30 minutes then centrifuged for 15 minutes at 12 500 g. Further ammonium sulphate was added to the supernatant to give 70% saturation (156 g/l) and after a further 30 minutes equilibration the mixture was centrifuged for 15 minutes at 12 500 g. The precipitate was then dissolved in 300 cm^3 of 0.005 M pH 7.3 phosphate buffer with a conductivity of 360 $\mu\Omega^{-1}$ at 4°C and dialysed against successive 20 litre changes of the same buffer until the conductivity reached 360 $\mu\Omega^{-1}$. This normally took about 36 hours with buffer changes every 2 hours during the day, with the pH of the crude enzyme being adjusted to pH 7.3 with 0.1 M NaOH after 30 hours. When the conductivity had reached the required value the enzyme sample was loaded onto a Whatman DE 52 cellulose resin column (20 x 5 cm) pre-equilibrated with dialysis buffer. The column outlet was connected to an LKB 8300 uvicord II ultraviolet monitor and the column then washed with dialysis buffer until the absorbance at 280 nm was less than 0.1. The enzyme was then eluted with 0.022 M pH 7.3 phosphate buffer, the eluate being collected on an LKB Ultrorac 7000 fraction collector at a rate of 10 cm^3 every 10 minutes. The aldehyde dehydrogenase first appeared after about 4 hours and another 4 hours were required to completely elute the enzyme. The fractions were assayed for aldehyde dehydrogenase, lactate dehydrogenase and alcohol dehydrogenase and those fractions containing significant quantities of lactate or alcohol dehydrogenase were discarded. The fractions containing aldehyde dehydrogenase were combined and reduced from 300 cm^3 to 8 cm^3 over 8 hours using a diaflow ultra-filtration apparatus with an XM 100 filter which retained all species with a molecular weight greater than 100 000. The concentrated sample was loaded onto a sephacryl S 300 gel filtration column (70 x 2.5 cm) and eluted with 0.0022 M pH 7.3 phosphate buffer. The eluate was collected on the LKB apparatus described above, at a rate of about 12 cm^3 per hour with the enzyme usually detected after 30 hours and completely eluted after a further 6 hours. The aldehyde

dehydrogenase samples were sealed with parafilm and stored at $4^{o}C$ until required.

Method 2

The initial homogenisation and centrifugation steps were the same as for the method described above up to and including the 20 000 g centrifuge spin. At this stage the supernatant was made up to 1500 cm^3 with 0.005 M pH 7.3 buffer containing 0.25 M sucrose with a conductivity of $360 \pm 30\ \mu\Omega^{-1}$ at $4^{o}C$, and powdered AR grade polyethylene glycol 6000 was added over 30 minutes with stirring to give a mixture containing 12% weight by volume (120 g/litre). The stirring was continued for a further 30 minutes to allow equilibration, then the mixture was centrifuged at 12 500 g for 15 minutes and the precipitate discarded. Further polyethylene glycol was added to the supernatant to bring the concentration up to 20% weight by volume (80 g/litre) and the stirring continued for 60 minutes. The mixture was centrifuged at 12 500 g for 15 minutes and the precipitate dissolved in 300 cm^3 of 0.005 M pH 7.3 phosphate buffer with a conductivity of $360\ \mu\Omega^{-1}$ then loaded directly onto a 20 x 5 cm DE cellulose column pre-equilibrated with the same buffer. The column was washed with 0.005 M pH 7.3 phosphate buffe until the absorbance at 280 nm was less than 0.1 then eluted with 0.022 M pH 7.3 phosphate buffer and the fractions collected using the LKB apparatus described in Method 1. The fractions containing aldehyde dehydrogenase were concentrated as in Method 1 to 8 cm^3 with the diaflow apparatus and loaded onto the sephacryl S 300 column which was eluted as described in Method 1.

2.2.3.2 Mitochondrial Aldehyde Dehydrogenase

The method used for the mitochondrial enzyme preparations was essentially that of Crow et al., (1974).

A 500 g sample of sheep liver was homogenised in 1 litre of 0.005 M pH 7.3 phosphate buffer containing 0.25 M sucrose as described in section 2.2.3.1. The mixture was centrifuged at 500 g for 5 minutes to remove whole cells and

debris then for 1 hour at 20 000 g to sediment the mitochondria. The mitochondria were resuspended in 300 cm^3 of 0.005 M pH 7.3 phosphate buffer by sonication with a Janke and Kunkel ultra-turrax T45 for 30 seconds then ruptured by sonicating for 5 x 30 seconds with an MSE 100 watt ultrasonic disintegrator, the suspensions being cooled in ice between sonications. After centrifuging for 1 hour at 20 000 g to remove mitochondrial debris, AR grade ammonium sulphate was added with stirring over 30 minutes to give 35% saturation (194 g/litre). The stirring was continued for a further 30 minutes to allow equilibration then the mixture was centrifuged for 15 minutes at 12 500 g and the precipitate discarded. Further ammonium sulphate was added to the supernatant over 30 minutes to give 70% saturation (218 g/litre) and after 30 minutes equilibration the mixture was centrifuged at 12 500 g for 15 minutes and the supernatant discarded. The precipitate was dissolved in 300 cm^3 of 0.005 M pH 7.3 phosphate buffer then loaded onto a Whatman DE 52 cellulose column (20 x 5 cm) and washed and eluted as described in section 2.2.3.1. Fractions containing aldehyde dehydrogenase were concentrated to 8 cm^3, loaded onto a sephacryl S 300 column (70 x 2.5 cm) and eluted as described in section 2.2.3.1.

2.3 RESULTS

2.3.1 Purity of Enzyme Preparations

2.3.1.1 Contamination by Other Protein

All three enzyme preparations have been shown to be essentially free of contaminant proteins by a number of methods. SDS gel electrophoresis carried out using an Ortec 4200 system with slab gels (8% acrylamide at pH 9.0) as described by Crow (1974), showed only one major band. Isoelectric focussing studies were carried out on samples from the enzyme preparations by Agnew *et al.*, (1981) using an LKB multiphor apparatus with ampholine polyacrylamide plates with a pH range of 3.5 to 9.5. These studies revealed that gels stained for protein showed only one major band which

corresponded to the band obtained when the gel was stained for aldehyde dehydrogenase activity.

Cytoplasmic aldehyde dehydrogenase samples stained for alcohol and lactate dehydrogenase activities failed to show any development of colour, however it should be noted that using very high enzyme concentrations in assays, very small traces of activity resulting from these enzymes could be found in fractions collected towards the end of the aldehyde dehydrogenase profile from the gel filtration column. These samples were not used for kinetic or equilibrium studies.

Catalase was found to be present in small quantities in cytoplasmic enzyme samples prepared by Method 1 (Crow, 1975), but not in samples prepared by Method 2 (R.L. Motion, personal communication). Catalase contamination was not found to be a problem in the mitochondrial preparation.

2.3.1.2 Cross Contamination of the Mitochondrial and Cytoplasmic Enzymes

The level of mitochondrial enzyme contamination in cytoplasmic enzyme preparations was estimated in two ways:

(1) Assaying for a mitochondrial marker enzyme
(2) Isoelectric focussing

Agnew et al., (1981) using glutamate dehydrogenase as a marker enzyme, have found that consistently no more than 2% of the mitochondria were ruptured during the homogenisation and separation procedures, a value in good agreement with that reported by Crow et al., (1974) also of 2%. The isoelectric focussing studies of Agnew et al., (1981) also enabled estimates of the cross contamination to be made, since on isoelectric focussing the cytoplasmic enzyme showed only two bands very close together at pH 5.22, whereas the mitochondrial enzyme showed an additional 5 bands at pH's 5.48, 5.56, 5.65, 5.70 and 5.76. The almost complete absence of these latter five bands in cytoplasmic samples, except under extreme loading conditions indicated that there

was virtually no cross contamination by the mitochondrial enzyme.

The presence of the two bands at pH 5.22 for both the cytoplasmic and mitochondrial enzymes makes isoelectric focussing unsuitable as a method for detecting whether the cytoplasmic enzyme was contaminating the mitochondrial enzyme preparations. However assays for a cytoplasmic marker enzyme, lactic dehydrogenase (Agnew et al., 1981) showed the presence of only 2% cytoplasmic contamination in the mitochondrial preparations.

2.3.2 Enzyme Yields

2.3.2.1 Cytoplasmic Enzyme

Enzyme concentrations were expressed in μM of NADH binding sites as determined by assay (Section 3.2.2.1) or NADH titration (Section 3.2.2.2). The two methods used for cytoplasmic enzyme preparations resulted in similar yields of enzyme, an average preparation resulting in 5 to 6 μmoles of active sites contained in about 100 cm^3. The peak activity being in the region of 150 μM to 200 μM of active sites.

2.3.2.2 Mitochondrial Enzyme

The yield from the mitochondrial preparation was rather less than that of the cytoplasmic preparation, with a considerable loss in activity being observed during the dialysis to remove the ammonium sulphate from the crude enzyme sample. Typically the preparation resulted in about 0.4 μmoles of enzyme active sites, with a peak activity of about 30 μM.

SECTION 3

STUDIES ON PROTON RELEASE KINETICS OF CYTOPLASMIC ALDEHYDE DEHYDROGENASE

3.1 INTRODUCTION

In steady-state kinetic studies the overall conversion of reactants to products is followed and in order to do this, enzyme concentrations of the order of 10^{-6} to 10^{-9} M are used so that the reaction takes place at a rate slow enough to be measureable. At enzyme concentrations this low any intermediates, which may be formed along the reaction pathway, will not normally be detectable. Steady-state kinetics therefore usually only allow the determination of a number of macroscopic steady-state parameters, such as the michaelis constant (Km) and the turnover number (k_{cat}). These parameters are complicated functions of the individual microscopic rate constants, the majority of which cannot be identified uniquely by steady-state kinetic studies especially where, as in the case of aldehyde dehydrogenase, the reaction is experimentally irreversible. However in some cases upper and lower limits for an individual, or combinations of rate constants, can be determined from steady-state kinetics.

The use of pre-steady-state kinetic studies, in which the approach to the steady-state is observed, provides more information about transient intermediates and the rate constants for the formation and destruction of these intermediates. In these methods, much higher enzyme concentrations are employed (10^{-5} to 10^{-3} M) and if any intermediate is formed which results in a change in a detectable physical property such as fluorescence, absorption or optical rotation, then it may be possible to directly observe the rate of formation of the intermediate.

Pre-steady-state kinetic studies require an apparatus capable of following changes in physical properties within a short time of the initiation of the reaction. The

stopped-flow spectrophotometer described by Gibson and Milnes (1964) is ideal for this purpose. In this apparatus two solutions are mixed within 3 ms and the subsequent reaction followed by monitoring physical changes in the mixed solutions, usually absorbance or fluorescence. Hiromi (1979) has reviewed the instrumentation and techniques for this method.

A number of dehydrogenases, such as glutamate dehydrogenase (Iwatsubo and Pantaloni, 1967), lactate dehydrogenase (Heck et al., 1968) and alcohol dehydrogenase (Theorell et al., 1967; Geraci and Gibson, 1967; Bernhard et al., 1970; Brooks and Shore, 1971) have been studied by stopped-flow methods. The analytical solution of pre-steady-state rate equations can be difficult. For example the rate equation describing the transient appearance of product, both enzyme bound and free, contains exponential terms equal to the number of enzyme-containing intermediates in the mechanism (Maguire et al., 1974). However in practice, the situation is generally much simpler, since nothing will be observed until the first step involving a change in the physical property being monitored occurs and there will be no contribution from any steps after the steady-state rate determining step. Also if there is more than one exponential term in the transient phase, some may not be observable if, for instance, the amplitude of the exponential term is very low due to an unfavourable combination of the rate constants describing their formation and destruction.

MacGibbon et al., (1977 b,c) have carried out extensive stopped-flow studies on the cytoplasmic aldehyde dehydrogenase from sheep liver. By monitoring nucleotide fluorescence during the pre-steady-state phase of the enzyme reaction, they observed a burst due to the appearance of an enzyme-NADH complex, and concluded that the rate-limiting step in the steady-state was the slow dissociation of NADH from the binary enzyme-NADH complex. Further evidence to support this conclusion came from their observation of a biphasic displacement of NADH from the binary enzyme-NADH complex with the slower process having a rate equal to the

turnover number (k_{cat}). Kinetic isotope experiments with deuterated propionaldehyde and acetaldehyde indicated that hydride transfer was not rate-limiting in the pre-steady-state phase of the reaction and steady-state product inhibition studies showed that the mechanism was ordered Bi Bi (MacGibbon et al., 1977a) with NAD^+ binding first. The simplest mechanism consistent with this data, was proposed by MacGibbon et al., (1977c) and is shown in scheme 3.1.

$$E \underset{k_{-1}}{\overset{k_{+1}[NAD^+]}{\rightleftharpoons}} E^{NAD^+} \underset{k_{-2}}{\overset{k_{+2}[Ald]}{\rightleftharpoons}} E^{NAD^+}_{Ald} \xrightarrow{k_{+3}} E^{NADH} \underset{k_{-4}}{\overset{k_{+4}}{\rightleftharpoons}} E + NADH$$

(Scheme 3.1)

It was assumed that $E^{NAD^+}_{Ald}$ and E^{NADH}_{Acid} are rapdily interconverted and that the concentration of E^{NADH}_{Acid} was so low that no transient results from this intermediate.

Computer simulations based on scheme 3.1 using rate constants determined from pre-steady-state and steady-state experiment gave a good approximation to the experimental data indicating that scheme 3.1 is a reasonable mechanistic model. However it was noted that additional steps may be needed to explain some of the experimental data, for example, the biphasic displacement of NADH from the enzyme really requires a two step dissociation rather than the single step shown in scheme 3.1. It was not possible on the basis of the reported results to identify the process which was rate-determining in the pre-steady-state, but it clearly occurs prior to the hydride transfer (included in the step with the rate constant k_{+3} in scheme 3.1).

The observation of the rate of formation of single transients, rather than the rate of overall appearance of products which generally contain contributions from several intermediates, can be useful in determining reaction mechanisms. For some reactions a transient release of protons may be observed, and a convenient means of measuring the pH changes in the stopped-flow apparatus associated with such proton releases, is to use a pH indicator. In this way

the transient release of protons from lactate dehydrogenase both H_4 and M_4 has been studied by a number of groups (Whitaker et al., 1974 ; Holbrook and Ingram, 1973; Holbrook and Gutfreund, 1973). For these enzymes a transient release of protons was observed with a rate of 240 s^{-1} which was attributed to the step:

$$\begin{matrix} \text{NADH} \\ \text{E} \\ \text{Pyruvate} \end{matrix} \longrightarrow \begin{matrix} \text{NADH} \\ \text{E} \end{matrix} + H^+ + \text{pyruvate}$$

The kinetics of the transient proton release for horse liver alcohol dehydrogenase have also been extensively studied. Shore et al., (1974) first studied the enzyme using phenol red as an indicator then Kvassman and Petterson (1980 a,b) extended this investigation using chlorophenol red as an indicator. For this enzyme a very fast transient release of protons is observed when the enzyme is mixed with NAD^+ in the stopped-flow apparatus, and a second slower transient is also observed when alcohol and NAD^+ are mixed with the enzyme. The first fast proton release has been postulated as arising from the perturbation of a functional group at the active site from a pKa of 9.0 to a pKa of 7.6 on formation of the binary enzyme-NAD^+ complex. The second slower proton release has been attributed by Kvassman and Petterson to the formation of an alcoholate ion in the enzyme-NAD^+-alcohol ternary complex.

Dickinson and Dickenson (1978) have carried out studies on the yeast alcohol dehydrogenase. Although proton release was observed when trifluoroethanol (an inhibitor competitive with ethanol) was mixed with enzyme-NAD^+, no transient proton release was observed when NAD^+ or alcohol and NAD^+ were mixed with the enzyme. The failure to observe a transient proton release was interpreted by these workers as indicating that proton release occurred after the formation of the enzyme-NADH-aldehyde ternary complex, and at the same rate as the steady-state reaction. The proton release seen with trifluoroethanol was attributed to the perturbation of the pKa of a functional group of the enzyme. A perturbation did not however take place when alcohol was mixed with the

binary complex.

As a number of proton releases have been successfully studied using phenol red as an indicator in the pH range of 7.4 to 8.0, it was decided to investigate the pre-steady-state release of protons for sheep liver cytoplasmic aldehyde dehydrogenase using phenol red as an indicator to monitor pH changes with the hope of obtaining further insight into the detailed sequence of events taking place during the pre-steady-state phase of the enzyme catalysed reaction.

3.1.1 The Measurement of Proton Release with Indicators

The pH indicators used to detect endpoints during simple acid-base titrations encountered in elementary chemistry are weak acids. Their suitability for use as indicators arises from the fact that there is usually a large difference in the visible spectra between the undissociated acid and its conjugate base. Phenol red (Fig. 5.1) has two absorption maxima in the visible region of the spectrum, one at 560 nm for the conjugate base and one at 510 nm for the undissociated acid. Changes in proton concentration in the pH range of 7.0 to 8.0 can be conveniently monitored by following changes in absorbance at 560 nm.

The change in proton concentration calculated by measuring the change in absorbance at 560 nm, assuming a molar extinction coefficient of 54×10^3 $M^{-1}cm^{-1}$ (Gutfreund, 1972) will only be equal to the actual change in proton concentration if there are no buffer systems present in solution. However, the absence of any buffer in an experiment can result in changes in the pH which are outside the region over which the change in colour with pH of the indicator is linear (approximately $pK \pm 0.5$). Also the rates of most enzyme catalysed reactions are dependant upon pH, thus reliable kinetic data can be obtained only if the change in pH over the time course of the reaction is relatively small. These problems can be circumvented by maintaining a low concentration of buffer (0.5 to 1 mM) in the experimental solutions and calculating changes in pH by

FIG 3.1 VISIBLE SPECTRUM OF PHENOL RED

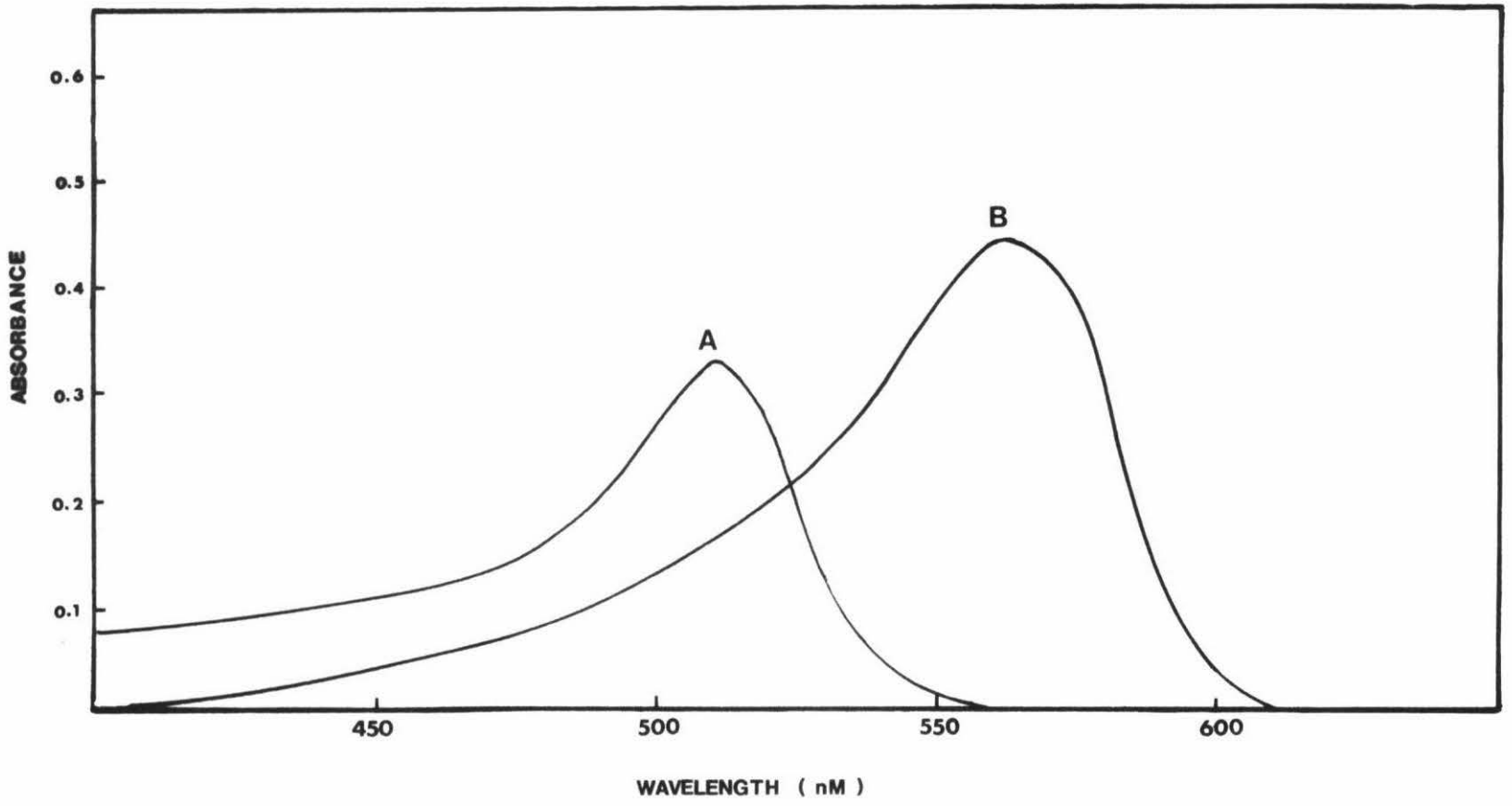

The cell contained 8.3 uM phenol red in A, 0.1 M HCl and B 0.1 M NaOH

measuring changes in absorbance at the appropriate wavelength for the indicator used, then using an apparent molar extinction coefficient ϵ_A which takes into account the buffering abilities of the solution. The apparent molar extinction coefficient can be calculated by adding a known quantity of acid to a solution containing indicator, enzyme and buffer, then using Beers law ($A = c\epsilon L$) to calculate ϵ_A.

Complications may arise if the indicator binds to the enzyme being studied. The binding of an indicator to protein molecules is generally characterised by changes in the spectra of either the dye or the enzyme and/or a change in the rate of the enzyme-catalysed reaction, and thus can normally be readily detected. As protonation reactions are extremely rapid, the presence of an indicator to monitor pH changes does not complicate the interpretation of kinetic data obtained from the stopped-flow experiments, for example Gutfreund (1972) has estimated that 10 μM phenol red at pH 8.0 when subjected to an instantaneous change in hydrogen ion concentration reaches equilibrium with a relaxation time of 10 μs. This is in excess of 500 times faster than the rate of fastest proton release measurable using a stopped-flow apparatus.

3.1.2 The Effects of Absorbed Carbon Dioxide on pH Measurement

Carbon dioxide is relatively soluble in water, which at a pressure of one atmosphere contains 10.35 μM of dissolved CO_2, although this concentration decreases in solutions containing electrolytes (Gutfreund, 1972). The dissolved CO_2 is present in solution as four species, CO_2, HCO_3^-, H_2CO_3 and CO_3^{2-}, however the dissociation constant for the equilibrium

$$HCO_3^- \rightleftharpoons CO_3^{2-} + H^+$$

is 4.67×10^{-11}, thus the concentration of CO_3^{2-} is negligible. However the presence of the other three species can cause unwanted buffering effects. Furthermore, any perturbation of the equilibrium of a solution containing HCO_3^- or H_2CO_3

will result in the release or uptake of protons according to the equilibrium shown below. For example, if a solution containing H_2CO_3 has its pH rapidly lowered from about 8.0

$$H_2CO_3 \rightleftharpoons HCO_3^- + H^+$$

to some lower value, a slow proton release will occur with a rate constant of 0.038 s^{-1}, which may be mistaken for a slow steady-state proton release. These problems can be circumvented by removing CO_2 from the experimental solutions. In the early part of this study experiments were carried out in the absence of carbon dioxide, the removal of CO_2 being accomplished by boiling the aqueous solutions then allowing them to cool under nitrogen. Further manipulations of the CO_2 free solutions were carried out in a glove box containing a nitrogen atmosphere. However since the same results were obtained in this study with and without the degassing procedures, provided the same amount of dissolved CO_2 was present in both solutions in the stopped-flow syringes, these procedures were relaxed.

3.1.3 Consecutive Reactions

When excess NAD^+ is premixed with enzyme the mechanism shown in scheme 3.1 simplifies to scheme 3.2.

$$E^{NAD^+} \underset{k_{-2}}{\overset{k_2[Ald]}{\rightleftharpoons}} E^{NAD^+}_{Ald} \xrightarrow{k_3} E^{NADH} \underset{k_{-4}}{\overset{k_4}{\rightleftharpoons}} E + NADH$$

(Scheme 3.2)

The dissociation step, shown as k_4, is slow compared with the other steps in the mechanism and can be disregarded (Shore and Gutfreund, 1970), and if the concentration of aldehyde is considerably larger than that of the enzyme, the aldehyde addition can be treated as a pseudo first-order process. With these assumptions, scheme 3.2 can be treated as two reversible first-order reactions, for which the solutions have been given by Frost and Pearsons(1961). For a reaction with three kinetically significant intermediate forms, as shown

in scheme 3.3, three decay constants, λ_1, λ_2 and λ_3 are obtained.

$$E_1 \underset{k_{-1}}{\overset{k_1}{\rightleftharpoons}} E_2 \underset{k_{-2}}{\overset{k_2}{\rightleftharpoons}} E_3$$

(Scheme 3.3)

The solutions for these decay constants are:

$$\lambda_1 = 0$$

$$\lambda_2 = \tfrac{1}{2}\,(P + Q) \qquad (3.1)$$

$$\lambda_3 = \tfrac{1}{2}\,(P - Q) \qquad (3.2)$$

where $$P = (k_1 + k_{-1} + k_2 + k_{-2}) \qquad (3.3)$$

and $$Q = [P^2 - 4\,(k_1k_2 + k_{-1}k_{-2} + k_1k_{-2})]^{\frac{1}{2}} \qquad (3.4)$$

The concentrations of the three species E_1, E_2 and E_3 can also be calculated,

since if $E_1 = E_1^{\,o}$ (where $E_1^{\,o}$ equals the initial concentration of E_1)

and $E_2 = E_3 = 0$ at time zero, then

$$E_1 = E_1^{\,o}\left(\frac{k_{-1}k_{-2}}{\lambda_2\lambda_3} + \frac{k_1(\lambda_2 - k_2 - k_{-2})}{\lambda_2(\lambda_2 - \lambda_3)}\,e^{-\lambda_2 t} + \frac{k_1(\lambda_3 - k_{-2})}{\lambda_3(\lambda_2 - \lambda_3)}\,e^{-\lambda_3 t}\right) \qquad (3.5)$$

$$E_2 = E_1^{\,o}\left(\frac{k_1k_{-2}}{\lambda_2\lambda_3} + \frac{k_1(k_{-2} - \lambda_2)}{\lambda_2(\lambda_2 - \lambda_3)}\,e^{-\lambda_2 t} + \frac{k_1(\lambda_3 - k_{-2})}{\lambda_3(\lambda_2 - \lambda_3)}\,e^{-\lambda_3 t}\right) \qquad (3.6)$$

$$E_3 = E_1^{\,o}\left(\frac{k_1k_2}{\lambda_2\lambda_3} + \frac{k_1k_2}{\lambda_2(\lambda_2 - \lambda_3)}\,e^{-\lambda_2 t} - \frac{k_1k_3}{\lambda_3(\lambda_2 - \lambda_3)}\,e^{-\lambda_3 t}\right) \qquad (3.7)$$

These decay constants can be used to derive the dependance of the observed rate constant (k_{obs}) on the aldehyde concentration. It can be seen from equation 3.7 that if the production of E_3 is monitored in the stopped-flow apparatus and only a single process is observed with a rate constant of k_{obs}, it will be the slower process with the decay constant λ_3. In scheme 3.2, $k_{-2} = 0$ and therefore does not appear in the equations, thus

$$\lambda_2 + \lambda_3 \text{ reduces to } k_2[\text{Ald}] + k_{-2} + k_3$$

and $$\lambda_2 \times \lambda_3 \text{ reduces to } k_2k_3[\text{Ald}].$$

Substituting for λ_2, which is assumed to be fast but not observed since the amplitude of the transient will be small (equation 3.7), gives:

$$1/\lambda_3 = \frac{1}{k_3} + \left(\frac{k_3 + k_{-2} - \lambda_3}{k_2k_3[\text{Ald}]}\right) \qquad (3.8)$$

It can be seen from equation 3.8 that as long as $(k_3 + k_{-2})$ is much larger than λ_3, a plot of $1/\lambda_3$ against aldehyde concentration will result in a straight line with an intercept on the y axis of $\frac{1}{k_3}$.

3.2 STEADY-STATE AND EQUILIBRIUM STUDIES

3.2.1 Methods

3.2.1.1 Spectrophotometric Assays

Assays were carried out using a Unicam SP 500 series II spectrophotometer fitted with a Unicam SP22 recorder and a water bath thermostatted at 25°C. The reaction progress was followed by either, monitoring the appearance of NADH at 340 nm assuming a molar extinction coefficient of 6220 $lmol^{-1}cm^{-1}$ (Horecker and Kornberg, 1948), or, monitoring the production of hydrogen ions at 560 nm using phenol red

as an indicator assuming a molar extinction coefficient of 54×10^3 $lmol^{-1}cm^{-1}$ (Gutfreund, 1972).

3.2.1.1.a Assays in 25 mM phosphate buffer

The assay mixture was as described in Section 2.2.2 and the reaction initiated by the addition of the aldehyde.

3.2.1.1.b Assays at low buffer concentrations

Enzyme solution was dialysed for four hours against two changes of 3 litres of 0.5 mM pH 7.6 phosphate buffer containing 0.1% v/v 2-mercaptoethanol. The dialysis tubing had been washed in hot deionised distilled water containing approximately 0.1 M $NaHCO_3$ before use. After dialysis the pH of the enzyme solution was adjusted to pH 7.6 with 0.1 M HCl or NaOH, using a radiometer 28 pH meter. Stock solutions of 14 mM NAD^+ and 240 mM propionaldehyde were prepared in the dialysing buffer and were adjusted to pH 7.6 with 0.1 NaOH prior to use. The assay mixture was as follows:

2.2 cm^3 of dialysis buffer
0.45 cm^3 of 14 mM NAD^+ solution
0.25 cm^3 of 240 mM propionaldehyde solution
0.1 cm^3 of enzyme solution

The reaction was initiated by the addition of aldehyde.

Assays with added electrolytes were carried out as described above, except that quantities of 1.0 M electrolytes were added in place of the dialysis buffer. Assays at pH values other than 7.6 were also carried out as described above, with the pH being adjusted to the appropriate value with 0.1 M HCl or NaOH.

2.3.1.2 NADH Titrations

NADH titrations were carried out using an American Instruments corporation Aminco SPF 500 fluorimeter thermostatted at 25°C. The excitation wavelength was 340 nm

with a 5 nm bandpass and the emission wavelength was 435 nm with a 10 nm bandpass. The fluorimeter was zeroed on a blank of 1.0 M H_2SO_4 then set to give a fluorescence reading of 1.0 with 0.1 $\mu g/cm^3$ quinine sulphate to enable comparisons to be made between data obtained on different days.

A glass syringe attached to a micrometer was used to deliver 0.01 cm^3 aliquots of NADH to the fluorimeter cell. Eighteen totwenty-five aliquots were added resulting in a final NADH concentration of 8 to 10 µM. A blank titration was always carried out first, in which NADH was added to a cell containing 3.0 cm^3 of 35 mM pH 7.6 phosphate buffer, then the titrations were performed in which NADH was added to an enzyme buffer mixture (3.0 cm^3). Both titrations were then repeated with 10 µM phenol red added. All solutions except the enzyme solution were filtered through a sintered glass funnel to remove dust before use.

3.2.2 TREATMENT OF DATA

3.2.2.1 Calculation of Active Site Concentration by Spectrophotometic Assay

The velocity of the enzyme-catalysed oxidation of propionaldehyde is equal to the amount of NADH produced per unit time;

$$v = \frac{\Delta c_{NADH}}{\Delta t} \qquad (3.9)$$

The concentration of an absorbing species, such as NADH, can be related to absorbance by Beers Law,

$$A = c\epsilon l$$

where A = absorbance

c = concentration of the absorbing species

l = path length

ϵ = molar extinction coefficient of the absorbing species at the wavelength being monitored

Rearranging $c = \frac{A}{\epsilon l}$

thus $\Delta c = \frac{\Delta A}{\epsilon l} \qquad (3.10)$

and substituting for Δc in equation 3.9

$$V = \frac{\Delta A_{340}}{\epsilon_{NADH}\ \Delta t} \qquad (3.11)$$

where ϵ for NADH at 340 nm is 6220 $M^{-1}cm^{-1}$

and A_{340} is the absorbance at 340 nm

As both NAD^+ and propionaldehyde are present at saturating concentrations with respect to the enzyme concentration, the velocity is equal to V_{max}, the velocity at infinite substrate concentrations. Since V_{max} is equal to the enzyme concentration multiplied by k_{cat}, then

$$[\text{Enzyme}] = \frac{V_{max}}{k_{cat}} \qquad (3.12)$$

$$\text{from 3.11} \quad [\text{Enzyme}] = \frac{\Delta A_{340}}{\varepsilon_{NADH}\Delta t k_{cat}} \qquad (3.13)$$

As k_{cat} at saturating concentrations of both NAD^+ and propionaldehyde at pH 7.6 is 0.25 s^{-1} (MacGibbon *et al.*, 1977a), l equals 1.0 cm, ε_{NADH} equals 6220 $lmol^{-1}cm^{-1}$ and $\Delta A_{340}/\Delta t$ can be measured by a spectrophotometer, the enzyme active site concentration can be calculated.

3.2.2.2 NADH Titrations

For the binding of ligands to a molecule we can define a dissociation constant:

$$K_D = \frac{[\text{free ligand}]\,[\text{free binding sites}]}{[\text{bound ligand}]}$$

In the case of NADH binding to an enzyme,

$$K_D = \frac{[NADH]\,[E]}{[E.NADH]} \qquad (3.14)$$

where [NADH] is the concentration of free NADH
[E] is the concentration of free binding sites
[E.NADH] is the concentration of occupied binding sites.

The concentration of free binding sites [E], equals the total concentration of binding sites minus the concentrations of bound sites,

$$[E] = [E]_o - [E.NADH] \qquad (3.15)$$

and the concentration of free NADH equals the total NADH concentration minus the concentration of bound NADH,

$$[NADH] = [NADH]_o - [E.NADH] \qquad (3.16)$$

Substituting for [E] and [NADH] in equation 3.14

$$K_D = \frac{([NADH]_o - [E.NADH])\ ([E]_o - [E.NADH])}{[E.NADH]} \qquad (3.17)$$

The fractional saturation of bindings sites, R, equals

$$\frac{[E.NADH]}{[E]_o}$$

Thus rearranging $[E.NADH] = R[E]_o$ (3.18)

and then substituting for [E.NADH] in eqn. 3.17

$$K_D = \frac{([NADH]_o - R[E]_o)\ ([E]_o - R[E]_o)}{R[E]_o} \qquad (3.19)$$

Rearranging eqn. 3.19 $$\frac{1}{(1-R)} = \frac{1}{K_D}\frac{[NADH]_o}{R} - \frac{[E]_o}{K_D} \qquad (3.20)$$

As can be seen from eqn 3.20 a plot of $\frac{1}{(1-R)}$ against $\frac{[NADH]_o}{R}$ will have a slope of $\frac{1}{K_D}$ and an intercept $[E]_o$ on the abscissa axis.

For a fluorescence titration where there is an enhancement of nucleotide fluorescence on NADH binding to the enzyme,

$$R = \frac{\Delta F}{\Delta F_{max}}$$

where ΔF is equal to the fluorescence difference between a blank containing NADH only and a titration containing enzyme and NADH. ΔF_{max} is the maximum change in fluorescence between the blank and the enzyme titration which is obtained when all the NADH sites are occupied.

3.2.3 RESULTS

3.2.3.1 Effect of Ionic Strength on Enzyme Activity

When enzyme samples were dialysed against 0.5 mM phosphate buffer, then assayed as described in Section 3.2.1.1.b, the enzyme activity was found to be only about 30% of the activity measured in 25 mM phosphate buffer before dialysis. The enzyme activity was found to be restored to greater than 95% of the predialysis value by the addition of KNO_3 (approx. 0.1 M) to the assay mixture, or by assaying the dialysed sample in 25 mM phosphate buffer. The addition of either Na_2SO_4 or KCl also resulted in the restoration of the activity of the dialysed enzyme but $NiSO_4$, $ZnSO_4$, $MnCl_2$, $CaCl_2$ and $MgCl_2$ (See Section 4.3) were found to lower the activity below that measured after dialysis.

The maximum reaction velocity showed a linear dependance on ionic strength at low concentrations of buffer or electrolytes, but reached a maximum value at an ionic strength of 100 mM (Fig. 3.2).

The pH profile for the enzyme activity showed a marked difference at an ionic strength of 250 mM (Fig. 3.3b) compared to the pH profile at an ionic strength of 3.3 mM (Fig. 3.3a). It can be seen that the highest activity at low ionic strength is observed at pH 5.2 approximately equal to the isoelectric point of the enzyme (Agnew *et al.*, 1981), while at a relatively high ionic strength V_{max} is greatest at about pH 7.6. This behaviour is in marked contrast to the results reported by MacGibbon *et al.*, (1977a) who found that V_{max} was relatively insensitive to pH in sodium barbital/HCl buffers but that V_{max} was greatest in the pH range 9-10.

FIG. 3.2 EFFECT OF IONIC STRENGTH ON ALDEHYDE DEHYDROGENASE ACTIVITY AT pH 7.6

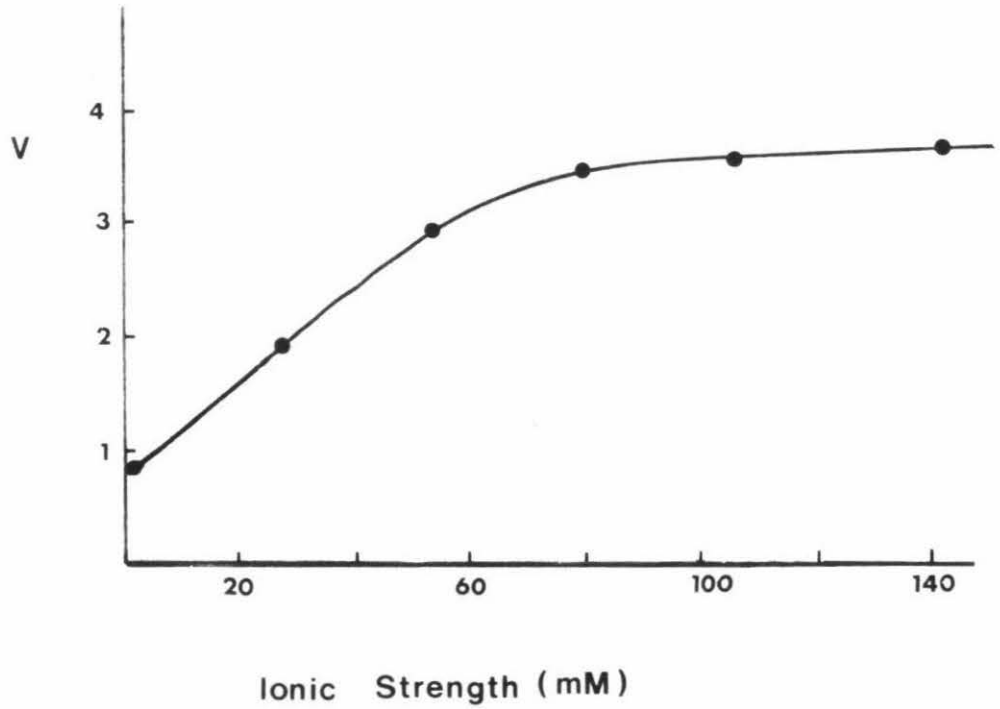

Na_2SO_4 was used to vary the ionic strength and 0.1 M HCl & NaOH to adjust the pH

FIG. 3.3 EFFECT OF pH ON Vmax

(a) AT LOW IONIC STRENGTH

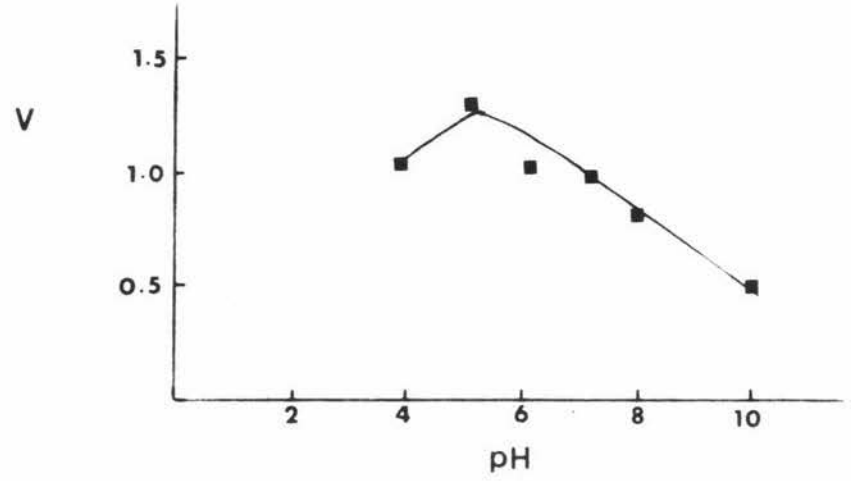

0.1 M HCl & NaOH were used to adjust the pH and the ionic strength was 3.3 mM

(b) AT HIGH IONIC STRENGTH

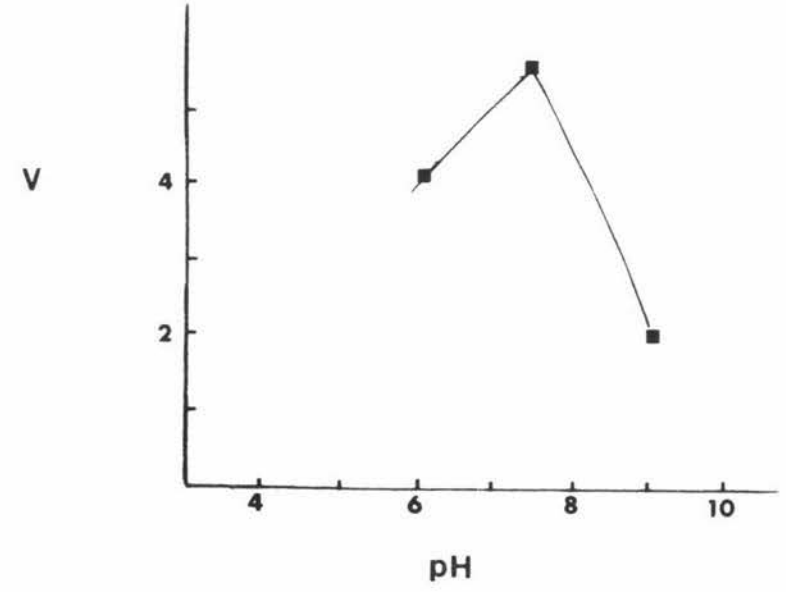

The pH was adjusted as above and the ionic strength maintained at 250mM with Na_2SO_4

3.2.3.2 NADH Titrations at Low Buffer Concentrations

When titrations were carried out on enzyme samples at an ionic strength of 3.3 mM the concentration of NADH binding sites was identical to that obtained by titration in the presence of 25 mM phosphate buffer. Titrations at an ionic strength of 100 mM Na_2SO_4 also resulted in no change in the binding site concentration. A small effect on the NADH dissociation constant was noted at low ionic strength, where a value of 0.9 µM was observed compared to 2.0 µM in 100 mM Na_2SO_4.

3.2.3.3 Effect of Phenol Red on Aldehyde Dehydrogenase Activity

The addition of phenol red (10 µM) to assays in 25 mM phosphate buffer had no effect on V_{max}, and also had no effect on assays at low buffer concentrations with and without added electrolytes.

NADH titrations with enzyme and NADH only, yielded enzyme binding site concentrations in good agreement with those calculated by assay at pH 7.6. The dissociation constant of 1.0 µM obtained, was in good agreement with the value of 1.2 µM reported by MacGibbon et al., (1979). The addition of phenol red (10 µM) to the fluorimeter cell resulted in a slight decrease in the fluorescence of both the blank and the enzyme titrations, probably as a result of the absorption of the fluoresced radiation by the acidic form of phenol red which has a moderate absorption at 435 nm (Fig. 3.1). However both the NADH binding site concentration and the K_D value were unchanged in the presence of phenol red.

Titrations carried out with chlorophenol red and thymol blue added also resulted in K_D values and NADH binding site concentrations identical to those in the absence of any indicator.

3.3 PROTON BURST EXPERIMENTS

3.3.1 Methods

3.3.1.1 Apparatus

Stopped-flow experiments were carried out using a Durrum-Gibson D110 stopped-flow spectrophotometer (Durrum Instruments Corporation, Palo Alto California U.S.A.). In the stopped-flow apparatus two solutions are forced into an observation chamber through mixing jets by compressed-gas driven plungers within about 3 ms (Fig. 3.4). The flow is halted by a stopping syringe which, on contacting with a trigger, activates a recording device. The reaction progress is followed by monitoring radiation of an appropriate wavelength with a photomultiplier after it has passed through a 1.7 cm observation chamber containing 0.3 cm^3 of the mixed solutions.

3.3.1.2 Observation and Recording of Data

In the absorbance mode, signals from the photomultiplier were passed through a log buffer amplifier to a Data Laboratories DL905 or DL901 transient recorder. The data was displayed on a Hewlett Packard 141B oscilloscope and, if a satisfactory trace was obtained, then transferred to a pdp 8/e computer (Digital Equipment Corporation) from the transient recorder via an interface. The data could then be processed immediately or punched to paper tape for processing at a later date. In each case a permanent record of the reaction trace was printed using a Bryans 29000 A4 x Y recorder (Fig. 3.5).

3.3.1.3 Preparation of Solutions

Solutions were prepared for use in the stopped-flow apparatus using 0.5 mM pH 7.6 phosphate buffer which had been degassed on a water pump for 30 minutes prior to use. The degassing procedure was carried out to remove air bubbles from the solutions as the presence of air bubbles in the observation chamber resulted in erratic data. The enzyme solution was dialysed for 3 hours in 2 x 3l of 0.5 mM pH 7.6

FIG. 3.4 SCHEMATIC DIAGRAM OF A STOPPED-FLOW APPARATUS

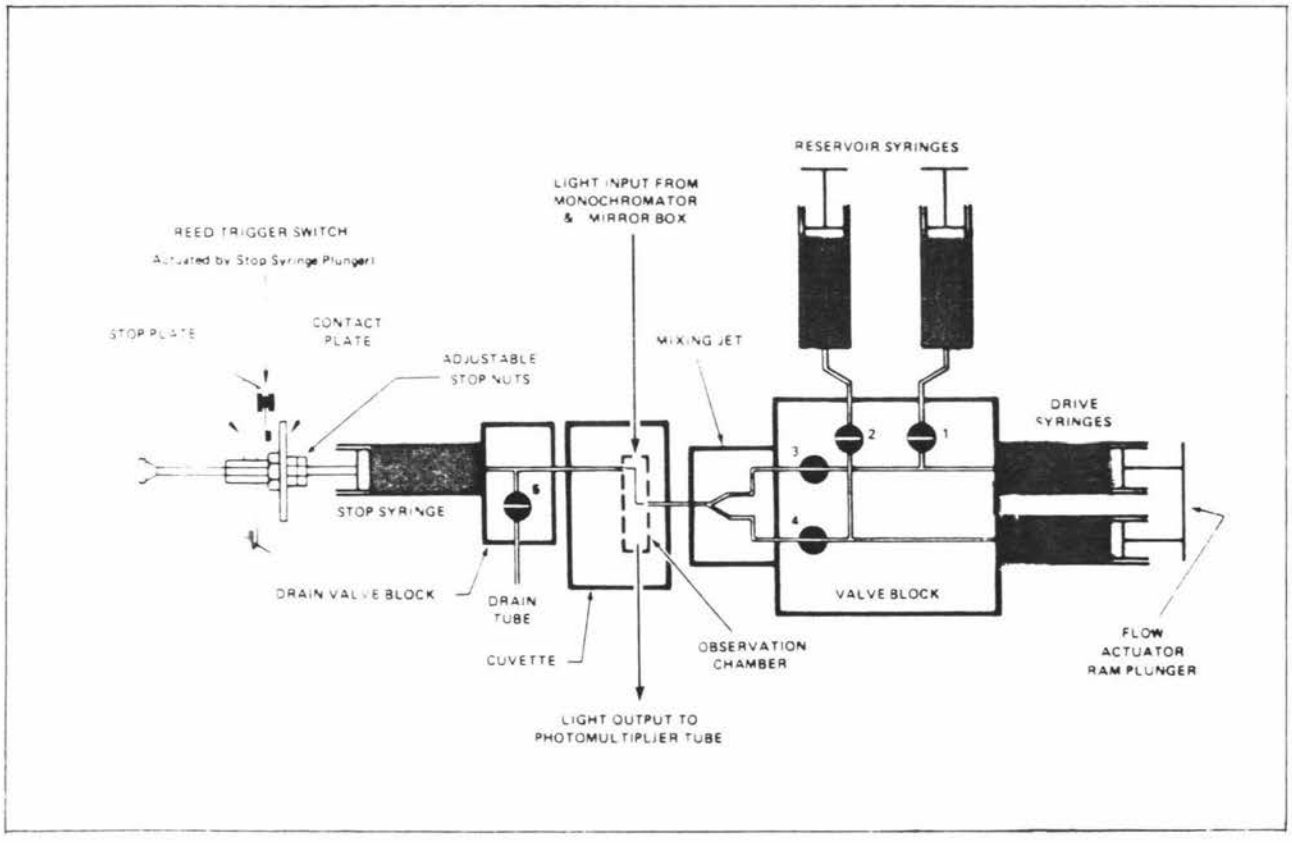

(Durrum Instruments Corporation Instruction manual (D110) 1974 P 3.14)

FIG 3.5 **BLOCK DIAGRAM OF THE STOPPED-FLOW APPARATUS AND ASSOCIATED EQUIPMENT**

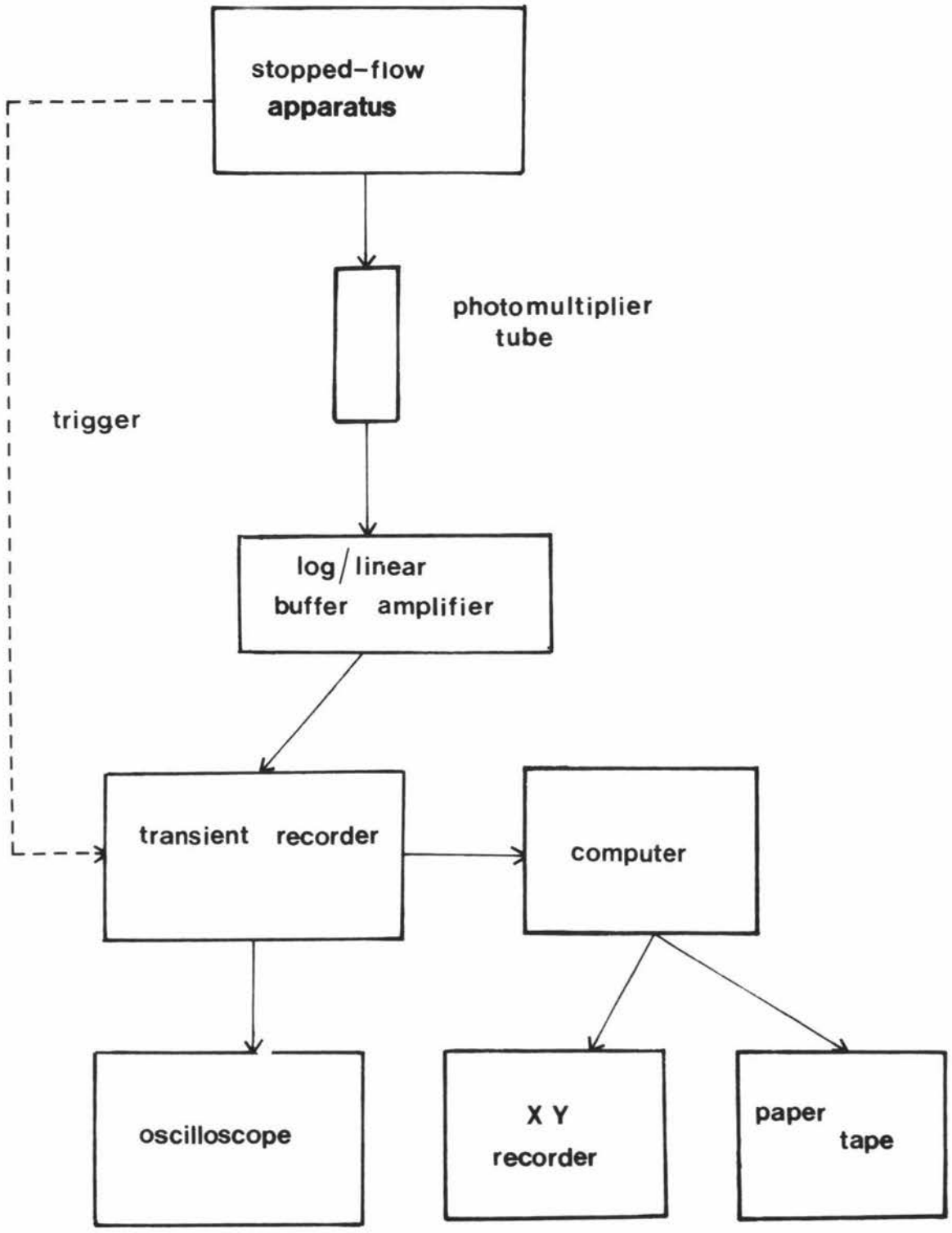

phosphate buffer containing 0.1% v/v β-mercaptoethanol. All solutions contained 10 to 20 μM phenol red, 0.1 M Na_2SO_4 and 0.1 M KNO_3 and were adjusted to pH 7.6 with 0.1 M HCl and 0.1 M NaOH using a Radiometer pH meter 28 immediately prior to use.

The enzyme was usually pushed against NAD^+ and propionaldehyde in the stopped-flow apparatus, although in some experiments it was convenient to have one of the substrates premixed with the enzyme.

For burst experiments using 4-nitrophenylacetate instead of aldehyde as the substrate, the ester was prepared as a stock solution in acetonitrile as it is relatively insoluble in water. The stock solution was subsequently diluted with 0.5 mM phosphate buffer for use in the stopped-flow experiments so that the final concentration of acetonitrile was less than 3% v/v, at which concentration there is no significant inhibition by acetonitrile.

3.3.1.4 Preparation of [1-^{2}H] Propionaldehyde

[1-^{2}H] Propionaldehyde was prepared by the Nef reaction using 1-nitro-[2- H]-propane as the starting material (Johnson and Degering, 1942). 1-Nitro-[2-^{2}H]-propane was dissolved in a solution containing NaOH (2 g) in distilled H_2O (20 cm^3), this mixture was then added dropwise with stirring over 30 minutes to a solution containing 12 M H_2SO_4 (3 cm^3) and distilled H_2O (20 cm^3) in an alcohol/ice bath. The aldehyde was distilled off at a b.p. of 48°C to 52°C, and after a further distillation was shown to be 90% deuterated by mass spectrometry. A 68% yield of aldehyde from the nitropopane was obtained from this process.

The 1-nitro-[2-^{2}H]-propane was prepared from 1-nitropropane by a method similar to that described by Leitch (1955). 1-nitropropane (50 g), which had been distilled through a vigreux column, was added to Na (0.8 g) and D_2O (35 g) then refluxed for 17 hours. The organic layer was separated from the aqueous layer then added to Na (0.4 g) and D_2O (15 g) then refluxed for a further 17 hours. The

recovery from this step was approximately 8%, mainly due to losses during over-vigorous refluxing.

3.3.1.5 Computer Simulations

Computer simulations were carried out using a Burroughs continuous simulation modelling package on a Burroughs B6700 computer. The program accepted as input data, the rate equations for the mechanism to be simulated, the rate constants for the individual steps in the mechanism and the initial concentrations of all reactants, intermediates and products involved in the proposed mechanism. The computer integrated the rate equations at time intervals specified by the program and outputted the concentration of products, reactants and intermediates at each integration interval. This data was then treated as described in section 3.3.2.2 to obtain the rate constant for the simulated burst.

3.3.2 Treatment of Data

3.3.2.1 Calibration of Activity at 340 nm and 560 nm

The stoichiometry of the enzyme-catalysed oxidation of aldehydes to acids indicates that two protons are released per NADH molecule produced.

$$H_2O + R\text{-}\underset{\underset{O}{\|}}{C}\text{-}H + NAD^+ \xrightarrow{\text{enzyme}} R\text{-}\underset{\underset{O}{\|}}{C}\text{-}O^- + NADH + 2H^+$$

The second proton comes from the almost complete dissociation of the carboxylic acid at pH 7.6. Consequently the change in concentration per unit time determined by monitoring the reaction at 340 nm with a spectrophotometer, assuming a molar extinction coefficient of 6220 $lcm^{-1}mol^{-1}$ should be half that resulting from following the reaction at 560 nm using a molar extinction coefficient of 54×10^3 $lcm^{-1}mol^{-1}$ (Gutfreund, 1972). However due to the presence of the 0.5 mM phosphate buffer in the solutions the change in concentration per unit time at 560 nm was considerably less than that at 340 nm, thus it was found necessary to assay the same solution at both 340 nm and 560 nm and relate the change in concentration

at 560 nm to that at 340 nm by a calibration factor. Usually this was carried out prior to each stopped-flow experiment using solutions which were to be mixed in the stopped-flow apparatus.

3.3.2.2 Processing of Burst Data

Photomultiplier signals were transferred by the transient recorder to the core of the pdp 8/e computer as 1024 8 bit data points by means of a machine language program similar to that described by Hardman et al., (1978). Statistical and kinetic calculations could then be carried out on the data using a number of machine language subroutines.

pH burst experiments which resulted in a single first order exponential were treated by a method described by Laidler (1973), in which the steady-state slope was extrapolated back to zero time to obtain a baseline, then the log of the difference between the transient and the baseline plotted against time. The rate constant for the process was obtained by multiplying the slope of log difference plot by -2.303. A least squares analysis was used by the computer program to fit the straight line through the log difference versus time plot, and after calculating the rate constant and amplitude of the exponential process, the computer reconstructed the burst curve using the calculated rate and amplitude (Fig. 3.7). The closeness of the computer drawn cure to the original reaction trace was taken as a measure of the accuracy of the calculated values.

When traces with a low signal to a noise ratio were obtained (Fig. 3.6), up to eight successive transients could be stored by the computer, then each 8 bit data point averaged to give a computed average transient or C.A.T. (Fig. 3.7) with a greatly improved signal to noise ratio. Kinetic calculations could then be performed on the averaged transient.

FIG. 3.6 Reaction Trace With a Low Signal to Noise Ratio

The trace shows the association of NADH (4.9 μM) and enzyme (4.9 μM). In nucleotide fluorescence, the vertical scale is 0.011 volt/cm and the horitzontal scale .47 s/cm.

FIG. 3.7 An Averaged Reaction Trace

The trace shows the results of averaging 6 single transients as in FIG. 3.6. The voltage and time scales are as in FIG. 3.6. The smooth line drawn through trace is a curve generated by the computer through the slower binding process (Section 5.4.4) utilizing the previously calculated rate and amplitude.

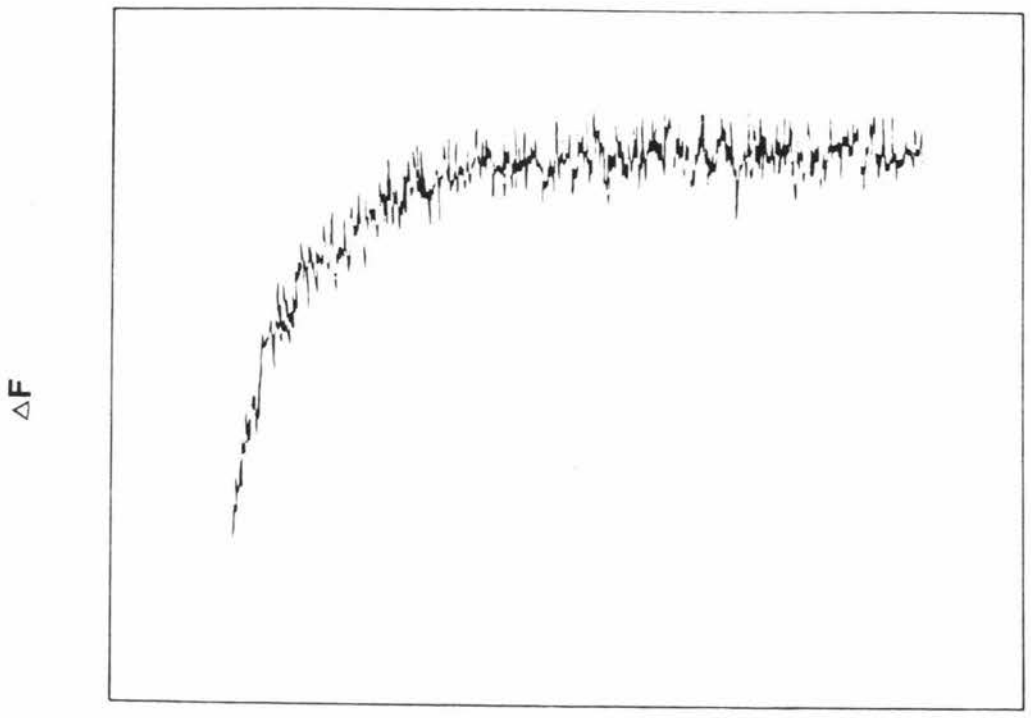
ΔF
Time (s)

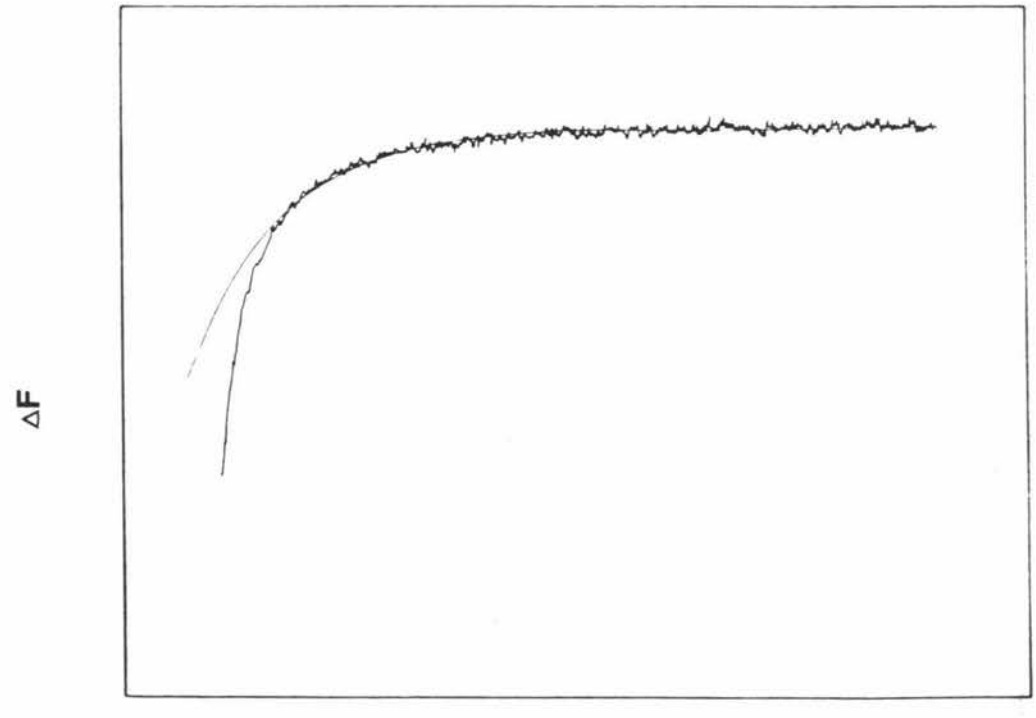
ΔF
Time (s)

3.3.3 Results

3.3.3.1 Calibration of Activity between 560 nm and 340 nm

The recorder traces obtained by monitoring the reaction of 560 nm were generally linear for 30 to 60 seconds while at 340 nm they were linear for 2 to 3 minutes. The calibration factor obtained by dividing the change in concentration of NADH per unit time (calculated from the absorbance data at 340 nm) by the apparent change in concentration of protons (calculated from the absorbance data at 560 nm) and multiplying by two, was an average 50 ± 10.

3.3.3.2 Proton Burst at pH 7.6

When a solution containing enzyme (30 μM), NAD^+ (2 mM), phenol red (15 μM), KNO_3 (0.1 M) and Na_2SO_4 (0.1 M) was pushed against a solution containing propionaldehyde (40 mM), phenol red (15 μM), KNO_3 (0.1 M) and Na_2SO_4 (0.1 M) in the stopped-flow apparatus, a burst in the production of protons was observed followed by a slow release of protons equivalent to the steady-state rate (Fig. 3.8a). The transient phase was first order with a rate constant of 11 s^{-1}, and the amplitude calculated using a calibration factor of 50 was equal to the enzyme active site concentration. No transient proton release was observed when the enzyme solution above was pushed against NAD^+ (2 mM), phenol red (15 μM), KNO_3 (0.1 M) and Na_2SO_4 (0.1 M). However a very slow proton release was observed with a rate of about 0.05 s^{-1}. This proton release, was also observed in the absence of NAD^+ and probably resulted from the presence of dissolved CO_2 in unequal concentrations in the two syringes which can result in a proton release as shown below.

$$H_2CO_3 \rightleftharpoons HCO_3^- + H^+$$

This process has a rate constant of 0.038 s^{-1} (Gutfreund, 1972).

FIG. 3.8 Proton Burst at pH 7.6

3.8a Proton Burst at Saturating Substrate Concentrations

The reaction mixture contained enzyme (16 μM), phenol red (15 μM), $NaNO_3$ (0.1 M), Na_2SO_4 (0.1 M), NAD^+ (1.1 mM) and propionaldehyde (20 mM). The rate of the burst was 11 s^{-1} and the amplitude was 14.3 μM.

3.8b Proton Burst at Low Propionaldehyde Concentrations

The reaction mixture contained enzyme (11 μM), phenol red (15 μM), $NaNO_3$ (0.1 M), Na_2SO_4 (0.1 M), NAD^+ (1.03 mM) and propionaldehyde (60 μM). The rate of the burst was 8.3 s^{-1} and the amplitude was 9.8 μM.

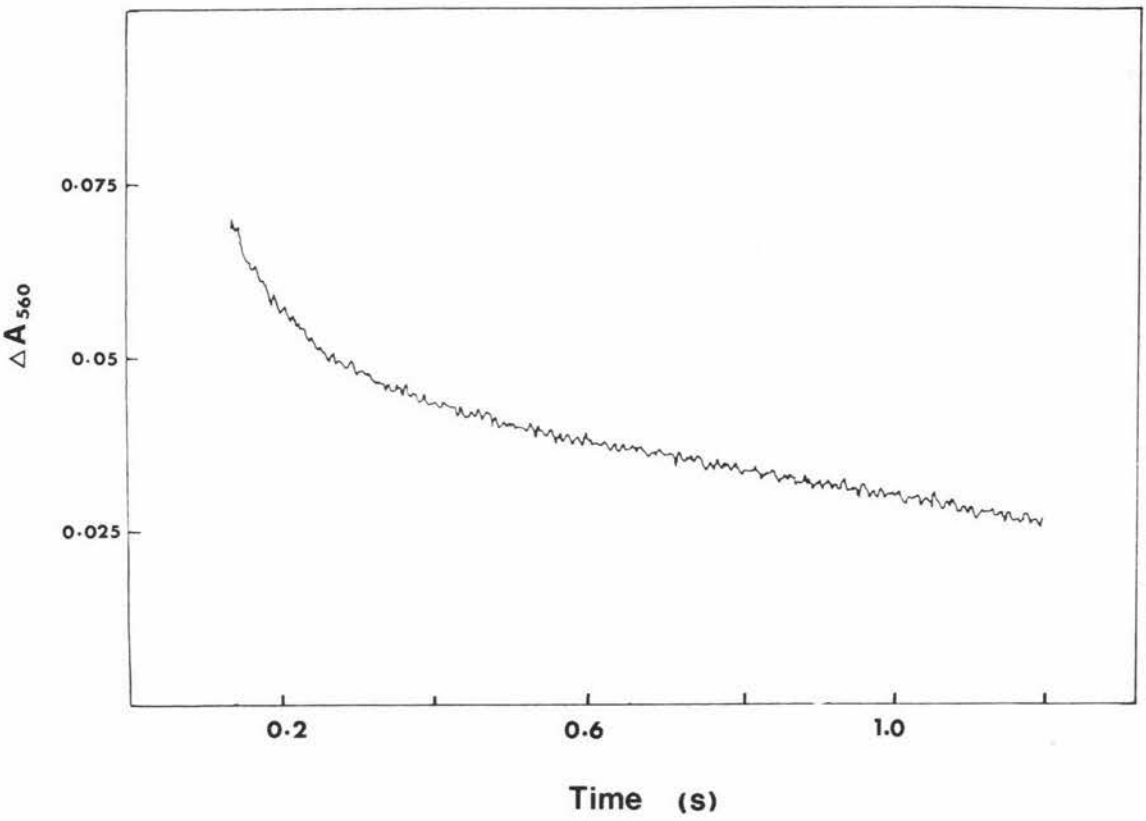
0·075
0·05
0·025
ΔA560
0·2
0·6
1.0
Time (s)

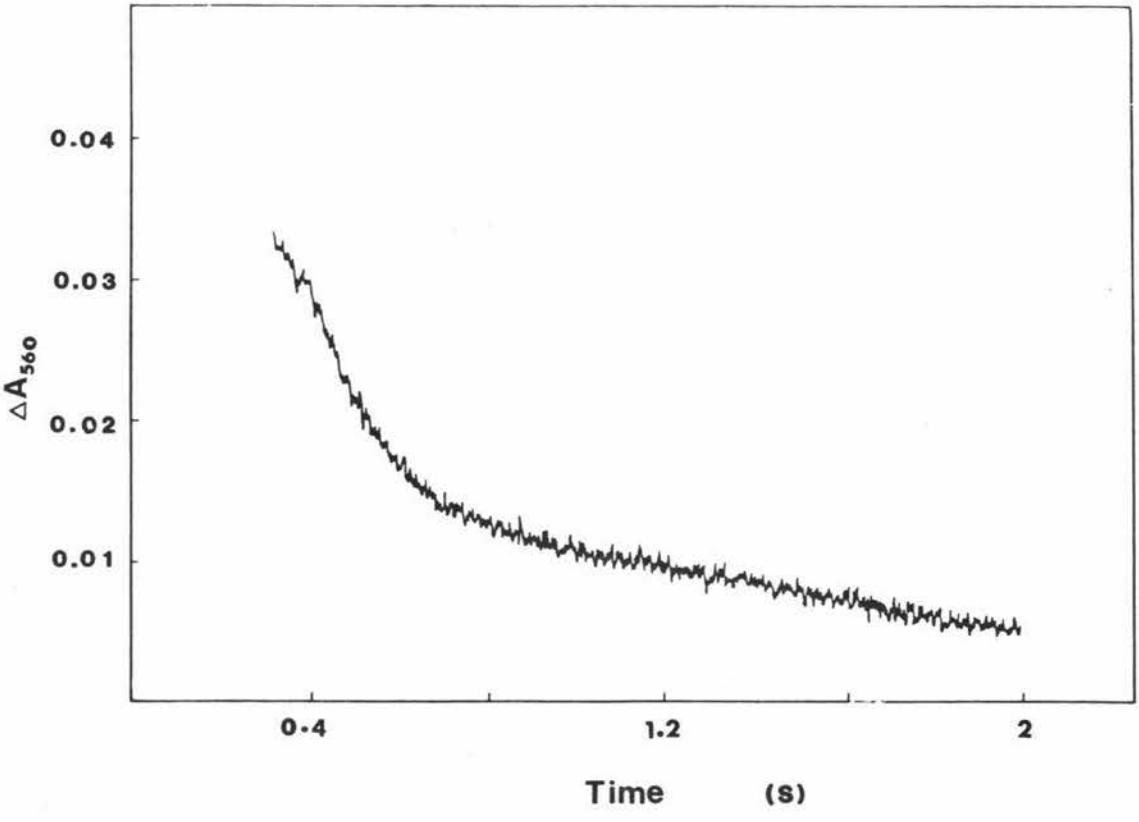
0.04
0.03
0.02
0.01
ΔA560
0·4
1.2
2
Time (s)

A proton burst equal in amplitude to the enzyme concentration was also observed when NAD^+ was not premixed with the enzyme, however in this case there was a slight decrease in rate to 7 s^{-1}. When the production of NADH was monitored at 340 nm in absorbance using the same solutions that were used in the proton burst experiments a burst was also observed with a rate of 13 s^{-1}.

3.3.3.3 Effect of Propionaldehyde Concentration on the Burst rate

The observed rate constant for the proton burst was found to vary with propionaldehyde concentration. Figure 3.9 shows the results of a double reciprocal plot of k_{obs} versus propionaldehyde concentration. The data resulted in a straight line with a slope of 3 x 10^{-6} Ms and a half-saturating concentration of 36 µM. The rate constant at infinite propionaldehyde concentration was 12 s^{-1}.

At low propionaldehyde concentrations (less than 100 µM) a lag phase was observable at the start of the transient (Fig. 3.8b) presumably caused by the build up of an enzyme.NAD^+.aldehyde intermediate. Using [1-^{2}H]-propionaldehyde as a substrate a moderate kinetic isotope effect of 2.0 was observed at propionaldehyde concentrations less than 100 µM. At higher concentrations however, there was no detectable isotope effect.

3.3.3.4 Effect of Acetaldehyde Concentration on the Burst Rate

When acetaldehyde was used as a substrate, a burst in the production of protons was also observed (Fig. 3.10). The double reciprocal plot of k_{obs} against acetaldehyde concentration again resulted in a straight line, the slope of which was 8.8 x 10^{-3} Ms. The half-saturating concentration of acetaldehyde was 2 mM and the rate constnat at infinite aldehyde concentration was 30 s^{-1} (Fig. 3.11).

FIG 3.9 **DOUBLE RECIPROCAL DEPENDENCE OF OBSERVED PROTON BURST RATE ON PROPIONALDEHYDE CONCENTRATION**

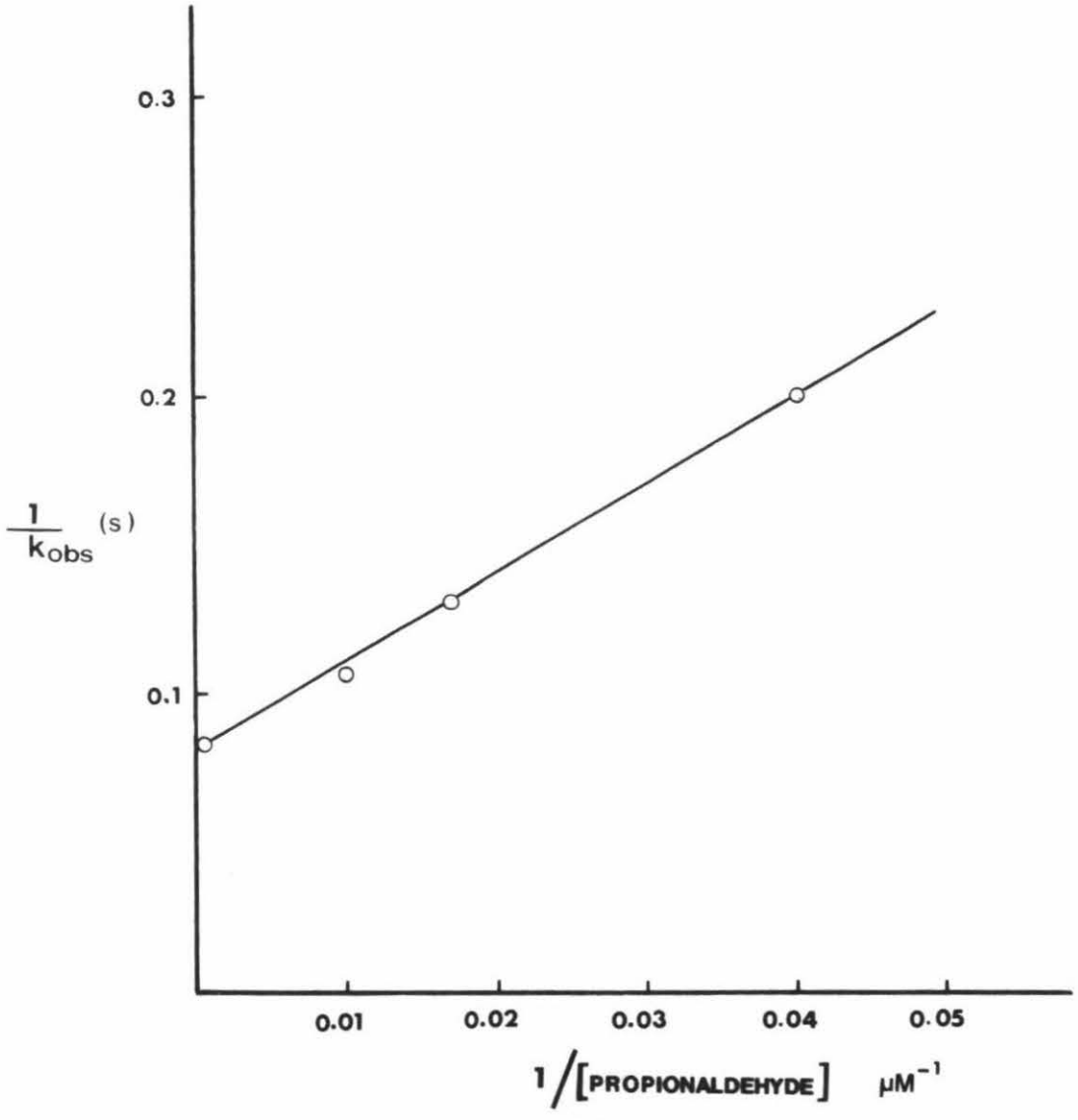

The reaction mixture contained 15 μM enzyme, 1 mM NAD^+, 0.1 M Na_2SO_4, 0.1 M $NaNO_3$ and 15 μM phenol red. The slope equals 3×10^{6} Ms^{-1} and the concentration at half the maximum burst rate is 36 μM.

FIG. 3.10 Burst With Acetaldehyde

The reaction mixture contained enzyme (18 μM), phenol red (15 μM), $NaNO_3$ (0.1 M), Na_2SO_4 (0.1 M), NAD^+ (1.1 mM) and acetaldehyde (20 mM). The rate of the burst was 24 s^{-1} and the amplitude was 14.7 μM.

FIG. 3.14 Proton Burst With Added Disulfiram

The reaction mixture contained enzyme (17μM), phenol red (15 μM), $NaNO_3$ (0.1 M), Na_2SO_4 (0.1 M), NAD^+ (1 mM), propionaldehyde (20 mM) and disulfiram (21μM) premixed with the enzyme. The rate of the burst was 10 s^{-1} and the amplitude was 3.15 μM.

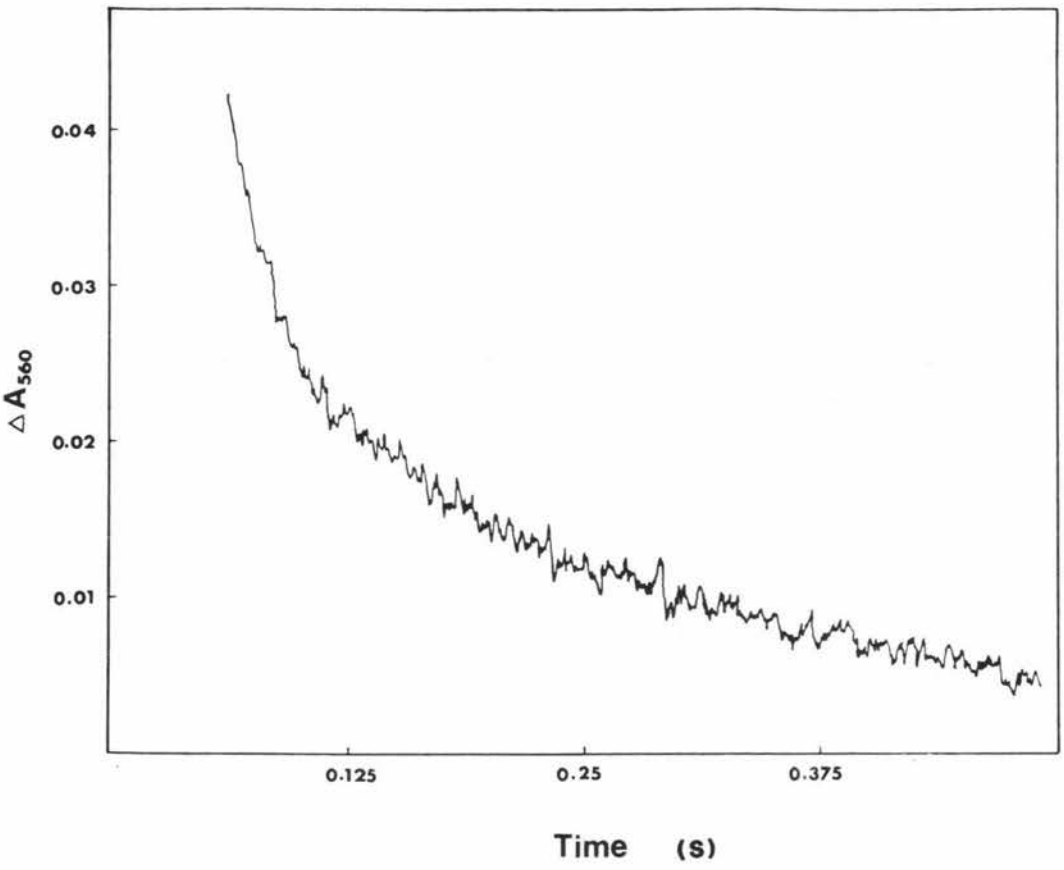
0.04
0.03
0.02
0.01
ΔA560
0.125
0.25
0.375
Time (s)

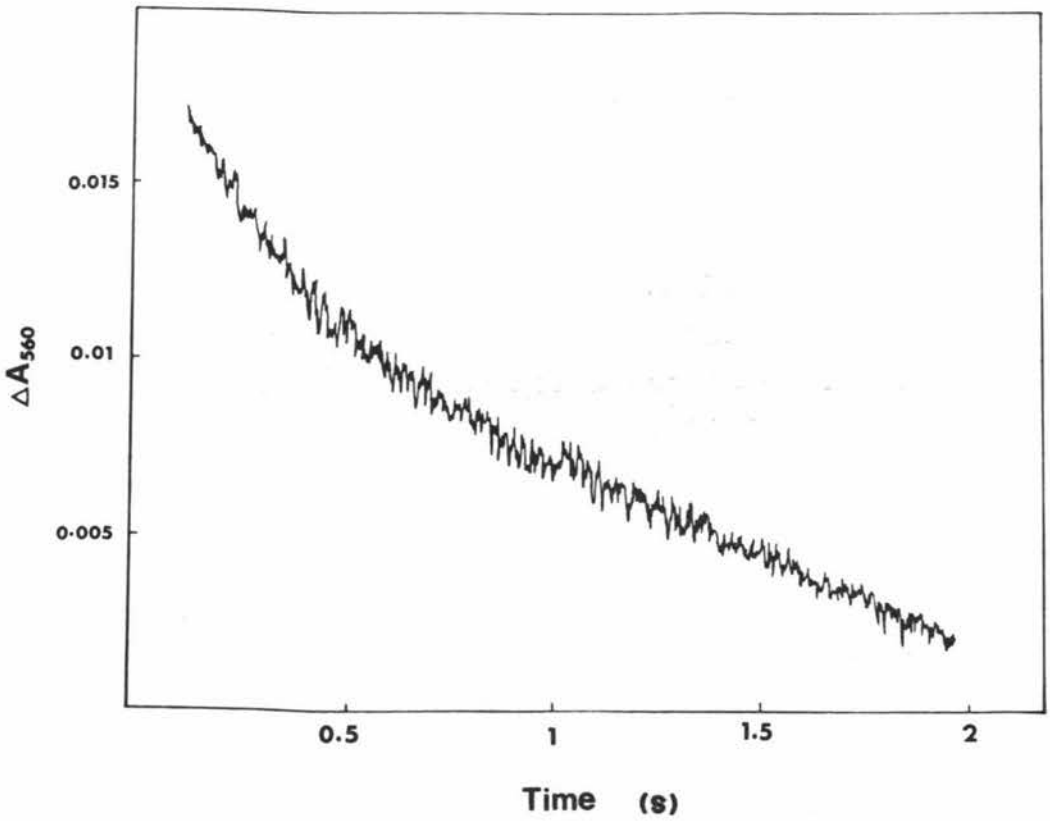
0.015
0.01
0.005
ΔA560
0.5
1
1.5
2
Time (s)

FIG 3.11 **DOUBLE RECIPROCAL DEPENDENCE OF OBSERVED PROTON BURST RATE ON ACETALDEHYDE CONCENTRATION**

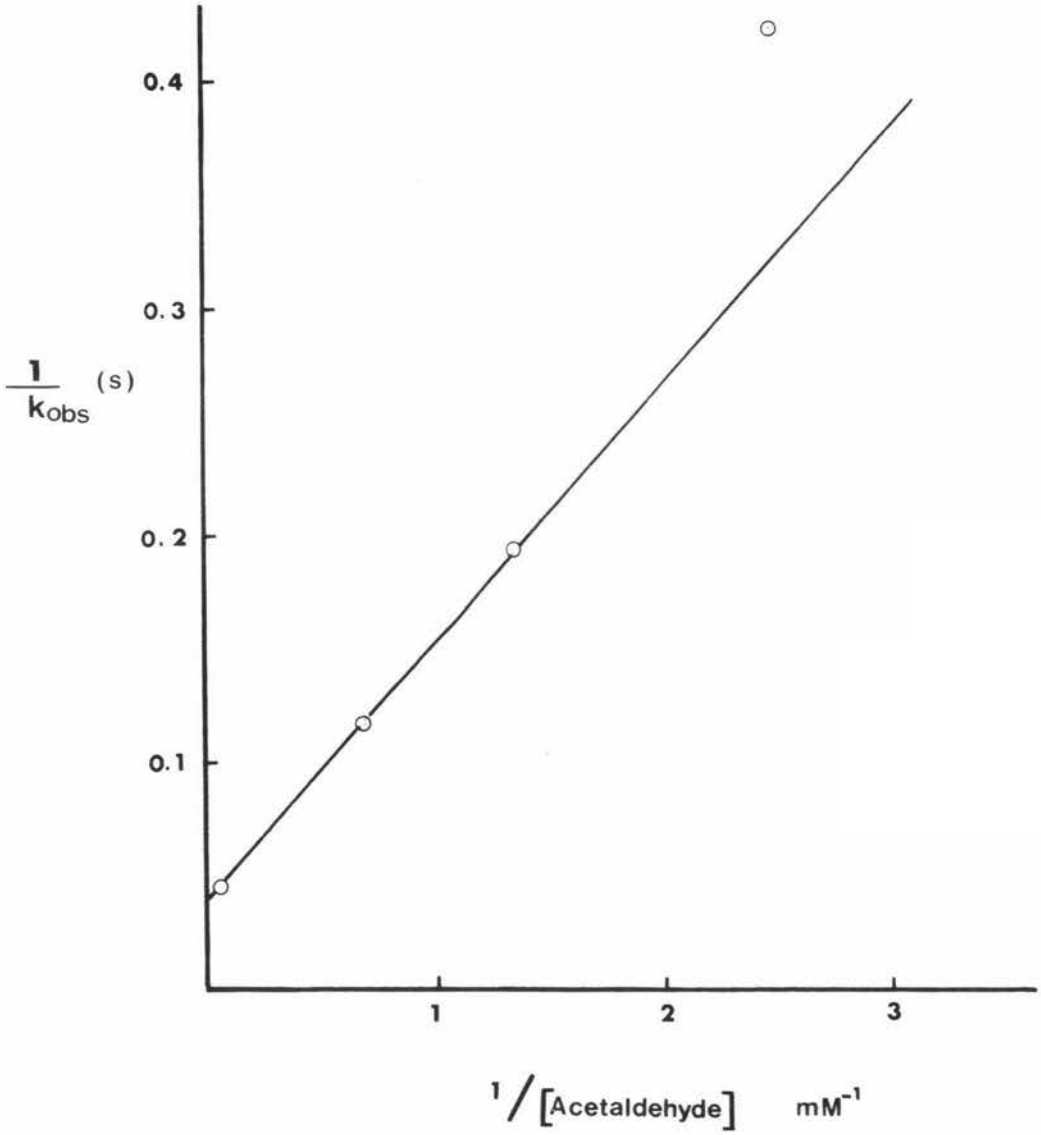

The reaction mixture contained 15 µM enzyme, 1 mM NAD^+, 0.1 M Na_2SO_4, 0.1 M $NaNO_3$ and 15µM phenol red. The slope equals 8.8×10^{-3} Ms^{-1} and the concentration at half the maximum burst rate is 2 mM.

Using [1,2,2,2-^{2}H] acetaldehyde as a substrate, a kinetic isotope effect of 2.1 was found at acetaldehyde concentrations less than 1 mM while no evidence for any isotope effect was found at higher concentrations.

3.3.3.5 Effect of NAD^+ Concentration on the Burst

The rate constant for the proton burst was found to vary with NAD^+ concentration at NAD^+ concentrations below saturating levels. A plot of the observed rate constant versus NAD^+ concentration resulted in a straight line with a slope of $1.14 \times 10^5\ M^{-1}s^{-1}$ (Fig. 3.12).

3.3.3.6 Effect of pH on the Burst

When a solution of enzyme (20 μM), chlorophenol red (15 μM), KNO_3 (0.1 M) and Na_2SO_4 (0.1 M) was pushed against NAD^+ (2 mM), chlorophenol red (15 μM), KNO_3 (0.1 M) and Na_2SO_4 (0.1 M) in the stopped-flow apparatus, a burst in the production of protons was observed at 580 nm. The transient was a single first order process with a rate constant of $5 \pm 1\ s^{-1}$ and the amplitude of the burst was equal to 90% of the enzyme active site concentration.

When the experiment was repeated at pH 9.0 using thymol blue as an indicator, there was no observable transient release of protons.

3.3.3.7 Proton Bursts with Other Aldehydes

Using benzaldehyde (1.0 mM) as a substrate, a proton burst was observed with a rate constant of $2.7\ s^{-1}$. The amplitude of the burst process corresponded to 90% of the enzyme active site concentration.

4-Nitrobenzaldehyde has been reported by MacGibbon *et al.*, (1977c) as exhibiting steady-state activity, but not exhibiting a pre-steady-state burst in NADH production. These workers interpreted this result as indicating a shift to hydride transfer as the rate limiting step in the steady-state. When 4-nitrobenzaldehyde was used as a substrate, no NADH burst was detected in this study, however on the addition of $MgCl_2$ (5 mM), a substance which has been shown to greatly

FIG 3.12 **DEPENDANCE OF OBSERVED PROTON BURST RATE CONSTANT ON NAD^+ CONCENTRATION**

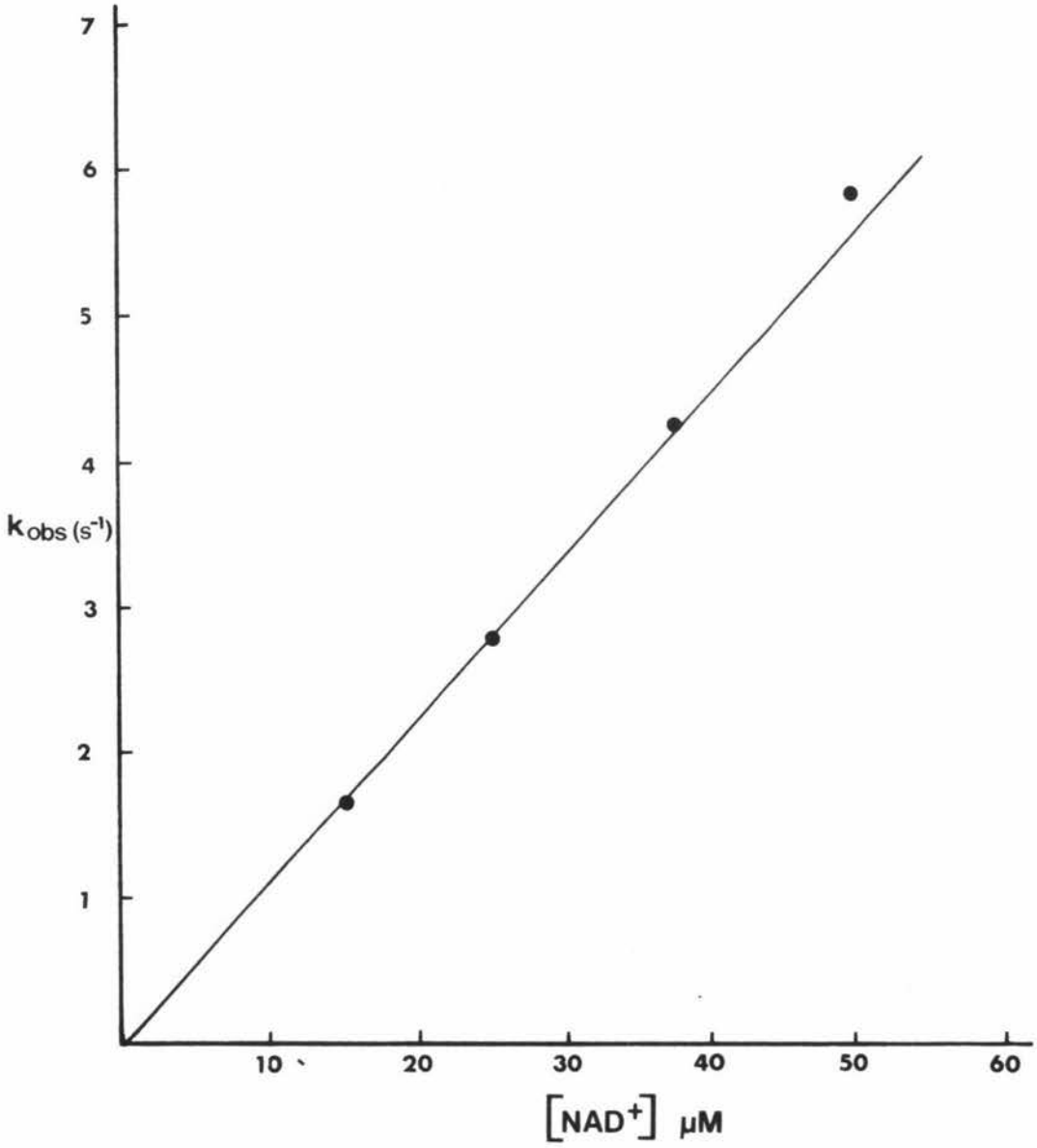

The reaction mixture contained 14.6 µM enzyme, 20 mM propionaldehyde, 0.1 M Na_2SO_4, 0.1 M $NaNO_3$ and 15 µM phenol red.

inhibit the steady-state production of NADH but not the burst rate (Sections 4.3.1, 6.3.4), a small NADH burst was observed with a rate constant of 0.02 s^{-1} (Fig. 3.13b). This rate constant is in good agreement with the turnover number k_{cat} calculated in the absence of $MgCl_2$ of 0.013 s^{-1}.

When the transient release of protons at 560 nm was monitored using 4-nitrobenzaldehyde as a substrate, a burst was observed with a rate constant of 3 s^{-1} (Fig. 3.13a). The amplitude of the burst was equal to 90% of the enzyme active site concentration.

3.3.3.8 4-Nitrophenylacetate as Substrate

Cytoplasmic sheep liver aldehyde dehydrogenase has been shown to catalyse the hydrolysis of nitrophenyl-esters (MacGibbon et al, 1978a) These workers also observed a burst in the production of the 4-nitrophenolate ion with the same rate (11 s^{-1}) as the NADH burst for the dehydrogenase reaction. As it has been suggested that the esterase and dehydrogenase active sites of aldehyde dehydrogenases are the same (Hart and Dickinson, 1978; Duncan, 1979; Eckfeldt and Yonetani, 1976; Feldman and Weiner, 1972b) it was decided to determine whether there was a transient release of protons associated with the esterase reaction.

When enzyme (27 µM) was pushed against 4-nitrophenylacetate (800 µM) in the stopped-flow apparatus, a slow steady-state release of protons was observed, but no burst in proton release was detected. The rate of the slow proton release, calculated assuming that the calibration factor of 50 calculated in Section 3.3.3.31 was unchanged by the substitution of the ester for the aldehyde, was almost identical to the steady-state production of the 4-nitrophenolate ion as measured by assay (Section 4.2). When the experiment was repeated with NAD^+ (1 mM) added there was again no detectable burst, although the rate of the steady-state proton release had increased, consistent with the observation of MacGibbon et al, (1978a).

FIG. 3.13 Proton and NADH Bursts with 4-Nitrobenzaldehyde

3.13a Proton Burst

The reaction mixture contained enzyme (13.5 μM), phenol red (15 μM), $NaNO_3$ (0.1 M), Na_2SO_4 (0.1 M), NAD^+ (1.2 mM), and 4-nitrobenzaldehyde (250 μM). The rate of the burst was 3 s^{-1} and the amplitude was 12.8 μM.

3.13b NADH Burst

The reaction mixture contained enzyme (8.2 μM), NAD^+ (1.1 mM), 4-nitrobenzaldehyde (250 μM), and $MgCl_2$ (5 mM). The rate of the burst is 0.021 s^{-1} and the amplitude was 1.1 μM. The vertical axis was 0.5 Volts which corresponds to the fluorescence of 8.5 μM of NADH .

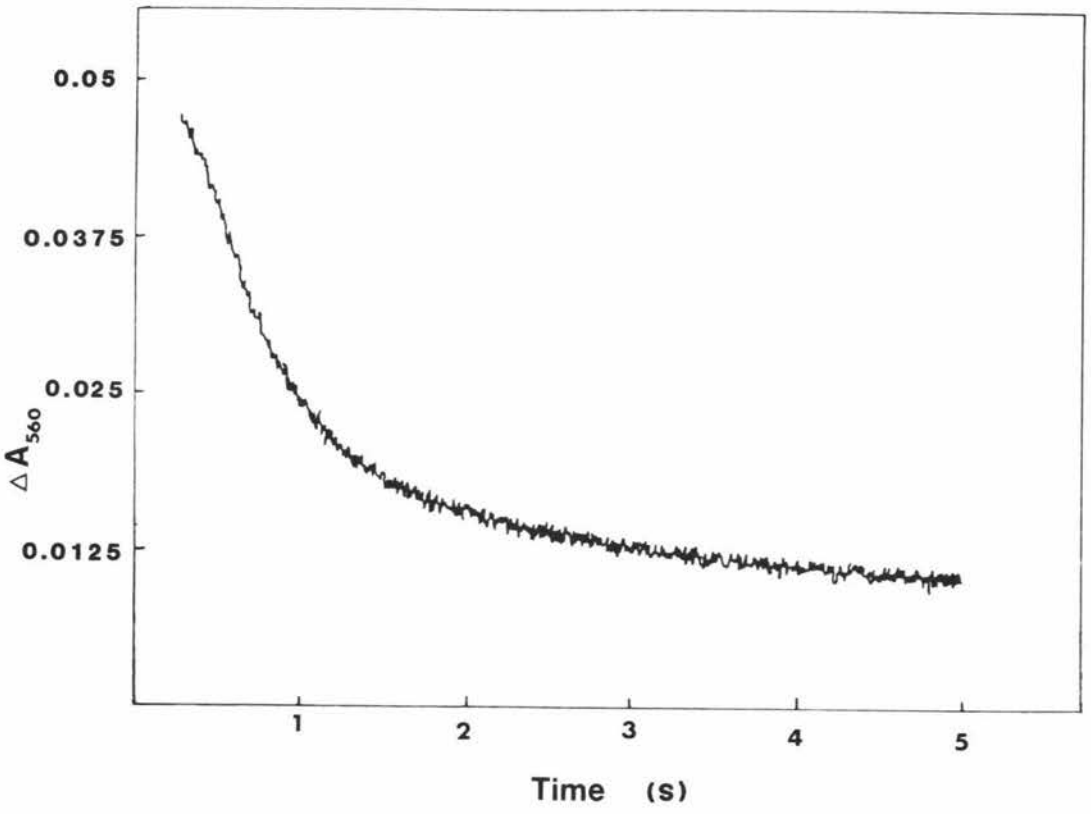
0.05
0.0375
0.025
0.0125
ΔA_{560}
1
2
3
4
5
Time (s)

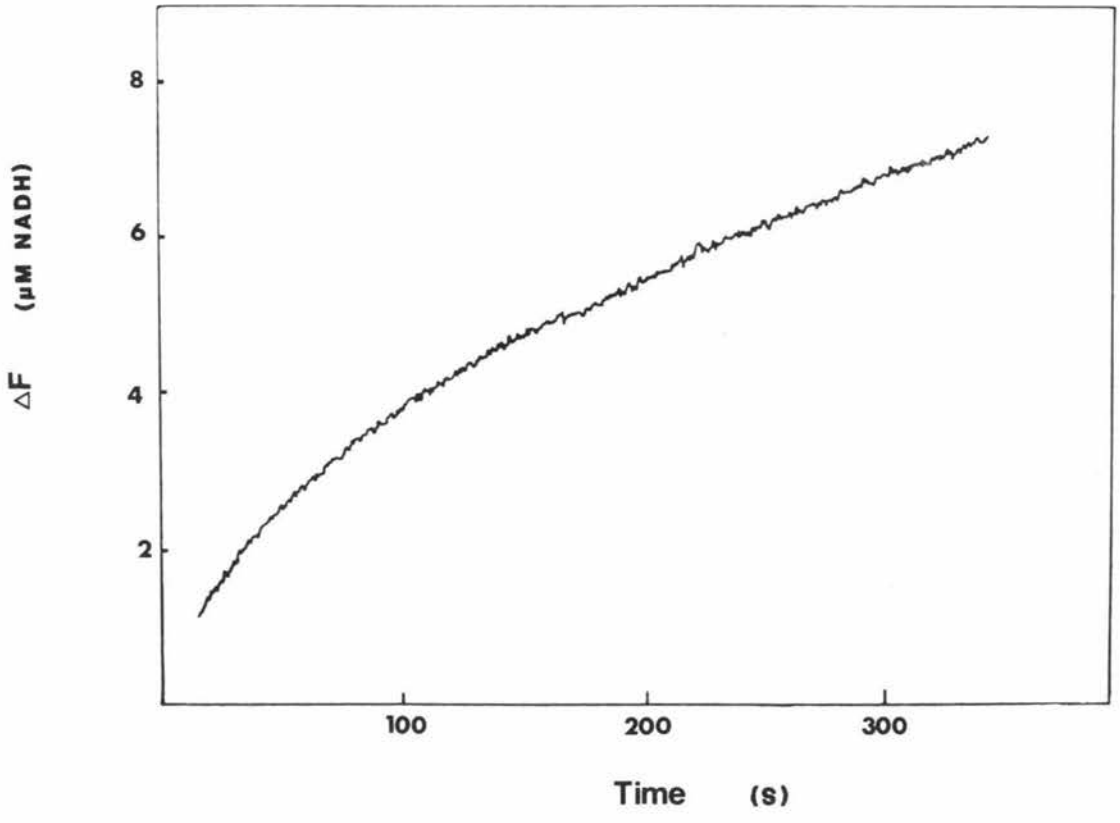
8
6
4
2
ΔF (μM NADH)
100
200
300
Time (s)

3.3.3.9 Burst Experiments with Steady-state Inhibitors Present

When burst experiments were carried out in which the enzyme (18 μM) was pretreated with disulfiram (25 μM) and NAD^+ (1 mM), a proton burst was observed with a rate of 10 s^{-1}. The amplitude of the burst was however only 18% of the enzyme active site concentration (Fig. 3.14).

The addition of glyoxylic acid (20 mM) (which acts as an inhibitor competitive with propionaldehyde at high concentrations of aldehyde but is not a reaction substrate (L. Deady, personal communication)), to the enzyme.NAD^+ mixture in the stopped-flow apparatus which was then pushed against propionaldehyde, resulted in a burst no longer being observed. Instead a lag phase with a rate constant of 0.1 s^{-1} and an amplitude equal to 60% of the enzyme concentration was observed followed by a steady-state proton release (Fig. 3.15). When glyoxylic acid (20 mM) was used in place of propionaldehyde in burst experiments, again no proton burst was observed. However in this case, a slow proton uptake was observed followed by an even slower proton release (Fig. 3.16). The amplitude of the proton uptake was equal to the enzyme active site concentration, however the slow proton release, which may be due to the presence of CO_2 in the solutions (Section 3.3.3.1), is probably masking some of the proton uptake amplitude. The rate constant for the proton uptake was 0.2 $\pm$ 0.02 s^{-1} and the rate constant for the proton release was 0.058 s^{-1}.

Acetone, which is similar to acetaldehyde in structure and size, has a relatively small inhibitory effect on the steady-state reaction (MacGibbon *et al.*, 1977b). However when it was mixed with enzyme and NAD^+ in the stopped-flow apparatus, no transient or steady-state proton release was observed.

FIG. 3.15 Lag Phase in Proton Release in the Presence of Glyoxylic Acid

The reaction mixture contained enzyme (18 μM), phenol red (15 μM), $NaNO_3$ (0.1 M), Na_2SO_4 (0.1 M), NAD^+ (2.1 mM), propionaldehyde (20 mM) and glyoxylic acid (20 mM) premixed with the enzyme. The amplitude of the lag process was 11 μM and its rate 0.1 s^{-1}.

FIG. 3.16 Proton Uptake with Glyoxylic Acid

The reaction mixture contained enzyme (18 μM), phenol red (15 μM), $NaNO_3$ (0.1 M), Na_2SO_4 (0.1 M) and 20 mM glyoxylic acid not premixed with the enzyme. The rate of the uptake was 0.2 s^{-1} and the amplitude 21 μM. The rate of the release was 0.058 s^{-1}.

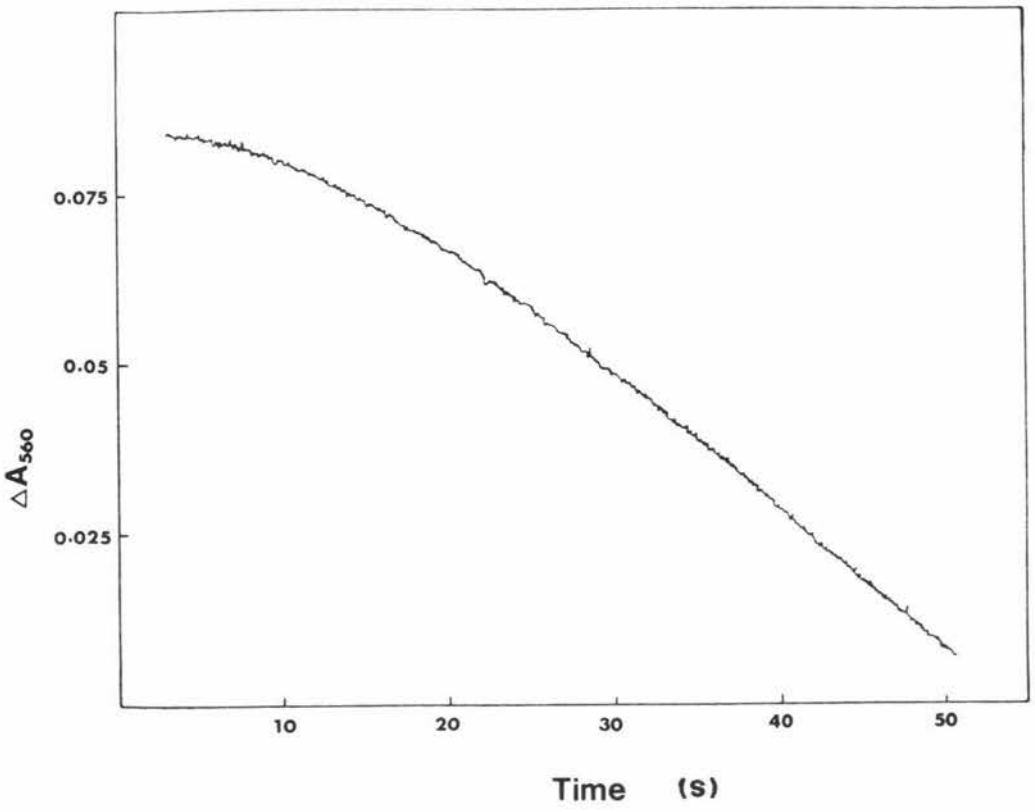
0.075
0.05
0.025
ΔA560
10
20
30
40
50
Time (s)

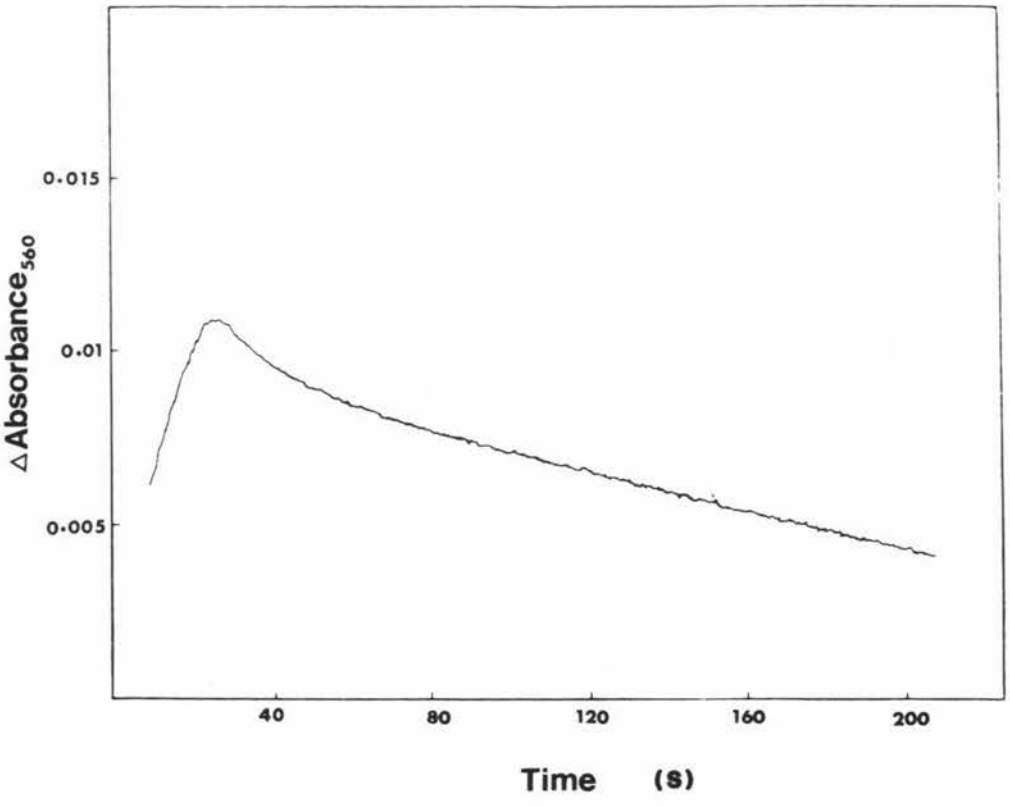
0.015
0.01
0.005
ΔAbsorbance560
40
80
120
160
200
Time (s)

3.3.4 Discussion

The observation of a transient release (or burst) of protons during the pre-steady-state phase of the oxidation of aldehydes by cytoplasmic sheep liver aldehyde dehydrogenase indicates that protons are released before the rate-determining step in the steady-state reaction. The fact that the observed rate constant for the proton burst is identical within experimental error to the rate constant observed for the burst in NADH production of 11 s^{-1} (MacGibbon et al., 1977c) means that the proton release is either associated with hydride transfer and NADH production, or is controlled by the same step that controls hydride transfer and NADH production.

Proton release resulting from the binding of NAD^+ to horse liver alcohol dehydrogenase has been observed by Shore et al., (1974), however this is not the case for aldehyde dehydrogenase since no proton release was observed when NAD^+ was mixed with enzyme in the stopped-flow apparatus.

The results of the burst experiments with 4-nitrobenzaldehyde show that proton release precedes the hydride transfer step. When the rate of production of NADH is monitored no burst is observed but a steady-state turnover number of 0.013 s^{-1} is obtained. When the experiment is repeated with 5 mM $MgCl_2$ added, a substance which slows the steady-state rate of the reaction but does not affect the rate of the NADH burst (Section 4.3), a burst in NADH production is seen with a rate constant of 0.021 s^{-1}. This indicates that the steady-state rate with 4-nitrobenzaldehyde as a substrate is largely controlled by the hydride transfer step as previously suggested by MacGibbon et al., (1977c). However, when the pre-steady-state production of protons with 4-nitrobenzaldehyde is monitored, a burst is still seen with a rate constant of 3 s^{-1} which is similar to the rate of 2.7 s^{-1} observed for benzaldehyde. Thus it is apparent that the proton is released before the hydride transfer step since if proton release occurred, with, or after, hydride transfer the rate for the proton release would

be expected to be 0.021 s^{-1}.

For all of the other aldehydes studied proton release is strongly coupled with hydride transfer as shown by the close similarity in the experimentally observed behaviour of the proton burst at various concentrations of acetaldehyde, propionaldehyde and NAD^+, to that of the NADH burst (MacGibbon et al., 1977c) under the same conditions. The change in the steady-state rate-limiting step for 4-nitrobenzaldehyde presumably results because of the strong electron withdrawing effect of the 4-nitro substituent which would be expected to destabilise any carbocation intermediates formed. The deuterium isotope experiments also lend support to the argument that, for most aldehydes, proton release and hydride transfer are controlled by the same step. Since proton release precedes hydride transfer, the kinetic isotope effect observed for the proton burst cannot result from the slowing of the hydride transfer step expected with deuterated aldehydes, but must result from some effect on either the actual proton release step or the step controlling both the proton and NADH bursts.

The observation of a linear relationship between the reciprocals of the observed proton burst rate constant and propionaldehyde concentration, with a slope of 3×10^{-6} Ms similar to that obtained for the NADH burst data of 4×10^{-6} Ms (MacGibbon et al., 1977c) indicates that the proton burst can legitimately be included in the composite step labelled k_{+3} in scheme 3.1. Since proton release occurs before NADH formation, the proton released cannot originate from the hydrolysis of any supposed NADH.acyl.enzyme intermediate resulting from the nucleophilic attack of water on the intermediate, or from the dissociation of the carboxylic acid formed as a reaction product, since both of these events take place after hydride transfer. The proton therefore, is probably released through the ionisation of some function group such as a sulfhydryl or protonated histidine at, or close to, the enzyme active site. The ionisation of an enzyme functional group could result from the covalent attachment of the aldehyde after binding or from the

perturbation of the pKa of the function group to some value below the pH of the solution. Since chemical steps are seldom rate limiting in enzyme reactions (Laidler, 1973) it seems probable that an ionisation step dependant on some prior rate-determining step is the cause of the proton release.

The rate-limiting step in the pre-steady-state has not previously been identified, but occurs after aldehyde binding (since as the second order rate constant for propionaldehyde binding is of the order of 10^6 Ms^{-1} the rate of aldehyde binding at saturating propionaldehyde concentrations is of the order of 10^3 s^{-1}) and as the 4-nitrobenzaldehyde data shows, before hydride transfer. The two most probable explanations for the rate-limiting step are:

(1) the covalent attachment of aldehyde to the enzyme after binding to form a tetrahedral intermediate.

(2) a conformational change resulting from aldehyde binding.

The first explanation appears unlikely, as a rate-limiting step involving covalent attachment of the aldehyde would be expected to show greater rates for aldehydes with electron withdrawing substituents. The Hammett rho value (ρ) for a nucleophilic attack on a carbonyl centre is usually about 2, and from the published $\sigma^*$and σ_I values for the CH_3^-, $CH_3CH_2^-$, $C_6H_5^-$ and $NO_2C_6H_5^-$ substituents (Kosower, 1968), the order of the rate constants for the proton burst should be acetaldehyde $\approx$ propionaldehyde $<$ benzaldehyde $<<$ 4-nitrobenzaldehyde. Experimentally however, this order is not observed since the rate constant for 4-nitrobenzaldehyde is about 7X slower than for acetaldehyde, and the rate constant for propionaldehyde less than half that for acetaldehyde.

The second explanation, that a conformational change is rate-limiting in the pre-steady-state, is more probable. MacGibbon *et al.*, (1977b) have reported evidence

for a conformational change in sheep liver aldehyde dehydrogenase which controls NADH dissociation. These workers observed a biphasic displacement of NADH by NAD^+ from the enzyme.NADH binary complex with rates of 0.85 s^{-1} and 0.20 s^{-1}, the rate of the slower process being identical with the turnover number (k_{cat}) for the enzyme at saturating propionaldehyde concentrations. They interpreted this data as arising from a situation where NADH binds to two forms of the enzyme, one where NADH dissociation occurs with a rate of 0.85 s^{-1} and another form from which NADH dissociation cannot occur until a conformational change with rate of 0.20 s^{-1} takes place. Further evidence to support this conclusion comes from NADH association experiments, where, as required by the two step dissociation model NADH binding is biphasic. The postulated conformational change on dissociation of NADH, results in the enzyme returning to the form to which NAD^+ and aldehyde bind, thus at some stage in the earlier part of the reaction mechanism another conformational change must have occurred. Such a conformational change is proposed here to explain the pre-steady-state proton release data obtained with 4-nitrobenzaldehyde and other aldehydes, and is presumably triggered by aldehyde binding and thus will show some dependance on aldehyde structure. Such a structure dependance would explain the variation in the dependance of the maximum burst rate with different aldehydes, as for example the bulkier aromatic aldehydes resulting in a slower conformational change.

Conformational changes have been observed for a number of dehydrogenases. Wonacott and Biesecker (1977) have shown by crystallographic studies that a conformational change is induced in glyceraldehyde-3-phosphate dehydrogenase from Bacillus stearothermophilus by NAD^+ binding and Eklund *et al.*, (1974) have shown that a conformational change occurs after NAD^+ binds to horse liver alcohol dehydrogeanse. Lactate dehydrogenase from dog fish also exhibits a conformational change after both NAD^+ and lactate have bound (Parker and Holbrook, 1977). Branden *et al.*, (1980) have

suggested that conformational changes in dehydrogenases arise because of a requirement for a non-polar environment around the active site in order to facilitate hydride transfer from the substrate to the carbon 4 of NAD^+, thus reducing the opportunity for water molecules to intercept the highly reactive hydride ions.

In order to determine the likely position of the conformational change and proton release steps in the reaction mechanism computer simulations were carried out. The first simulation was of the mechanism shown in scheme 3.3. In this model the binding of NAD^+ results in a

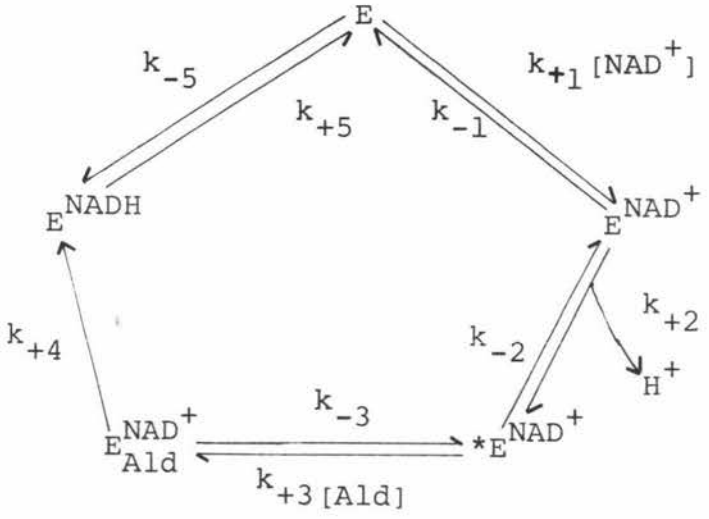

(Scheme 3.3)

conformational change and subsequent proton release. It is necessary to assume that the equilibrium for the conformational change lies well to the left ($k_{-2} >> k_{+2}$) in order that, as was observed experimentally, proton release should not occur when NAD^+ is mixed with enzyme alone in the stopped-flow apparatus. The values of k_{+1}, k_{-1}, k_{+3}, k_{-3}, k_{+5} and k_{-5} were 2 x 10^5 l $mol^{-1}s^{-1}$, 1.6 s^{-1}, 10^6 l $mol^{-1}s^{-1}$, 50 s^{-1}, 0.25 s^{-1} and 5 x 10^5 l $mol^{-1}s^{-1}$ respectively as reported by MacGibbon et al., (1977c). It was assumed that k_{+2} had a value of 11 s^{-1} and a value of 50 s^{-1} was assigned to k_{+4}. This value was arrived at by comparing the rate of hydride transfer for 4-nitrobenzaldehyde (0.02 s^{-1}) with that expected for propionaldehyde by using Taft σ^* values. With k_{+4} equal to 50 s^{-1}, ρ is about 4, but any increase in

k_{+4} above this value requires a ρ value greater than 4 which is highly improbable. However if k_{+4} was much less than 50 s^{-1}, the substitution of propionaldehyde by [1-^{2}H] propionaldehyde would result in k_4 being reduced to 10 s^{-1} or less (assuming an isotope effect of about 5), and at such values for k_{+4} the simulations showed pronounced lag phases at saturating propionaldehyde concentrations. k_{-2} was estimated by trial and error.

The results of the simulation showed that with k_{-2} greater than about 500 s^{-1} simulations of scheme 3.3 produced both proton and NADH bursts with amplitudes equal to 95% of the enzyme concentration and rates of 9.8 s^{-1} at 280 μM propionaldehyde which is in good agreement with the experimentally determined values. However, it was found that the rate constant for the simulated proton burst was independant of propionaldehyde concentration. Clearly this model cannot be correct since experimentally the proton burst rate constant was observed to have a linear double reciprocal relationship with propionaldehyde concentration. Thus the simulations exclude models in which the rate limiting step precedes aldehyde binding.

The second model simulated was one in which both proton release and the rate-limiting step occur after aldehyde binding, but proton release precedes the slow step (scheme 3.4). In this model k_{-3} is assumed much greater than k_{+3} so that proton release is controlled by the steps following the

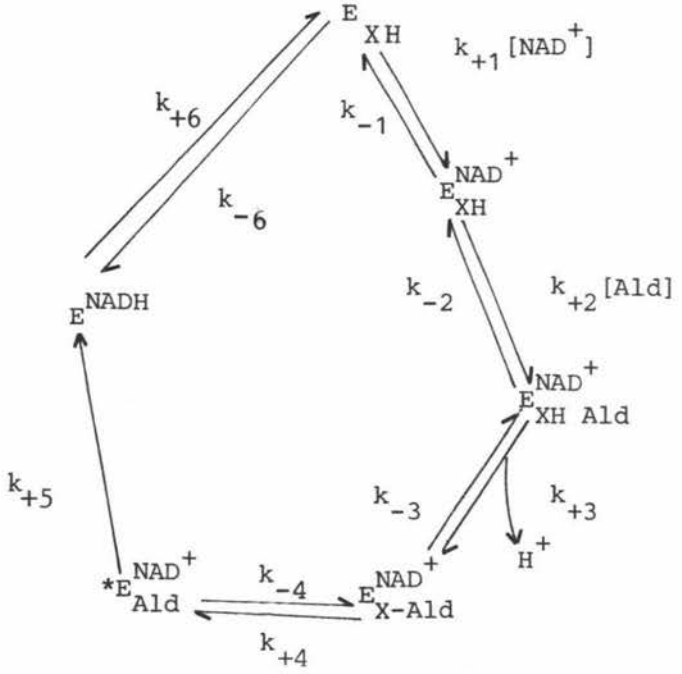

(Scheme 3.4)

release. The simulations showed that for this model, unless k_{-3} was much greater than k_{+3} a large hidden proton burst would be expected, and it was also observed that simulations using values of k_{-3} which reduced the size of the hidden burst, resulted in proton bursts of markedly reduced rate and amplitude compared with those observed experimentally. If k_{+3} was reduced to 11 s^{-1} and k_{-3} reduced to a similar value, a proton burst equal in amplitude and rate to the experimental values was observed but in this case a pronounced lag phase was observed for the NADH burst. The results of simulations of scheme 3.4 clearly show that the proton release does not occur before the rate-limiting pre-steady-state step.

Scheme 3.5 shows a model in which proton release follows a slow pre-steady-state step (such as a conformational change), although for simplicity the proton release is shown in the same step as the conformation change. Simulations of this model using the same parameters as in scheme 3.3. resulted in proton and NADH bursts equal to the experimental

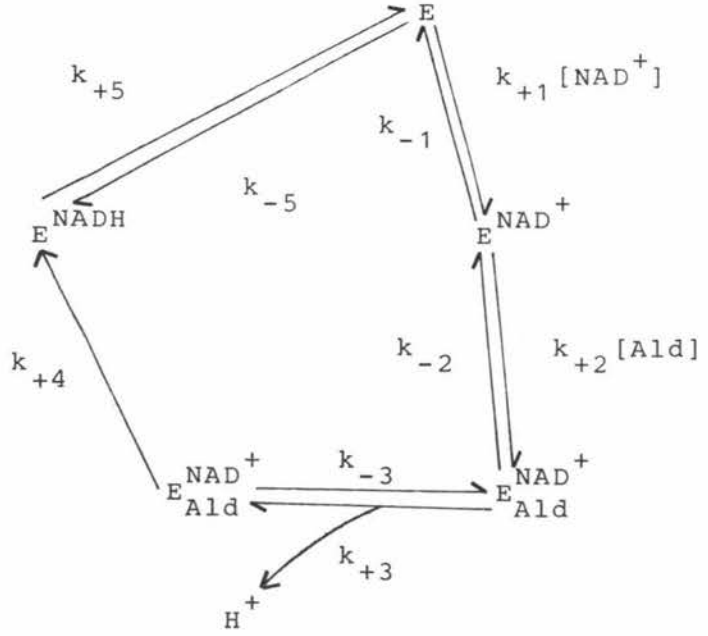

(Scheme 3.5)

values as long as k_{-3} was less than or equal to k_{+4}. While no upper limit could be placed on k_{+4} from the simulations it is unlikely to exceed 50 s^{-1} as this would result in an absurdly high ρ value for the hydride transfer step. However the simulations did show that k_{+4} could not be less than 15 s^{-1} without introducing a lag phase into the NADH burst, and as a lag phase was not observed experimentally with deuterated aldehydes at saturating concentrations, k_{+4} is not likely to be much less than 50 s^{-1}. From the simulations it was observed that k_{-3} could not be greater than k_{+4} without a resultant reduction in the NADH burst rate and amplitude, and while no lower limit could be placed on k_{-3} from simulations it is unlikely to be less than the turnover number for the reaction where the enzyme catalyses the reduction of anhydride to aldehyde of 0.1 s^{-1} (Hart and Dickinson, 1978). Both the proton and NADH bursts simulated using scheme 3.5 were found to vary with aldehyde concentration. A double reciprocal plot of k_{obs} versus propionaldehyde concentration resulted in a straight line with a slope of 5×10^{-6} Ms, in good agreement with the values of 3×10^{-6} Ms and 4×10^{-6} Ms for the proton and NADH bursts found experimentally.

Proton release can result from a conformational change, such as in scheme 3.5, if the conformational change results in the perturbation of the pKa of some acidic or protonated functional group to a value below that of the solution. In this case, since the proton burst amplitude at both pH 7.6 and pH 6.0 was equal to the enzyme active site concentration, the pKa value for the functional group must be at least 8.6 and perturbed to a value of about 5.0, otherwise amplitudes less than the formal enzyme concentration would be observed.

A burst in proton production was not observed at pH 9.0, presumably since the functional group is virtually completely ionised at this pH before the reaction is initiated by the mixing of enzyme and substrates, in which case the perturbation of the functional group would result in only a small proton release. The detection of a small proton burst

(10-20%) would be difficult, especially as the molar extinction coefficient for thymol blue is only about half that of phenol red. The pKa value of about 8.5 required to explain the proton release is in the region usually expected for thiol groups, which is consistent with the data reported for disulfiram (Kitson, 1975, 1978), 2-nitrobenzoate and iodoacetamide (Hart and Dickinson, 1977). These compounds are thiol modifiers which, when added to most aldehyde dehydrogenases, cause a loss of activity indicating the existence of a thiol group at, or near, the active site.

The absence of any transient proton release when an enzyme-NAD^+ mixture was pushed against a number of steady-state inhibitors such as acetone and chloral hydrate indicates that the inhibitors may be binding at a different site to the substrate, or as for chloral hydrate (a competitive inhibitor with respect to propionaldehyde) may bind at the substrate binding site, but due to differences in structure and electronic properties don't induce the same, if any, conformational change.

Glyoxylic acid, which contains an aldehyde functional group but does not function as a substrate and acts instead as an inhibitor of the steady-state reaction, has been observed to induce hysteretic effects in the steady-state kinetics of aldehyde dehydrogenase (L. Deady, personal communication). If glyoxylic acid is premixed with enzyme and NAD^+ then the reaction, initiated by the addition of propionaldehyde, shows a lag phase before a constant steady-state velocity is obtained. Also if glyoxylic acid is added to a cell containing enzyme, NAD^+ and propionaldehyde, the reaction velocity decreases until after about 10 minutes a constant inhibited rate of reaction is reached. The uptake of protons observed when glyoxylic acid is pushed against enzyme and NAD^+ in the stopped-flow apparatus may be caused by the same event which causes the lag phase in the steady-state. Steady-state inhibition studies with glyoxylic acid (L.F. Blackwell, personal communication) have shown that at low propionaldehyde concentrations (2-100 μM),

glyoxylic acid exhibits mixed or partial inhibition. This indicates that glyoxylic acid may be binding at a different site to propionaldehyde at low concentrations. Glyoxylic acid bound to this site appears to either, prevent the conformational change and thus the proton release, or prevent the proton release which follows the conformational change, since a lag phase equal to 60% of the enzyme active site concentration was observed rather than a proton burst when enzyme and NAD^+ were pushed against propionaldehyde in the stopped-flow apparatus.

Disulfiram, a potent inhibitor of the steady-state reaction (Kitson, 1975, 1978) has been shown to modify the NADH burst (L.F. Blackwell, personal communication), an enzyme to disulfiram ratio of 1:1 resulting in a reduction of the burst amplitude to 22% of the enzyme active site concentration. A similar result was obtained in this study, where an enzyme to disulfiram ratio of 1:1.3 caused a reduction in the proton burst amplitude to 18% of the active site concentration but no change in the burst rate constant. The similarity of the two burst processes in the presence of disulfiram again shows that for propionaldehyde the proton release and hydride transfer steps are closely coupled. The reduction in amplitude of the burst processes can be explained if disulfiram is partially modifying an active site sulfhydryl group (Kitson, 1978). An alternative explanation involves the formation of a disulphide bridge subsequent to modification of a thiol group by disulfiram. The modified thiol group may then undergo a disulphide exchange reaction which locks the enzyme into an unfavourable conformation (Scheme 3.6). The first explanation would mean that only

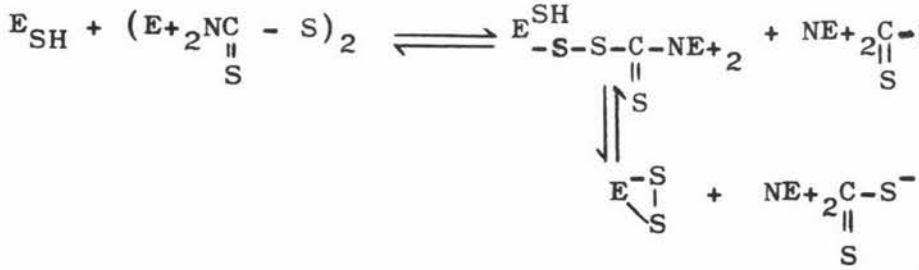

(Scheme 3.6)

a small percentage of the enzyme active sites would be available to bind aldehyde, whereas the second would require that only a small percentage of the bound aldehyde could trigger the conformational change. In either case the NADH burst would be reduced to the same amplitude as the proton burst since hydride transfer could only take place from a conformationally changed $E^{NAD^+}_{Ald}$ ternary complex. The residual activity is more difficult to explain since even in the presence of a large excess of disulfiram the residual activity is only reduced to 2% (Dickinson et al, 1981) furthermore Agnew et al., (1981) have shown that the residual activity is not caused by the relatively disulfiram insensitive mitochondrial enzyme as was suggested by Dickinson and Berrieman (1979). However while the experimental results show that disulfiram modifies or alters a thiol group on the enzyme, and that the proton may be released from a thiol group, the possibility cannot be ruled out that the proton is released from a different group to that modified by disulfiram.

Most aldehyde dehydrogenases studied to date exhibit esterase activity as well as the ability to oxidase aldehydes. Feldman and Weiner (1972b) first showed this for the F_2 horse liver enzyme which catalysed the hydrolysis of 4-nitrophenol esters, and that the addition of both NAD^+ and NADH activated the esterase reaction. Subsequently the same results were obtained for the F_2 horse liver enzyme (Eckfeldt and Yonetani, 1976), the human liver enzyme (Sidhu and Blair, 1975) and the rabbit liver enzyme (Duncan, 1977). It has been proposed that ester hydrolysis catalysed by aldehyde dehydrogenases takes place by a mechanism which involves the formation of an acyl-enzyme intermediate followed by hydrolysis to give products (Weiner et al, 1976). In the presence of NADH these steps would be expected to be identical to those for the dehydrogenase reaction following the hydride transfer step (Jakoby, 1963).

Both reactions have been assumed to take place at the same site on the enzyme (Feldman and Weiner, 1972b; Sidhu and Blair, 1975; Hart and Dickinson, 1978). If this is in fact the case, a burst in proton production similar to

that observed for the dehydrogenase reaction might be expected. That a burst was not in fact observed can be explained in a number of possible ways. Firstly, the ester may bind at a different site to propionaldehyde, and secondly the ester may bind at the same site as propionaldehyde but not induce the conformational change thought to be responsible for proton release. There is some evidence that the former suggestion may be correct, as it has been observed (L.F. Blackwell, personal communication) that 4-nitrophenyl-acetate gives mixed inhibition with respect to propionaldehyde at low concentrations (2-100 μM) of the aldehyde in the presence of NAD^+, but competitive inhibition with respect to propionaldehyde at high concentrations in the absence of NAD^+. This data is consistent with a 2 site or 2 enzyme model as suggested by MacGibbon et al., (1977a), with a site for which aldehydes have a high affinity but esters do not bind to, and a second site for which aldehydes have a low affinity and esters can bind to. If proton release only results from the binding of aldehydes to the high affinity site, then a proton burst would not be expected for the esterase reaction.

The second alternative, that the ester binds to the same site as the aldehyde is a possibility, although in this case the inhibition pattern of the esterase would be expected to be competitive rather than mixed, as observed experimentally. Even if the ester did bind at the aldehyde site it may not induce the same (if any) conformational change as aldehydes, presumably due (as was proposed for aldehyde analogues like chloral hydrate and glyoxylic acid) to its different physical and electronic structure. Indeed the requirement for the recognition of an aldehyde carbonyl group before a conformational change takes place resulting the subsequent covalent attachment and oxidation of the aldehyde, can explain the specificity of aldehyde dehydrogenases for aldehydes only, and its lack of marked inhibition by compounds such as ketones which closely resemble aldehydes.

3.3.5 Conclusion

Scheme 3.5 shows the most probable mechanism for the oxidation of aldehydes by aldehyde dehydrogenase. Computer simulations of this scheme showed that the model could reproduce the experimental data with good accuracy. The rate-limiting step in the pre-steady-state is labelled as k_{+3} while it has not been possible to unambiguously identify this step, it appears that it is a conformational change induced by aldehyde binding. However regardless of the nature of the rate-limiting step, the proton released during the burst must originate from the enzyme itself, since the proton burst precedes hydride transfer.

While scheme 3.5 is a good approximation to the actual experimental mechanism it is an oversimplification. The step involving hydride transfer (k_4) is a composite step rather than the single irreversible step shown in scheme 3.5, and in reality this step should include a reversible hydride transfer step, as Hart and Dickinson (1978b) have shown that under certain conditions the reaction is reversible. A slow hydrolysis of the acyl. enzyme intermediate by water is also indicated by the lack of a second transient proton release or by a proton burst with an amplitude equal to twice that of the NADH burst. Also the NADH dissociation step shown as k_5 has been shown to be a two step dissociation by MacGibbon *et al.*, (1977b) with a conformational change preceding NADH dissociations. Further work however, will be needed to verify or disprove the existence of any further steps in the reaction mechanism inducing any further conformational changes.

SECTION 4

THE EFFECTS OF $MgCl_2$ ON THE STEADY-STATE AND EQUILIBRIUM BEHAVIOUR OF CYTOPLASMIC ALDEHYDE DEHYDROGENASE

4.1 INTRODUCTION

Metallo-enzymes are enzymes which contain one or more metal atoms whose presence is required for catalytic activity or structural integrity. An example of such an enzyme is horse liver alcohol dehydrogenase which contains zinc atoms which are essential for its catalytic activity. Although aldehyde dehydrogenases are not metallo-enzymes, a number have exhibited a marked sensitivity to the presence of some metal ions. Stoppani *et al.* (1959) found that a wide range of metal ions inhibited yeast aldehyde dehydrogenase by competing with the essential activating alkali ion (which may be K^+, Na^+, Cs^+ or Rb^+). Venteicher *et al.* (1977) have studied the effects of a variety of divalent and trivalent metal ions on the F_1 and F_2 isoenzymes of aldehyde dehydrogenase from horse liver. They observed that most of the metal ions produced an initial activation of the enzyme at low concentrations (0.1 to 10 μM) while at higher concentrations (> 20 μM) the enzyme activity was inhibited. They also observed that the esterase activity of the aldehyde dehydrogenase isoenzymes was unaffected by any of the metal ions, with the exception of Zn^{2+} which inhibited the reaction velocity.

The F_1 isoenzyme, which is thought to be of cytoplasmic origin (Eckfeldt *et al.*, 1976) was found to be considerably more sensitive to the presence of metal ions than was the F_2 isoenzyme which is thought to be of mitochondrial origin. Venteicher *et al.* were unable to explain the mechanism of activation by metal ions, but because the dissociation constant of NADH was observed to decrease at inhibitory levels of metal ions, they did suggest that the

mechanism of inhibition may be a slowing of the rate-determining NADH dissociation step caused by tighter binding of the coenzyme.

Takahashi and Weiner (1980) and Takahashi *et al.* (1980) have made extensive studies of the mitochondrial horse liver aldehyde dehydrogenase in the presence of $MgCl_2$ (0.1 to 1.0 mM). They observed that this metal ion caused a two-fold activation of the reaction velocity in this concentration region, with similar behaviour being observed in the presence of the same concentrations of $MnCl_2$ and $CaCl_2$. Takahashi and Weiner (1980) were able to show by analytical ultracentrifugation experiments, that the observed two-fold activity was associated with a dissociation of enzyme subunits from tetramers to dimers. NAD^+ and NADH titration experiments also showed that the stoichiometry of coenzyme binding changed from two molecules of coenzyme per tetramer in the absence of $MgCl_2$ to four per tetramer in the presence of 0.5 to 1.0 mM $MgCl_2$.

Cytoplasmic sheep liver aldehyde dehydrogenase has been shown to exhibit a marked sensitivity to a number of metal ions including Mg^{2+}, Mn^{2+} and Ca^{2+} (Section 3.2.3). These metal ions, especially Mg^{2+} and Ca^{2+}, are important physiological ions which occur in relatively high concentrations in mammalian tissue. All enzyme systems which utilize ATP show an absolute requirement for the Mg^{2+} ion, of which there is quite a large amount present in cells. Soman *et al.* (1970) have estimated that the Mg^{2+} content of human liver is 20 meq per kg of wet tissue. It is therefore of some interest to study the effect of Mg^{2+} on aldehyde dehydrogenase in order to obtain information that might be relevant to the behaviour of the enzyme *in vivo*.

4.1.1 Steady-State Kinetics

The existence of enzyme-substrate complexes has been known for some considerable time, and was first proposed in 1902 by Brown for invertase. Michaelis and Menten (1913)

developed a kinetic treatment based on Scheme 4.1 by making a number of assumptions about the enzyme-substrate (E.S) complex;

$$E \underset{k_{-1}}{\overset{k_{+1}\ S}{\rightleftharpoons}} E.S \xrightarrow{k_{+2}} E + P \qquad \text{(Scheme 4.1)}$$

(1) the concentration of the substrate S is large compared with the concentration of enzyme E, so that the formation of E.S does not significantly change the concentration of S.

(2) the concentration of product P is zero during the establishment of the steady-state

(3) the rate of release of product is slow compared to dissociation of S from the E.S complex, allowing E and E.S to be considered as being in equilibrium.

The general velocity equation based on this treatment for Scheme 4.1 is:

$$v = \frac{k_{+2}\ E\ [S]}{[S] + \frac{k_{-1}}{k_{+1}}} \qquad (4.1)$$

v = reaction velocity

E = total enzyme concentration

The Michaelis-Menten or equilibrium kinetics treatment has been generally superseded by the less restrictive steady-state approach of Briggs and Haldane (1925), but was used in this study for deriving equations to model the experimentally observed behaviour by computer simulation techniques.

The main difference between the assumptions of rapid equilibrium and steady-state kinetics is that in steady-state kinetics, the rate of formation of E.S is assumed to be equal to it's rate of breakdown by all available pathways, rather than E and S are in equilibrium as is the case for the rapid equilibrium model.

For Scheme 4.1 the rate of ES formation can be expressed as:

$$\frac{d\,[E.S]}{dt} = k_{+1}\,[E]\,[S]$$

and its rate of removal as:

$$-\frac{d\,[E.S]}{dt} = k_{-1}\,[ES] + k_{+2}\,[E.S]$$

at steady-state $\frac{d\,[E.S]}{dt} = 0$

and $k_{+1}\,[E]\,[S] = k_{-1}\,[E.S] + k_{+2}\,[E.S]$

rearranging $[E.S] = k_{+1}\,\frac{[E]\,[S]}{(k_{+2} + k_{-1})}$ (4.2)

The maximum reaction velocity $V_{max} = k_{+2}\,[E]_t$ (4.3)

where $[E]_t$ equals the sum of all the enzyme species,

$$[E]_t = [E] + [E.S] \quad (4.4)$$

and the actual reaction $v = k_{+2}\,[E.S]$ (4.5)

dividing equation 4.5 by $[E]_t$

$$\frac{v}{[E]_t} = \frac{k_{+2}\,[E.S]}{[E] + [E.S]}$$

and substituting for [E.S] from equation 4.2

$$\frac{v}{[E]_t} = \frac{k_{+2}\,k_{+1}\,\frac{[E]\,[S]}{(k_{-1} + k_{+2})}}{[E] + \frac{k_{+1}\,[E]\,[S]}{(k_{-1} + k_{+2})}}$$

dividing by k_{+2} and substituting for $k_{+2}\,[E]_t$ from equation 4.3

$$\frac{v}{V} = \frac{\dfrac{k_{+1}\,[S]}{(k_{-1} + k_{+2})}}{1 + \dfrac{k_{+1}\,[S]}{k_{-1} + k_{+2}}} \qquad (4.6)$$

If $\left(\dfrac{k_{-1} + k_{+2}}{k_{+1}}\right)$ is replaced by Km, the Michaelis constant, then

4.6 reduces to $$\frac{v}{V_{max}} = \frac{[S]}{K_m + [S]} \qquad (4.7)$$

A plot of v versus [S] results in a rectangular hyperbola with assymptotes of $v = V_{max}$ and [S] = Km, enabling estimates of V_{max} and Km to be obtained, however it is more convenient to rearrange equation 4.7 in the form of Lineweaver and Burk

$$\frac{1}{v} = \frac{1}{V_{max}} + \frac{Km}{V_{max}} \cdot \frac{1}{[S]}$$

A plot of $\frac{1}{v}$ versus $\frac{1}{[S]}$ results in a straight line with slope $\frac{Km}{V_{max}}$ and an intercept of $\frac{1}{V_{max}}$ on the ordinate axis.

4.1.2 Two Substrate Reactions

One substrate enzyme reactions are somewhat infrequent in nature with most reactions involving two or more substrates. The general rate equation for most two substrate reactions can be expressed by equation 4.8, where A and B are the reaction substrates and K_{ia}, K_a and K_b are constants

$$v = \frac{V_{max}\,[A]\,[B]}{K_{ia}\,K_b + K_a[B] + K_b[A] + [A]\,[B]} \qquad (4.8)$$

(Cleland, 1963a). In general mechanisms involving two or more substrates are classed in two categories, sequential or ping pong. Sequential mechanisms are those in which all substrates must be bound before any product is released and can be subdivided into two classes, ordered, where the second substrate can only bind after the first has bound (Fig. 4.1.a) and random, where the substrates may bind in any order (Fig. 4.1.b). Ping Pong mechanisms are those in which a product or products may be released before all the substrates have bound (Fig. 4.2).

Initial velocity studies can determine whether a sequential or ping pong mechanism is operating in any particular case, as a Lineweaver-Burk plot with one substrate at a fixed concentration and the other varied, results, in straight lines which intersect to the left of the ordinate axis for sequential mechanisms and parallel lines for ping pong mechanisms. If for the sequential mechanism, data obtained from initial velocity measurements with the concentration of B fixed and the concentration of A varied is plotted as the reciprocals of initial velocity versus the concentration of A (as shown in Fig. 4.3), the intercepts and slopes of the intersecting lines can be plotted against the inverse of the concentration of B to obtain V_{max}, K_{ia}, K_a and K_b in equation 4.8. It is not possible to determine whether a sequential mechanism is random or ordered from Lineweaver-Burk plots alone, however product inhibition studies (Cleland, 1963b) can give information about the order of substrate addition.

4.1.3 Inhibition in Steady-State Kinetics

Reversible inhibition in an enzyme-catalysed reaction occurs when a substance, which is added to the enzyme assay mixture, results in a lowering of the initial reaction velocity. An inhibitor may be a reaction product which, for a reversible reaction, shifts the equilibrium in favour of the reverse reaction, and for an irreversible

Fig. 4.1 Sequential Bi-Substrate Mechanisms

4.1.a Ordered Bi Bi

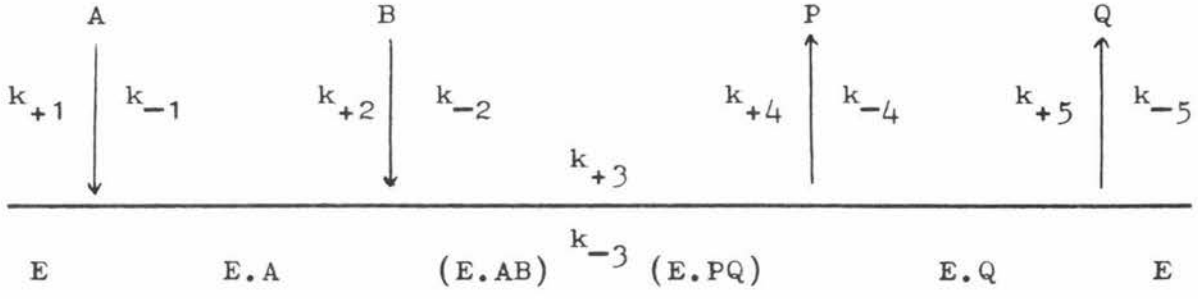

4.1b Random Bi Bi

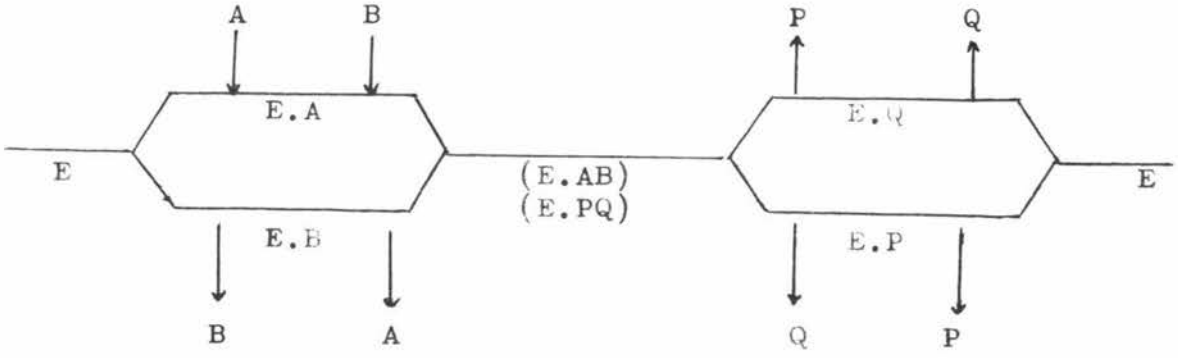

Fig. 4.2 Ping Pong Bi-Substrate Mechanism

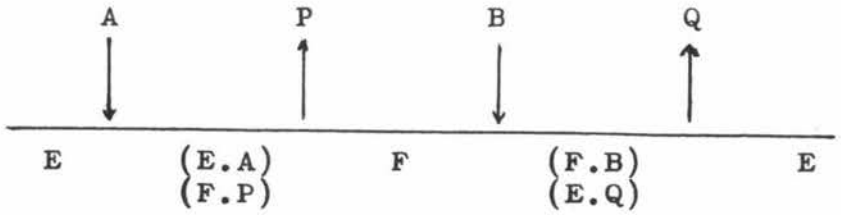

FIG. 4.3 DOUBLE RECIPROCAL PLOTS FOR A TWO SUBSTRATE REACTION

(a) PRIMARY PLOT

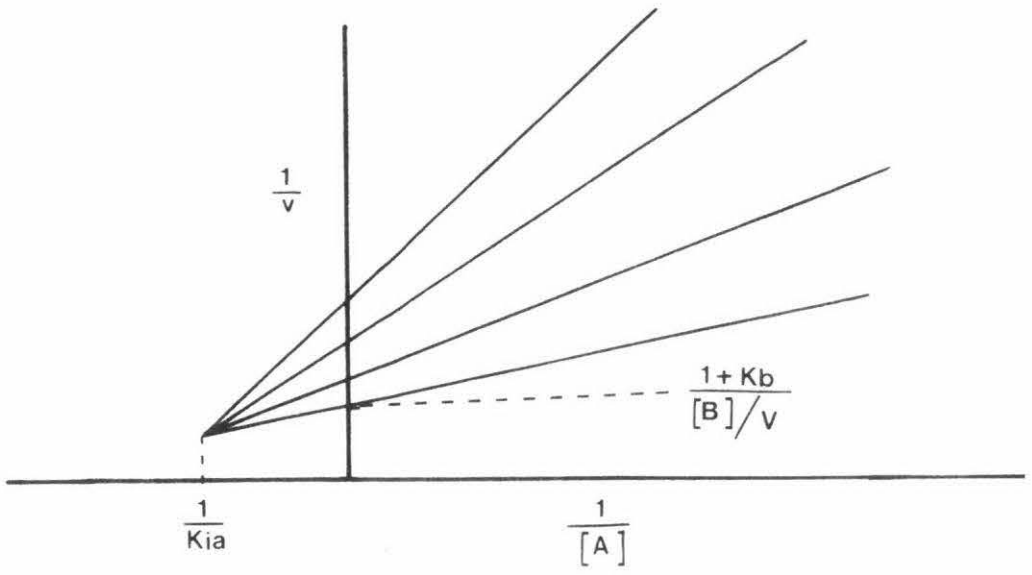

(b) SECONDARY REPLOTS

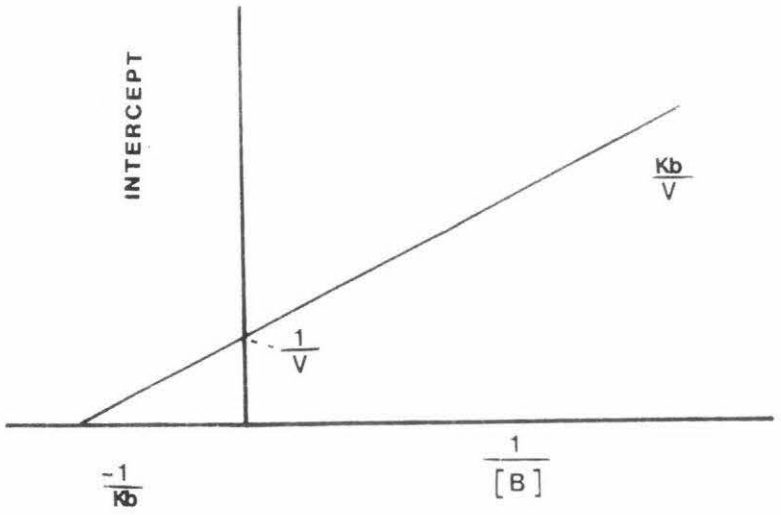

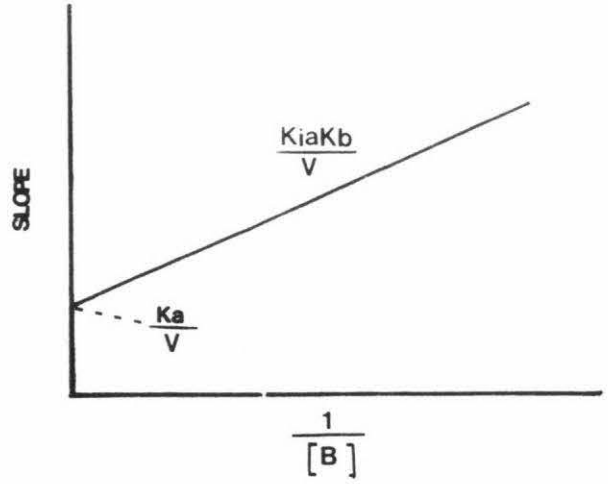

reaction may result in the formation of an unreactive or dead-end enzyme complex. Other substrates which often act as inhibitors are substrate analogues, which bind to the enzyme like substrates, but do not react to form products. However a large number of compounds with widely differing structures and properties, which are neither reaction products nor substrate analogues, are able to inhibit enzyme reactions. The mechanism of inhibition in these cases usually involves binding of the inhibitor to either the enzyme or one of the enzyme-substrate complexes.

Inhibition is usually classed as one of three types, competitive, noncompetitive or uncompetitive, depending on how the inhibitor affects the slopes and intercepts of a Lineweaver-Burk plot.

(1) Competitive inhibition

Competitive inhibition arises when the inhibitor combines with the same enzyme form as the substrate with which it is competitive, and prevents that substrate from binding. Increasing the concentration of a competitive inhibitor lowers the reaction velocity, until at an infinite concentration the reaction velocity is zero. Similarly, increasing the concentration of the substrate will increase the reaction velocity until V_{max} is reached.

The general equation for competitive inhibition for a two substrate enzyme is:

$$\frac{1}{v} = \frac{Km}{V_{max}}\left(1 + \frac{[I]}{Ki}\right)\frac{1}{[S]} + \frac{1}{V_{max}}$$

Fig. 4.4 shows the effect of a competitive inhibitor on the $\frac{1}{v}$ versus $\frac{1}{[S]}$ plot.

It can be seen that only the slopes are affected, with the intercept on the ordinate axis remaining unchanged. Thus the overall effect of a competitive inhibitor is to increase the Km value for the substrate with which it is competitive, but leave V_{max} unchanged.

FIG. 4.4 EFFECT OF INHIBITION ON DOUBLE RECIPROCAL PLOTS

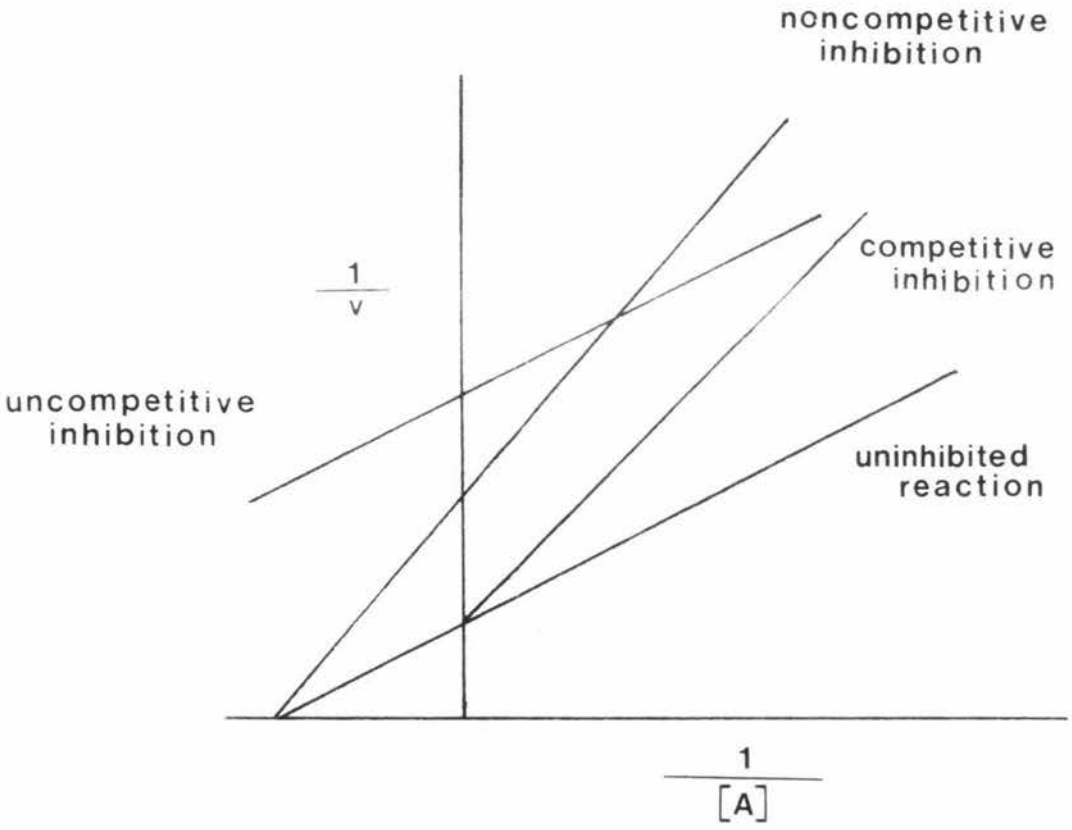

(2) Uncompetitive Inhibition

An uncompetitive inhibitor binds to the enzyme-substrate complex which contains the substrate with which the inhibitor is uncompetitive, yielding an inactive E.SI complex, but does not bind to the free enzyme. The V_{max} value is lowered, since some of the E.SI complex will always be present even at very high substrate concentrations. The effect of an uncompetitive inhibitor on the Lineweaver-Burk plot is to change the ordinate intercept, but not the slope as the inhibitor does not affect the substrate binding (Fig. 4.4). The general rate equation is:

$$\frac{1}{v} = \frac{Km}{V_{max}} \frac{1}{[S]} + \frac{1}{V_{max}} \left(1 + \frac{[I]}{K_i}\right)$$

Therefore strict uncompetitive inhibition results in a series of parallel lines. However in many cases lines which are apparently parallel, are in fact converging and result from noncompetitive rather than uncompetitive inhibition.

(3) Noncompetitive Inhibition

For simple noncompetitive inhibition the binding and dissociation of the substrate, with which the inhibitor is noncompetitive, is unaffected by the inhibitor and the substrate can bind to the E.I complex, and the inhibitor can bind to the E.S complex. The Km value is therefore unaltered but as the E.SI complex is catalytically inactive the reaction velocity is decreased and since on infinite concentration of the substrate cannot remove the effects of the inhibitor the V_{max} value is decreased. The general rate equation for noncompetitive inhibition is:

$$\frac{1}{v} = \frac{Km}{V_{max}} \left(1 + \frac{[I]}{K_i}\right) \frac{1}{[S]} + \frac{1}{V_{max}} \left(1 + \frac{[I]}{K_i}\right)$$

The effects of a noncompetitive inhibitor on the double reciprocal plot are shown in Fig. 4.4, where it can be seen that there is an effect on both the slope and intercept.

The three types of inhibition discussed above are all simple examples which yield straight lines when replots of data obtained from a Lineweaver-Burk plot are made ($\frac{1}{v}$ against [I] and slope against [I]). More complicated forms of inhibition patterns can arise where the replots are nonlinear, for example, partial competitive inhibition and some mixed inhibition systems. Nonlinear double reciprocal plots as well as nonlinear replots can also be obtained in some cases. The most common cause of this phenomenon is the presence of two enzymes or isoenzymes in an assay which both catalyse the same reaction, but show different sensitivities to the inhibitor. A similar situation arises if the enzyme being studied contains two substrate binding sites, and the substrate binding or subsequent catalytic activity of one site is affected to a different extent by the inhibitor than the second site (Segel, 1975).

4.2 METHODS

4.2.1 Spectrophotometric Assays at pH 7.6

Assays were carried out using the apparatus described in Section 3.2.1.1.

4.2.1.1 Assays for aldehyde dehydrogenase activity

The assay mixture was as described in Section 2.2.2. Grade III NAD^+ (Sigma) was used to prepare NAD^+ solutions and the propionaldehyde stock solution (240 mM) was prepared from propionaldehyde freshly distilled under nitrogen. Where assays were carried out in the presence of $MgCl_2$, volumes of 50 mM $MgCl_2$ were added in place of phosphate buffer to keep the final assay volume at 3.0 cm^3. The assay was initiated by the addition of the aldehyde and the reaction progress followed by monitoring the production of NADH of 340 nm.

4.2.1.2 Assays for esterase activity

The assay mixture consisted of:

0.1 cm^3 of 5 mM 4-nitrophenylacetate solution
0.1 cm^3 of enzyme solution
2.8 cm^3 of pH 7.6 35 mM phosphate buffer

The 5 mM 4-nitrophenylacetate stock solution was prepared in either acetone or acetonitrile as the ester is relatively insoluble in water. The final concentration of solvent was less than 3.3% v/v at which levels the inhibition of both acetone (MacGibbon et al, 1978a) and acetonitrile (R.L. Motion personal communication) is insignificant. The reaction was initiated by the addition of the ester and the reaction rate was followed by observing the appearance of the 4-nitrophenolate ion at 400 nm. Blank assays were also carried out (without enzyme) to determine the spontaneous rate of ester hydrolysis, this rate, which was found to be negligible at ester concentrations less than 50 μM, was then subtracted from the rate in the presence of enzyme.

4.2.2 Fluorimetric Assays

Where the concentration of enzyme, NAD^+ of aldehyde was very low, it was found convenient to use the more sensitive fluorimetric technique to follow the reaction progress. Assays were carried out using an Aminco SPF 500 fluorimeter thermostatted at 25°C, connected to a Tohshin Electron recorder. The excitation wavelength was 340 nm with a 5 nm bandpass and the emission wavelength was 460 nm with a 10 nm bandpass. A standard NADH solution of known concentration was used to relate fluorescence changes to NADH production. The assay mixture was as described in Section 2.2.2 and the reaction initiated by the addition of propionaldehyde.

4.2.3 NAD^+ Titrations

NAD^+ titrations were carried out using the apparatus described in Section 4.2.2. The excitation wavelength was 280 nm with a 5 nm bandpass and the emission wavelength 340 nm with a 10 nm bandpass. The excitation shutter was kept closed except when readings were being taken, to minimise the slow photolytic quenching of protein fluorescence that occurs when the enzyme is subject to radiation at 280 nm (P.D. Buckley, personal communication).

NAD^+ was added in 0.01 cm^3 aliquots using the apparatus described in Section 2.3.1.2, each aliquot adding approximately 0.5 μM NAD^+. A standard titration with NAD^+ and enzyme was always carried out first, followed by titrations with added $MgCl_2$.

4.2.4 NADH Titrations

NADH titrations were carried out as described in Section 2.3.1.2, control titrations being always carried out with enzyme and NADH only, followed by titrations with added $MgCl_2$.

4.2.5 UV Difference Spectra

The ultra violet difference spectrum between enzyme-bound and free NADH with and without $MgCl_2$ present was determined using a Shimadzu MPS-5000 spectrophotometer. Two quartz UV cells were mounted in tandem in both the sample and reference compartments. One cell in the reference compartment contained enzyme (40 μM) and the other NADH (26 μM), while in the sample compartment one cell contained enzyme and NADH and the other buffer only. After the difference spectrum had been determined with these solutions, $MgCl_2$ was added to all the cells and the difference spectrum redetermined.

The enzyme, NADH and $MgCl_2$ were added to the cells using a glass syringe attached to a micrometer which delivered 0.01 cm^3 aliquots. A blank was also run with all four cells containing buffer only, to determine the difference spectrum

between the two sets of cells. This difference was subsequently subtracted from the difference spectrum obtained with the various samples present.

4.2.6 Gel Chromatography

Gel filtration chromatography was carried out using a 70 cm x 2.5 cm Sephacryl S 300 column. The column was equilibrated with 0.022 M pH 7.3 phosphate buffer containing 0.1% v/v β-mercaptoethanol for 24 hours prior to use. 7 cm^3 samples were loaded onto the column, which was eluted at a rate of 9.0 cm^3 per hour with the equilibration buffer. Samples were collected using an LKB 7000 Ultrorac fraction collector with a drop counter attachment set at 70 drops per fraction.

An initial run was carried out with the enzyme only, then the column was washed with elution buffer (2 l) containing 5 mM $MgCl_2$ and an enzyme sample containing 5 mM $MgCl_2$ run through the column. A standard, yeast alcohol dehydrogenase, with a molecular weight of 150 000 was also run. The presence of aldehyde dehydrogenase was detected by assay, and the yeast alcohol dehydrogenase by absorbance measurements at 280 nm. Where $MgCl_2$ was present the aldehyde dehydrogenase assays were carried out in 33 mM pH 5.6 citrate buffer which removes the inhibitory effect of $MgCl_2$ (Section 4.4.8).

4.2.7 Gel Electrophoresis Experiments

Gel electrophoresis experiments were carried out using an Ortec 4200 electrophoresis system with an Ortec 4100 power pack. Tris-sulphate 8% acrylamide gels were prepared according to the Ortec 4200 instruction manual (Ortec Incorp., 1969). For the $MgCl_2$ run, the gel solutions and running buffers were prepared with 5 mM $MgCl_2$ and the samples also contained 5 mM $MgCl_2$. Catalase (bovine liver), alcolase (rabbit muscle) and yeast alcohol dehydrogenase were run as standards in conjunction with aldehyde dehydrogenase.

4.2.8 Laser Light Scattering Experiments

The laser used in the light scattering experiments was a Spectra Physics model 125A helium-neon laser with a power output of 55 mW at 623 nm. The laser was coupled to a Precision Devices 4300 spectrometer and an ITT FW130 photomultiplier tube, the voltage for which was supplied by an EMI PM25A power supply. The apparatus was mounted on a 2 tonne reinforced concrete table.

Signals from the photomultiplier tube was stored in a correlator which was interfaced to a pdp 11/03 computer (Digital Equipment Corporation) to facilitate analysis of the data. The data accumulating in the correlator was also displayed on an oscilloscope after digital-to-analogue conversion. The correlator used in this experiment incorporated a device known as a blinker which minimised the effects of light scattering by contaminent dust particles. A comprehensive description of the correlator's design and circuitry has been published by O'Driscoll and Pinder (1980), and a more detailed description of the entire light scattering apparatus has been reported by Trotter (1980).

Cells polished on four sides were sonicated in hot radioactive decontamination detergent (Decon 75) for 90 s with an MSE 100 W ultrasonicator, then washed 10 x with hot water, twice with acetone and ethanol then with filtered distilled deionized water. Analar cyclohexane (16 cm^3) was centrifuged at 11 000 $\underline{g}$ for 2 hours in stoppered glass tubes then used to rinse both the laser cells and a glass syringe. The rinsing was carried out in an atmosphere of air filtered through a 0.22 μm millipore filter. The enzyme and enzyme-$MgCl_2$ samples were centrifuged for two hours at 11 000 $\underline{g}$ in stoppered plastic centrifuge tubes, then transferred to the glass cells in the filtered atmosphere, using the cyclohexane rinsed syringe. The cells were immediately stoppered then kept under refrigeration until needed.

4.2.9 Computer Simulations

Computer simulations of the steady-state behaviour of the enzyme in the presence of $MgCl_2$ were carried out using a Cromemco Z2D minicomputer. Equations were derived for a number of possible mechanistic models assuming that rapid equilibrium conditions prevailed (Segel, 1975). The computer was programmed in Basic to calculate the reaction velocity at varying substrate concentrations using the derived equations and various steady-state parameters entered into the program.

4.3 TREATMENT OF DATA

4.3.1 Steady-State Assays

The initial velocity, which was linear for more than 10 minutes, and the concentration of the varied substrate were plotted as reciprocals for a range of inhibitor concentrations, to obtain the inhibition type. The $\frac{1}{V_{max}}$ values and the slopes of the double-reciprocal plots were plotted against the inhibitor concentration to obtain the inhibitor constants.

4.3.2 NADH Titrations

The titration data was treated as described in Section 3.2.2 to obtain the dissociation constant K_D, and the NADH binding site concentration. To enable a better comparison between the concentration of NADH binding sites to be made in the presence and absence of $MgCl_2$, the titration data was also plotted according to the method of Scatchard (1949). In this method a plot of

$$\frac{[NADH]_B}{[NADH]_F[E]_t} \quad \text{against} \quad \frac{[NADH]_B}{[E]_t} \qquad (4.9)$$

where $[NADH]_B$ is the concentration of bound NADH
$[NADH]_F$ is the concentration of free NADH
$[E]_t$ is the total enzyme concentration

(assuming equivalent binding sites) results in a line with a slope of $-\frac{1}{K_D}$ and an intercept on the abscissa axis equal to n, the number of NADH binding sites per tetramer. $[E]_t$ was calculated from absorbance measurements at 280 nm or from plots of equation 3.20 and $[NADH]_B$ calculated by multiplying $[E]_t$ by R, the fractional saturation of binding sites. $[NADH]_F$ was obtained by subtracting $[NADH]_B$ from the total NADH concentration. The enhancement of nucleotide fluorescence on NADH binding to the enzyme was also determined. MacGibbon (1976) has shown that the fluorescence of free NADH varies linearly with concentration (equation 4.10)

$$F_1 = [NADH]_F Q_1 \qquad (4.10)$$

where F_1 is the fluorescence of free NADH
Q_1 is the molar fluorescence of NADH
$[NADH]_F$ is the concentration of free NADH

With enzyme and NADH present, the fluorescence is due to both free and enzyme-bound NADH (equation 4.11)

$$F_2 = Q[NADH]_F + (Q_2-Q_1)\,[E.NADH] \qquad (4.11)$$

where F_2 is the fluorescence of free and bound NADH
Q_2 is the molar fluorescence of bound NADH
[E.NADH] is the concentration of bound NADH

Subtracting 4.10 from 4.11 gives

$$\Delta F_{max} = F_2-F_1 = (Q_2-Q_2)\,[E.NADH] \qquad (4.12)$$

where ΔF_{max} is equal to the maximum difference between the blank titration and a titration containing enzyme and NADH. This value was determined graphically from the titration data by plotting $1/\Delta F$ against $1/[NADH]$ from which ΔF_{max} was determined as the intercept on the ordinate axis. Q_1 was determined from the slope of the blank NADH titration, and the fluorescence enhancement factor Q was equal to Q_2/Q_1.

4.3.3 NAD^+ Titration Experiments

The concentration of NAD^+ binding sites was determined by plotting the quenching data as a Scatchard plot (equation 4.9). The enzyme concentration was determined either by NADH titration or by absorption measurements at 280 nm assuming that a solution with an absorption of 1.13 contained 1 mg cm^{-3} of protein (Dickinson *et al.*, 1981). The molecular weight was taken as 212 000 (MacGibbon *et al.*, 1979), and the fractional saturation R was equal to the fluorescence quenching at each NAD^+ concentration (q) divided by the maximum fluorescence quenching (q_{max}) obtained when all the binding sites are occupied. R was estimated by plotting $1/\Delta$fluorescence versus $1/NAD^+$ and extrapolating to zero on the abscissa axis. The fluorescence was corrected for the dilution caused by the addition of the NAD^+.

4.3.4 Gel Filtration Experiments

The elution volume for the gel filtration experiments was taken as the point at which the concentration of the enzyme had reached 50% of its maximum value. The volume of the fractions collected was calculated by weighing 20 tubes at random then averaging them, to obtain the average volume.

4.3.5 Laser Light Scattering Experiments

The quasi-elastic light scattering exhibited by macromolecules when subject to laser light, enables the calculation of a macromolecular diffusion coeficient D_o, which is the diffusion coefficient at infinite dilution. D_o is related to the radius of a macromolecule by the Stokes-Einstein law (equation 4.13).

$$D_o = \frac{K_B T}{(6 \pi \eta_o R_H)} \qquad (4.13)$$

where η_o is the solvent viscosity

R_H is the hydrodynamic radius of the solvated macromolecule

K_B is the Boltzman constant

T is the temperature

From equation 4.13 it can be seen that;

$$D_o \quad \alpha \quad \frac{1}{R_H} \tag{4.14}$$

Assuming that the macromolecule under study is a sphere, then its volume is given by:

$$V = \frac{4}{3}\pi r^3 \tag{4.15}$$

rearranging 4.15 $$r = (\frac{3}{4}.\frac{v}{\pi})^{\frac{1}{3}} \tag{4.16}$$

substituting $\frac{M}{\rho}$ for V in equation 4.

where M is the mass of the macromolecule

ρ is the density of the macromolecule

$$r = (\frac{3}{4\pi})^{\frac{1}{3}}(\frac{M}{\rho})^{\frac{1}{3}} \tag{4.17}$$

From equation 4.17 $r \alpha M^{\frac{1}{3}}$

and $$D_o \alpha \frac{1}{M^{\frac{1}{3}}} \tag{4.18}$$

Intensity fluctuations in the laser light, scattered by macromolecules in solutión, with time, can be characterised by the formation of a normalised intensity autocorrelation function or NIAF (Jakeman and Pike, 1969). NIAF's can be conveniently formed by photocount autocorrelation (Jakeman and Pike, 1969), and this experiment a computer programmed by N. Pinder and C. Trotter, carried out this procedure using data accumulated in the correlator via the photomultiplier tube. The output from the computer was ln (NIAF-1) for each angle at which the macromolecular light was observed, and a plot of:

$$\ln (NIAF-1) \text{ against } \frac{1}{2} (4 \pi n_o \sin(\theta/2)/ \lambda_o)^2$$

where θ is the scattering angle

λ_o is the wavelength of the incident radiation

n_o is the refractive index of the sample solution

yielded a straight line of slope D_o.

4.4 RESULTS

4.4.1 Effect of $MgCl_2$ on V_{max}

When $MgCl_2$ was added as a solid or in solution to an aldehyde dehydrogenase assay as described in Section 3.2.1.1 a substantial decrease in activity was observed. The inactivation occurred within the time taken to add the $MgCl_2$ to the assay and the recorder traces obtained after the $MgCl_2$ addition were linear for at least 10 minutes. The order of addition of $MgCl_2$ and substrates had no effect on the degree of inhibition produced, and plots of the percentage of initial velocity remaining versus $MgCl_2$ concentration at both high (>1 mM) and low (<100 µM) propionaldehyde concentrations resulted in hyperbolic inhibition curves with greater than 90% inhibition being obtained at $MgCl_2$ concentrations greater than 2 mM (Fig. 4.5).

4.4.2 Effect of $MgCl_2$ on Other Aldehydes

$MgCl_2$ was also observed to inhibit aldehyde dehydrogenase activity when other aldehydes were used as substrates. A similar degree of inhibition was induced by $MgCl_2$ at the same concentration, for each aldehyde used. Table 4.1 summarises the effects of $MgCl_2$ on V_{max} with other aldehydes as substrates.

FIG. 4.5 EFFECT OF $MgCl_2$ ON V_{max}

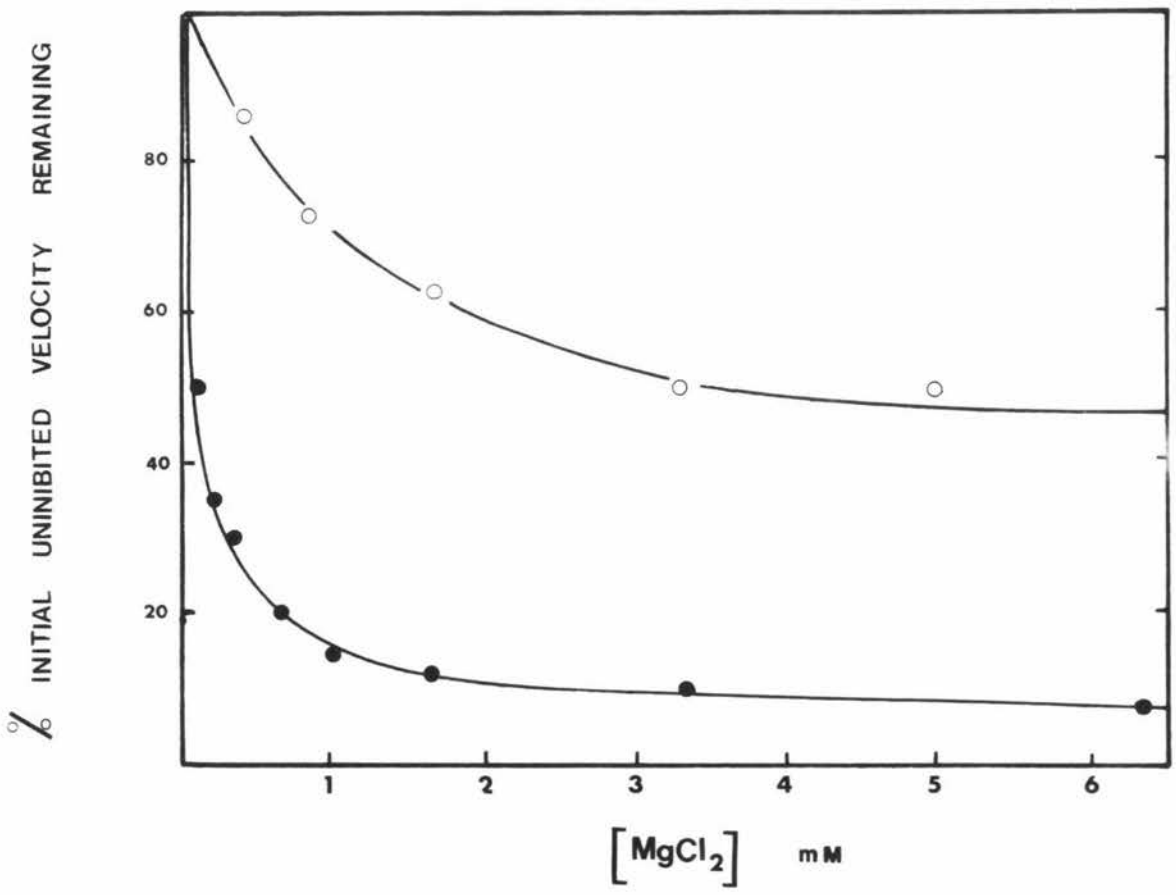

The assay mixture contained NAD^+ (2 mM), propionaldehyde (20 mM) and enzyme 2 µM. The open circles are replots of the data at low $MgCl_2$ concentrations at $1/50^{th}$ of the values shown.

Table 4.1 The effect of $MgCl_2$ of V_{max} with various aldehydes

Aldehyde	Concentration in Assay	[$MgCl_2$]	% Inhibition
Propionaldehyde	20 mM	1.6 mM	88
Acetaldehyde	20 mM	1.5 mM	87
4-Nitrobenzaldehyde	148 µM	1.6 mM	90
Benzaldehyde	5 mM	1.6 mM	82
4-Methoxybenzaldehyde	100 µM	1.6 mM	90
2-Hydroxybenzaldehyde	100 µM	1.6 mM	80

4.4.3 pH Profile of $MgCl_2$ Inhibition

An attempt was made to determine the pH profile of the $MgCl_2$ inhibition over a range of pH values from 5.0 to 9.0 using 35 mM citrate, phosphate and pyrophosphate buffers. However it was observed that $MgCl_2$ had no inhibitory effect on the enzyme activity in either the pyrophosphate or citrate buffers. Over the pH range 6.0 to 8.0 in the phosphate buffer, the percentage inhibition obtained when $MgCl_2$ (1.6 mM) was added to enzyme assays, remained constant at 88.

4.4.4 Double Reciprocal Plots of Initial Velocity versus Substrate Concentration with added $MgCl_2$

The double reciprocal plot with propionaldehyde as the varied substrate and the concentration of NAD^+ kept constant, resulted in a complicated inhibition pattern. The inhibition at propionaldehyde concentrations less than about 3 mM appeared to be uncompetitive (Fig. 4.6.a) and a replot of the ordinate intercepts of the double reciprocal plot versus the magnesium concentration resulted in an inhibition constant (Ki) of 240 µM. At higher propionaldehyde concentrations the double reciprocal plots were non linear, curving downward toward faster rates at very high

FIG. 4.6 **DOUBLE RECIPROCAL PLOT OF INITIAL VELOCITY VERSUS PROPIONALDEHYDE CONCENTRATION WITH ADDED $MgCl_2$ AT LOW LEVELS OF PROPIONALDEHYDE**

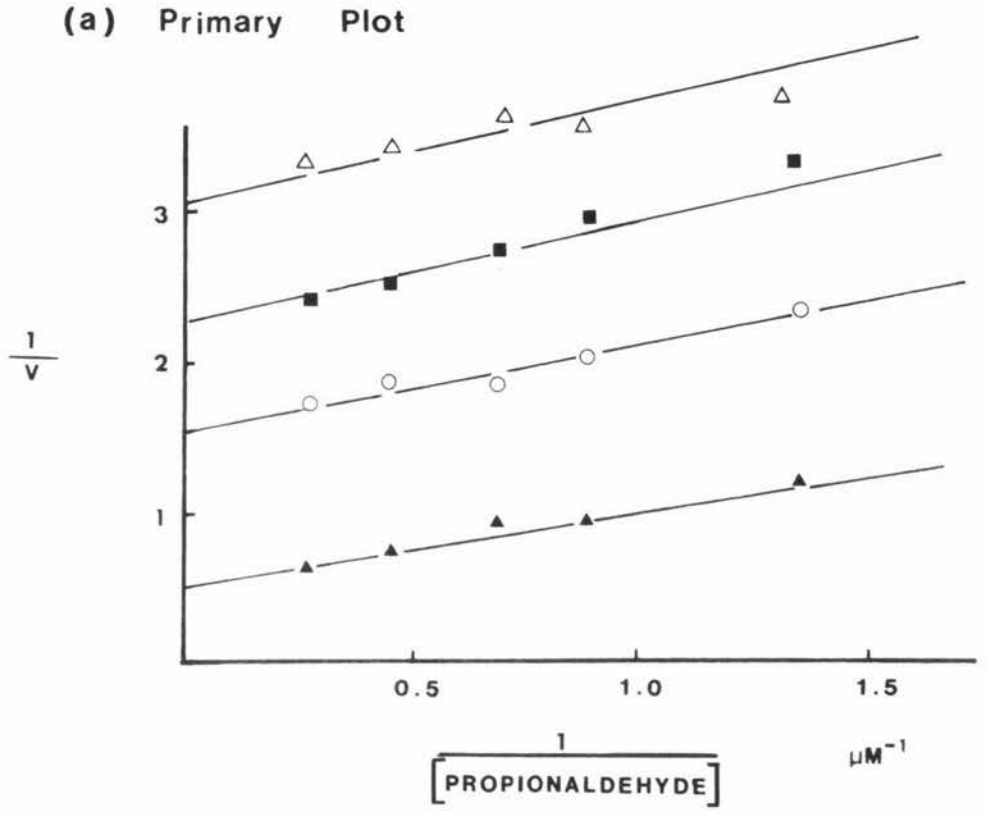

The NAD^+ concentration was 2 mM and the $MgCl_2$ concentration varied as follows, △ 1.0 mM, ■ 0.66 mM, ○ 0.33 mM and ▲ no $MgCl_2$.

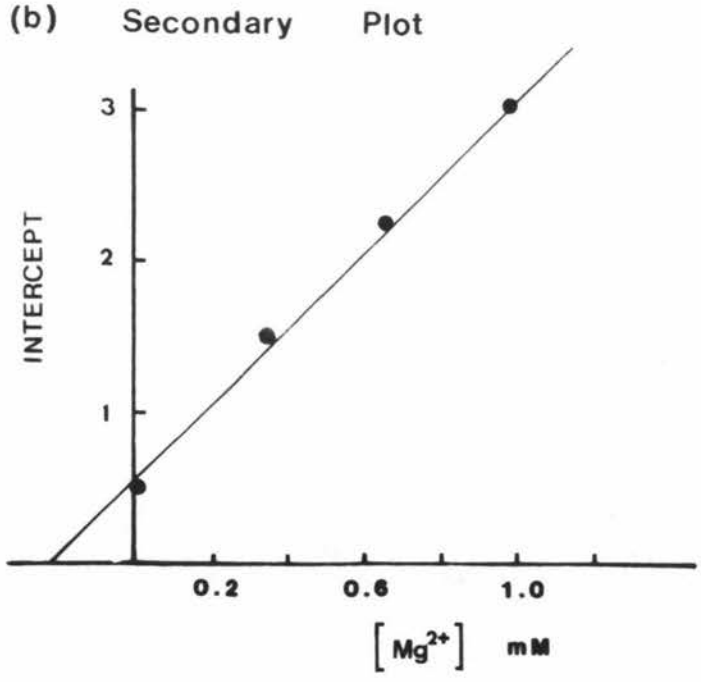

propionaldehyde concentrations (Fig. 4.7.a). The inhibition pattern appears to be either mixed or noncompetitive, although the possibility that plots may eventually become competitive at very high propionaldehyde concentrations cannot be entirely excluded. However the latter conclusion appears unlikely as the reaction velocity with 100 mM propionaldehyde and 1.6 mM $MgCl_2$ was almost identical to that at 20 mM propionaldehyde and 1.6 mM $MgCl_2$. The replots of the slopes and intercepts were both non-linear (Fig. 4.7.b). Non-linear replots which curve downward are characteristic of hyperbolic mixed type inhibition (Segel, 1975) and make the estimation of K_i values difficult. While K_i values can be determined from a plot of the reciprocals of the change in intercept or slope versus the $MgCl_2$ concentration, this procedure requires a large number of lines in the initial double reciprocal plot.

The double reciprocal plot with NAD^+ as the variable substrate and propionaldehyde as the fixed substrate, for various levels of $MgCl_2$, resulted in what appeared to be simple uncompetitive inhibition (Fig. 4.8a). The intercept replot was linear and resulted in an inhibition constant of 250 μM (Fig. 4.8.b).

4.4.5 The Effect of $MgCl_2$ on the Esterase Reaction

The addition of $MgCl_2$ (1.6 mM) to an esterase assay had no effect on the rate of the hydrolysis reaction and increasing the concentration of $MgCl_2$ to 15 mM also resulted in no inhibition of the esterase activity of the enzyme. Since it has been reported that the presence of both NAD^+ and NADH stimulate the esterase reaction (MacGibbon et al., 1978a) it was decided to determine whether $MgCl_2$ had any effect on the esterase activity in the presence of these coenzymes. When $MgCl_2$ was added to an assay containing enzyme (2 μM), PNPA (300 μM) and NAD^+ (100 μM), an immediate inhibition of the esterase activity was observed. The recorder traces were linear for the first few minutes, but

FIG. 4.7 DOUBLE RECIPROCAL PLOT OF INITIAL VELOCITY VERSUS PROPIONALDEHYDE CONCENTRATION WITH $MgCl_2$ ADDED

(a) Primary Plot

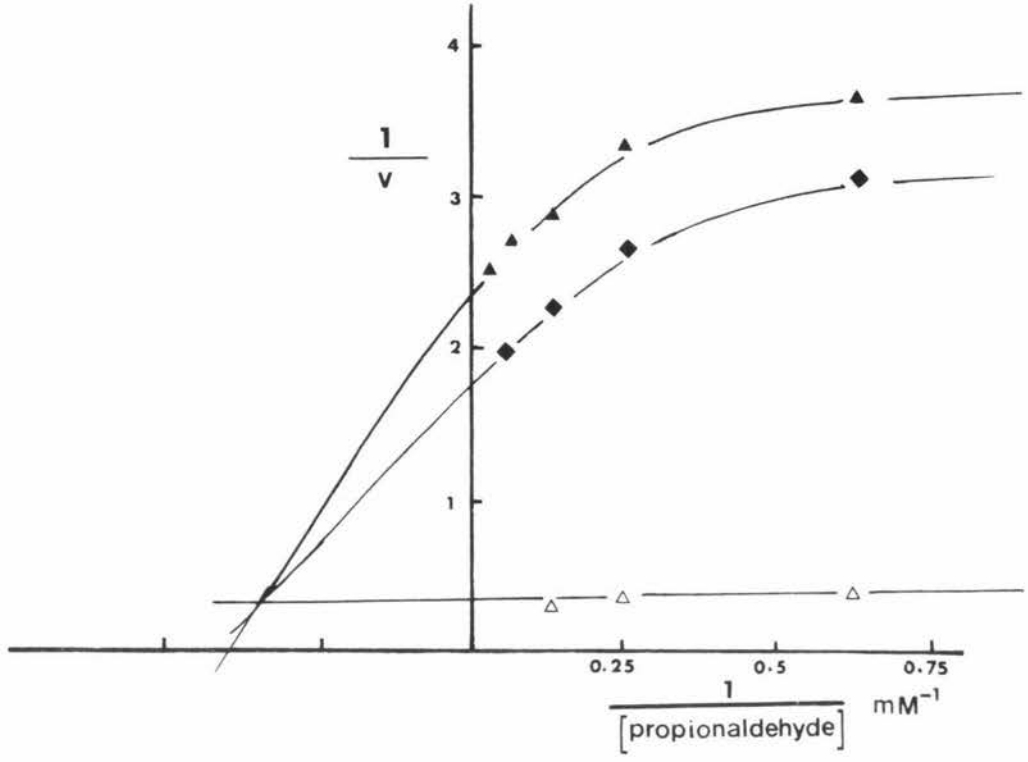

The NAD^+ concentration was 2 mM and the $MgCl_2$ concentration varied as follows, ▲ 1.6 mM, ◆ 0·83 mM and △ no $MgCl_2$.

(b) Secondary Plot

(1) INTERCEPT REPLOT

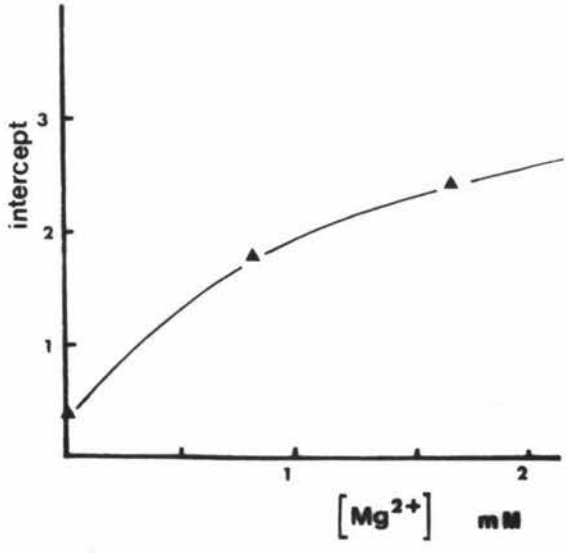

(2) SLOPE REPLOT

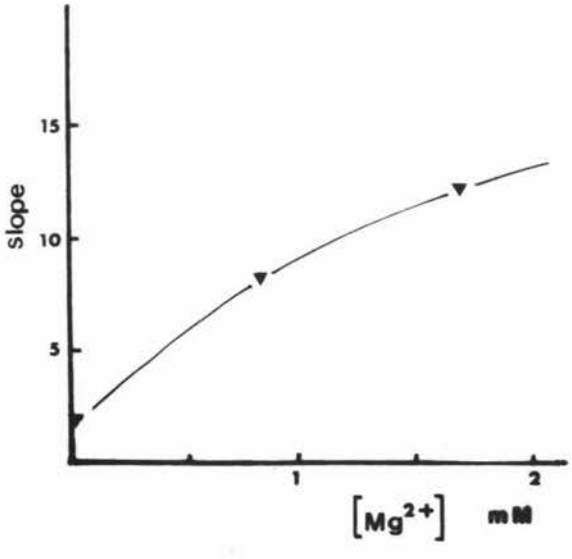

FIG. 4.8 **DOUBLE RECIPROCAL PLOT OF INITIAL VELOCITY VERSUS NAD^+ CONCENTRATION WITH ADDED $MgCl_2$**

(a) PRIMARY PLOT

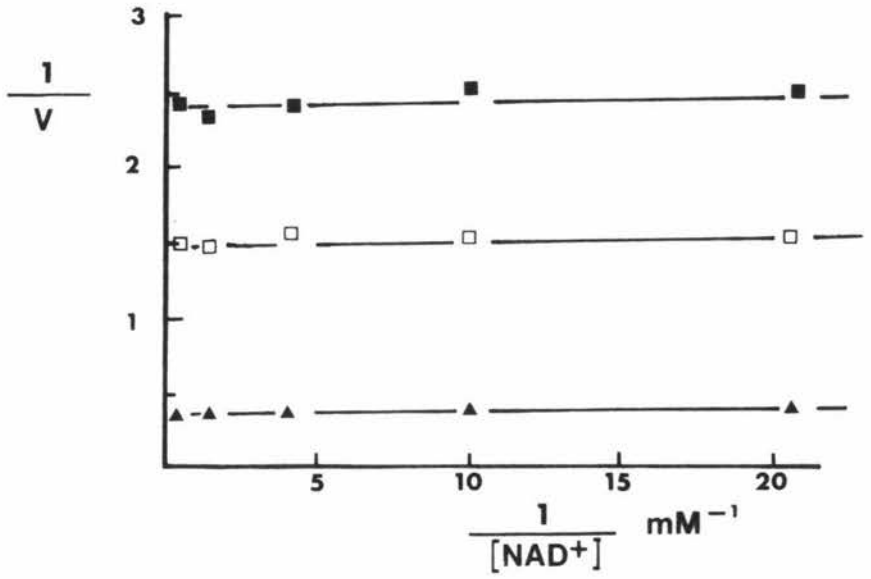

The concentration of propionaldehyde was kept constant at 60 µM while the concentration of MgCl was varied as follows ,■ 1.67 mM,□ 0.83 mM and ▲ no $MgCl_2$

(b) SECONDARY PLOT

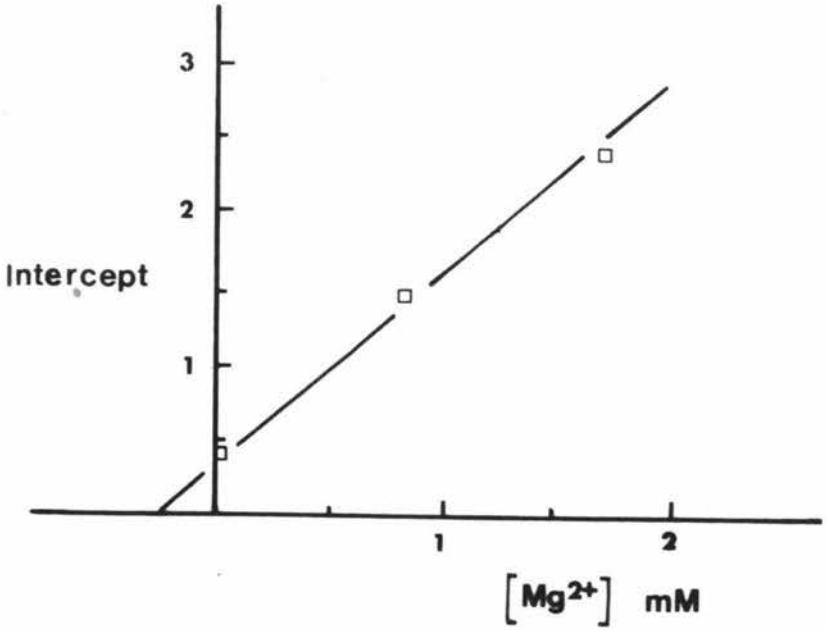

after an absorbance change of about 0.3, curved downward. The non-linearity of the recorder trace appeared to be related to the appearance of products from the ester hydrolysis, since the initial rate after the addition of $MgCl_2$ to enzyme-ester-NAD^+ mixture was less if the $MgCl_2$ was added after the reaction had proceeded for several minutes, than if it was added immediately after the reaction was initiated.

A double reciprocal plot of initial velocity versus PNPA concentration for various levels of $MgCl_2$ at an NAD^+ concentration of 100 µM, resulted in apparent competitive inhibition (Fig. 4.9.a), however the slope replot appeared to be non-linear (Fig. 4.9.b), more characteristic of partial competitive inhibition.

The addition of $MgCl_2$ (1.6 mM) to an esterase assay containing 100 µM NADH resulted in only a small amount of inhibition of the order of 4.9 %. The addition of higher $MgCl_2$ concentrations did not result in any further inhibition.

4.4.6 The Effects of NAD^+ Analogues and $MgCl_2$ on the Esterase Reaction

Since $MgCl_2$ inhibited the esterase activity only in the presence of NAD^+, it was decided to see whether NAD^+ analogues behaved in a similar manner. Deamino-NAD^+ (Nicotinamide hypoxanthine dinucleotide) has been reported to act as a coenzyme in the dehydrogenase reaction (MacGibbon *et al.*, 1977b), and when added to an esterase assay in this study, it was observed to stimulate the rate of ester hydrolysis in a similar fashion to NAD^+. Maximum stimulation was achieved at 800 µM compared to 100 µM for NAD^+. The addition of $MgCl_2$ (1.6 mM) to an esterase assay containing Deamino-NAD^+ (800 µM) also resulted in inhibited reaction velocities which curved downward, as seen where NAD^+ and $MgCl_2$ are added to an esterase assay.

FIG. 4.9 DOUBLE RECIPROCAL PLOT OF INITIAL VELOCITY VERSUS PNPA CONCENTRATION WITH ADDED NAD^+ AND $MgCl_2$

(a) Primary plot

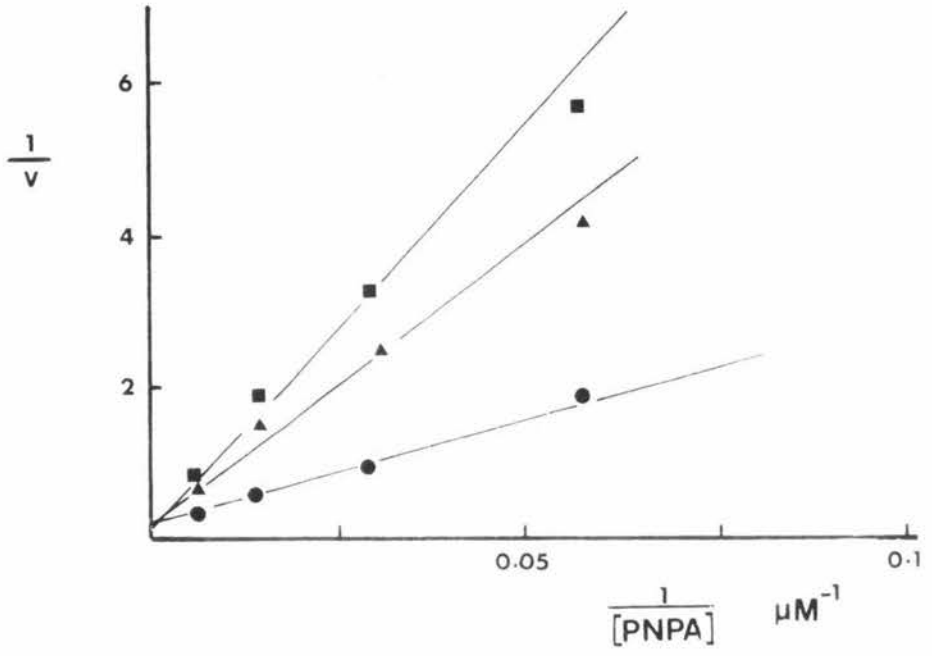

The NAD^+ concentration was 100 μM and the $MgCl_2$ concentration varied as follows , ■ 1·6 mM , ▲ 0·8 m , ● zero .

(b) Secondary plot

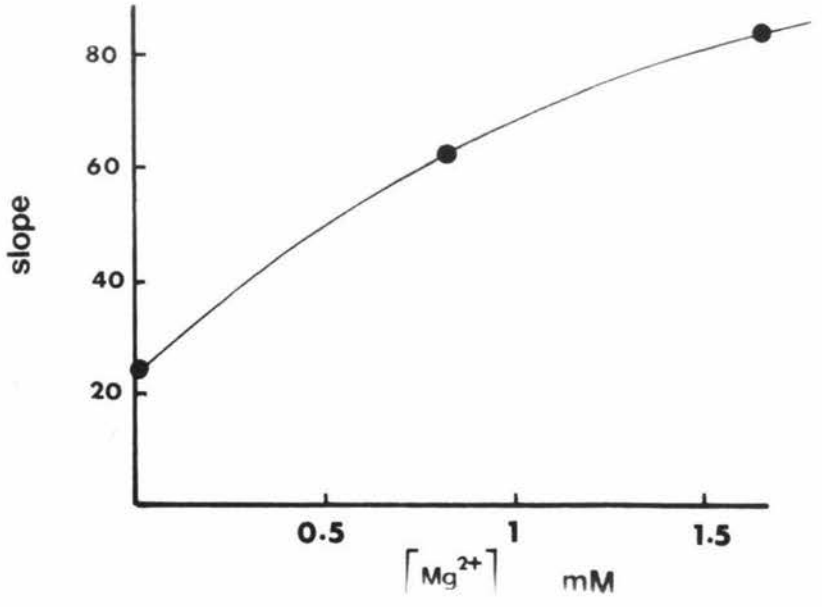

When 3-pyridine-aldehyde adenine-dinucleotide (100 μM) was added to an esterase assay, the rate of ester hydrolysis was reduced to 45% of the rate in the absence of the nucleotide. The addition of $MgCl_2$ (3.3 mM) to the 3-pyridine-aldehyde adenine dinucleotide esterase assay resulted in an increase in activity to 70% of the control obtained in the absence of the nucleotide and $MgCl_2$. There was no evidence of non-linearity in the recorder traces when assays contained 3-pyridine-aldehyde adenine dinucleotide and $MgCl_2$.

The addition of 3-acetyl-pyridine adenine dinucleotide (100 μM) caused 10% inhibition of the enzyme activity when added to esterase assays, and when added with $MgCl_2$ (3.3 mM) resulted in non-linear recorder traces which had an initial velocity greater than in the absence of the NAD^+ analogue but curved downward to give considerable inhibition.

ADP-ribose (100 μM) resulted in a 40% inhibition of the reaction rate when added to esterase assays, and the addition of $MgCl_2$ (3.3 mM) to an esterase assay containing ADP-ribose had no further effect on the degree of inhibition.

4.4.7 Hysteric Effects Induced by 3-Pyridine-aldehyde adenine dinucleotide

When 3-pyridine-aldehyde adenine dinucleotide (100 μM) was added to an esterase assay containing enzyme (2.0 μM), PNPA (220 μM) and NAD^+ (100 μM), the rate of reaction was initially reduced to 30% of the rate before the addition of the NAD^+ analogue, then after about 60 seconds the rate slowed to about 12% of the original rate (Fig. 4.10.a). The final rate was slightly less than that of an esterase assay containing enzyme-PNPA and 3-pyridine-aldehyde adenine dinucleotide (100 μM) only. A similar reaction rate versus time plot is observed when NAD^+ (100 μM) is added to an assay containing enzyme PNPA and 3-pyridine-aldehyde adenine dinucleotide (100 μM) (Fig. 4.10.b). In this case the reaction rate is initially increased to 156%

FIG. 4.10 HYSTERETIC EFFECTS INDUCED BY 3-PYRIDINE-ALDEHYDE ADENINE DINUCLEOTIDE

4.10a NAD^+ Premixed with the Enzyme

The recorder trace shows increase in absorbance at 400 nm due to the production of 4-nitrophenoxide ions. The reaction mixture contained enzyme (2μM), NAD^+ (100μM) and PNPA (220μM). At point a, 3-pyridine-aldehyde-NAD^+ (100μM) was added.

4.10b 3-Pyridine-Aldehyde-NAD^+ Premixed with the Enzyme

The reaction mixture contained (2μM), PNPA (220μM) and 3-pyridine-aldehyde-NAD^+ (100μM). At point a, NAD^+ (100μM) was added.

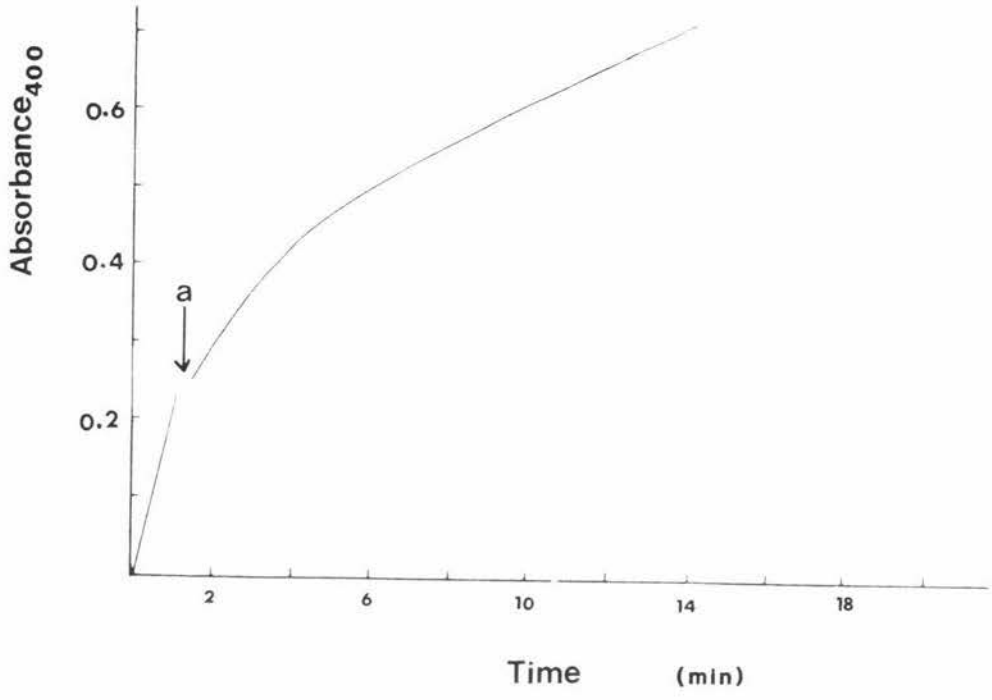
Absorbance400
0.6
0.4
0.2
a
2
6
10
14
18
Time (min)

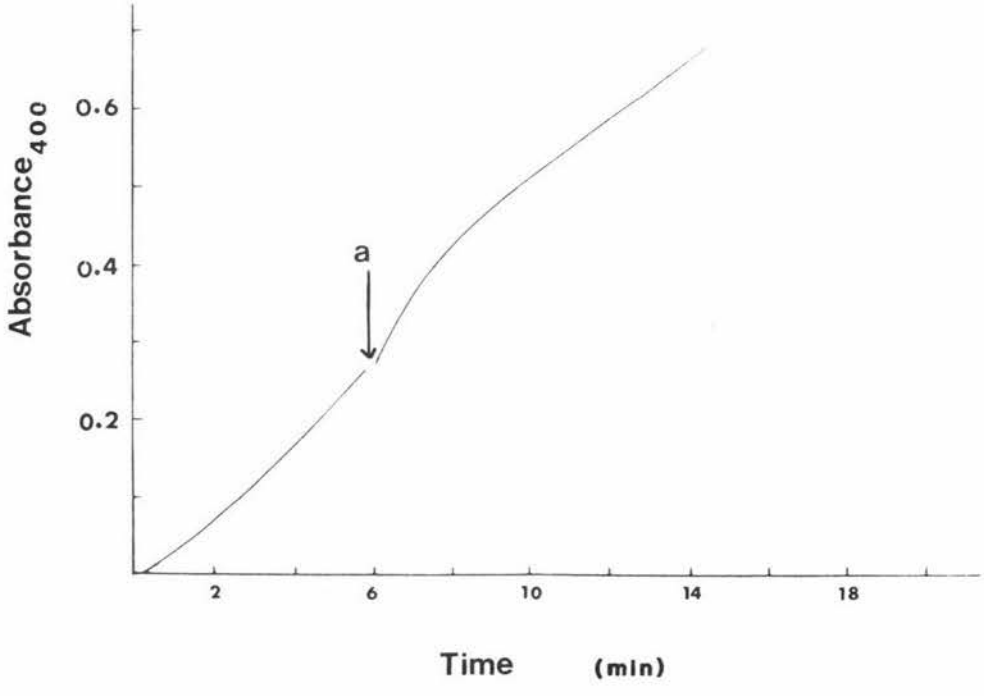
Absorbance400
0.6
0.4
0.2
a
2
6
10
14
18
Time (min)

of the original rate then after about 60 seconds decreases to 74% of the original rate.

4.4.8 The Effect of Chelating Agents on $MgCl_2$ Inhibition

Trisodium citrate and tetrasodium pyrophosphate, when added to assays for dehydrogenase activity, caused a 30% activation of the reaction velocity, EDTA however had no effect on the reaction velocity. The addition of all three substances, in concentrations in excess of the $MgCl_2$ concentrations to assays containing $MgCl_2$ resulted in an immediate increase in activity. Continued addition of these substances eventually resulted in the complete removal of all inhibition. A double reciprocal plot of initial velocity versus citrate concentration at fixed NAD^+ and propionaldehyde concentrations, with varying concentrations of $MgCl_2$, showed that trisodium citrate was competitive with $MgCl_2$ (Fig. 4.11) and the slope replot resulted in a K_i value of 330 μM.

4.4.9 Ultra-Violet Difference Spectra

The difference spectrum between enzyme-bound and free NADH has been determined by MacGibbon *et al.* (1979). They reported that the enzyme-NADH species absorbed less strongly in the region of 300 nm to 350 nm, with a maximum difference in the molar extinction coefficient (ε) of 940 1 $cm^{-1}mol^{-1}$ at 328 nm. These results are somewhat different from those obtained in this study, where the largest change in ε was found to be 585 1 $cm^{-1}mol^{-1}$ at 305 nm, and the $\Delta\varepsilon$ at 328 nm was 270 1 $cm^{-1}mol^{-1}$ (Fig. 4.12). The addition of $MgCl_2$ (4.0 mM) to the enzyme-NADH solution resulted in significant changes in the difference spectrum (Fig. 4.12). The maximum change in ε was now found to be 731 1 $cm^{-1}mol^{-1}$ at 310 nm and $\Delta\varepsilon$ at 328 nm was 673 1 $cm^{-1}mol^{-1}$.

FIG. 4.11 DOUBLE RECIPROCAL PLOT OF INITIAL VELOCITY VERSUS CITRATE AT FIXED CONCENTRATIONS OF Mg^{2+}

(a) Primary Plot

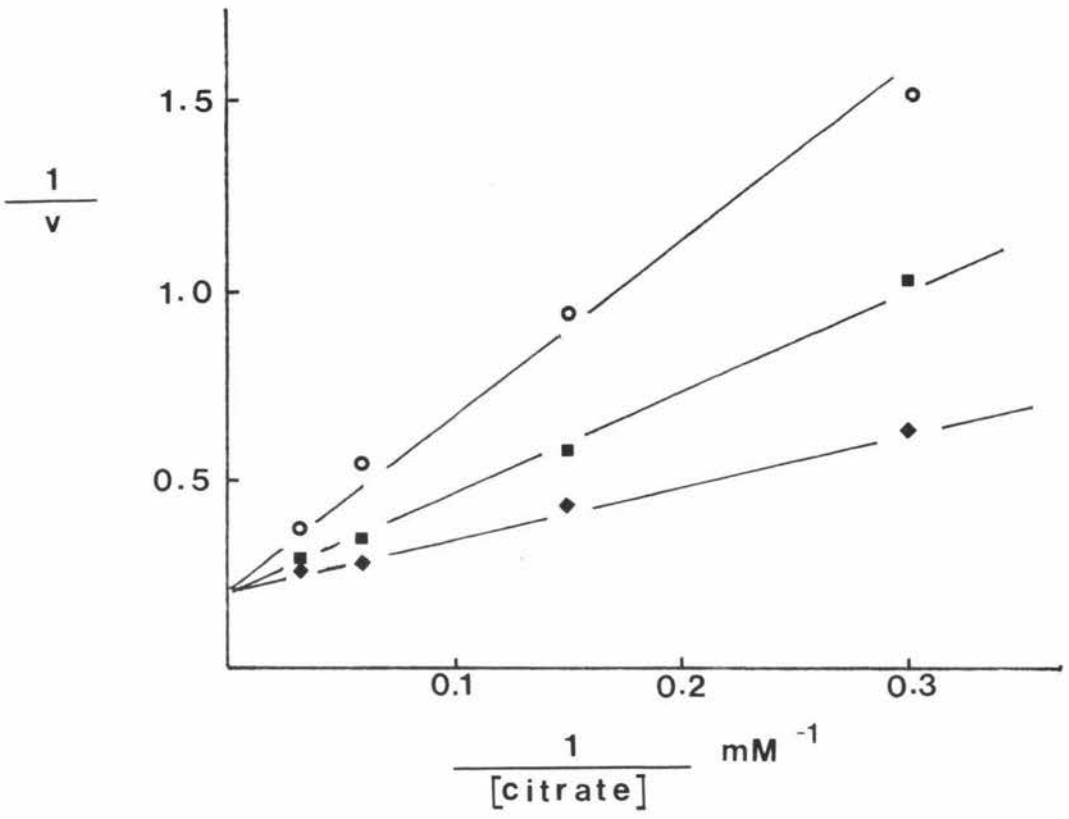

The concentrations of NAD^+ and propionaldehde were kept constant while Mg^{2+} was varied as follows, ○ 1.67 mM, ■ 0.83 mM, ◆ 0.5 mM.

(b) Secondary Plot

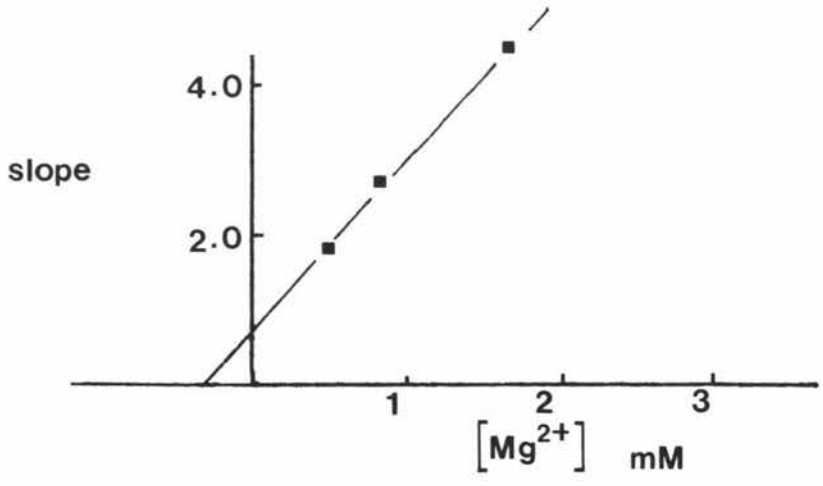

FIG. 4.12 Ultra Violet Difference Spectra Between Free and Enzyme Bound NADH With and Without Added $MgCl_2$

Line I shows the difference spectra obtained with one cell in the sample compartment containing enzyme (40 μM) and NADH (26 μM) and the other buffer, while in the reference compartment one cell contained enzyme (40 μM) and the other NADH (26 μM).

Line II shows the difference spectra obtained when $MgCl_2$ (3.3 mM) was added to all four cells.

FIG. 4.12 ULTRA VIOLET DIFFERENCE SPECTRA BETWEEN FREE AND ENZYME BOUND NADH WITH AND WITHOUT ADDED $MgCl_2$

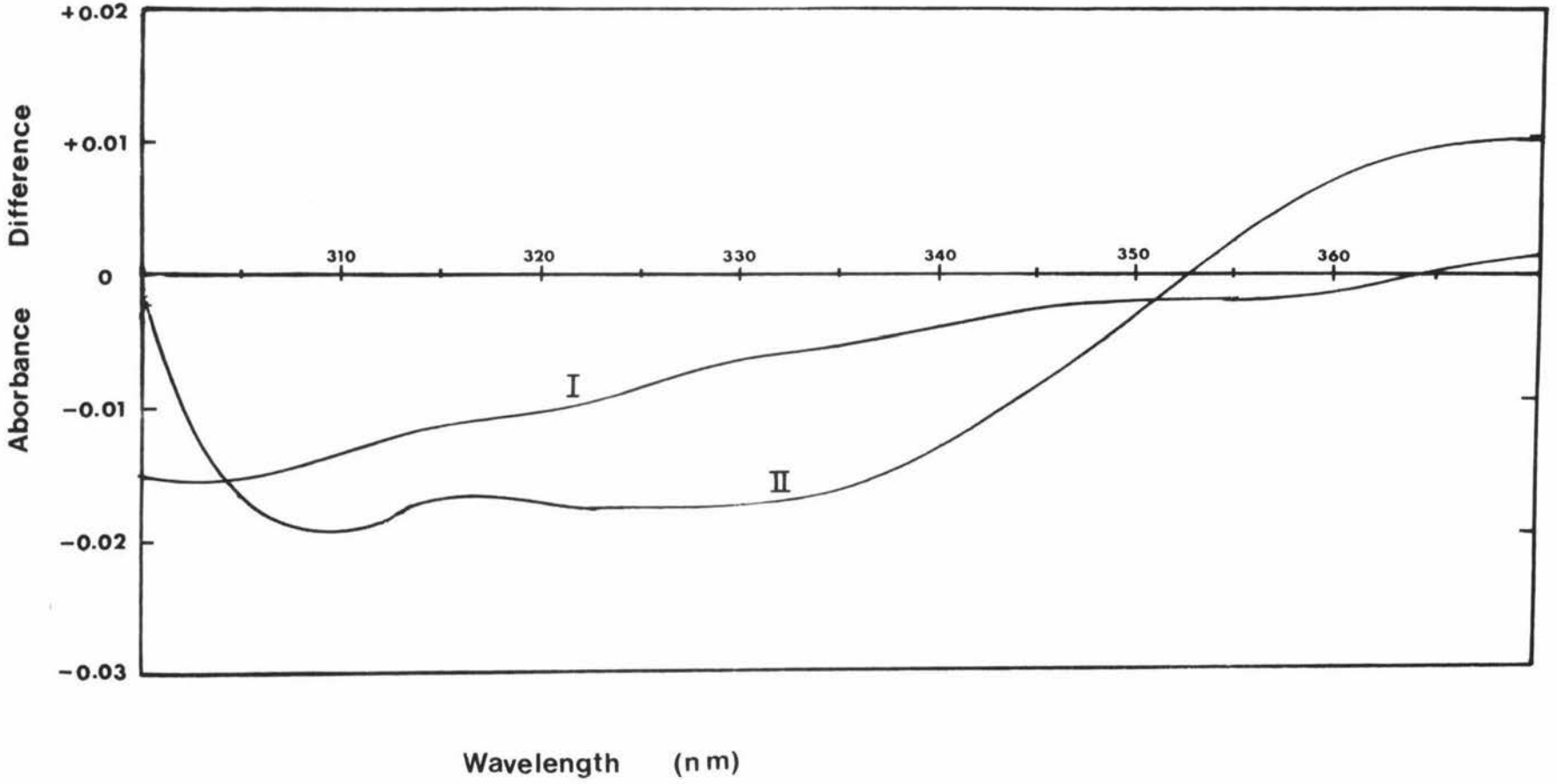

4.4.10 NADH Titrations

The stepwise addition of NADH to enzyme in the fluorimeter resulted in a smooth titration cruve (Fig. 4.13), the replots of which resulted in a K_D value of 1.0 μM and a fluorescence enhancement factor of 5.8. These values are in good agreement with the values of 1.2 μM and 5.6 reported by MacGibbon (1976). When $MgCl_2$ (1.6 mM) was added to a titration mixture a significant increases in the fluorescence was observed (Fig. 4.13), and a control titration showed that the fluorescence of free NADH was unaffected by the presence of $MgCl_2$. Replots of the titration data showed that the dissociation constant had decreased to 0.2 μM but the concentration of NADH binding sites was unchanged (Fig. 4.14). The average fluorescence enhancement factor in the presence of $MgCl_2$ was calculated to be 18. The tighter binding of NADH to the enzyme in the presence of $MgCl_2$ results in a much sharper titration curve, enabling estimates of the binding site concentration to be obtained directly from the titration curve in a manner similar to that described for the F_1 horse liver with Zn^{2+} (Venteicher *et al.*, 1977) and for horse liver alcohol dehydrogenase with isobutyramide (Theorell and McKinley-McKee, 1961).

Trisodium citrate (6.6 mM) caused a decrease in the fluorescence observed on NADH binding (Fig. 4.13) and a control titration showed that the citrate was not affecting the fluorescence of free NADH. The scatchard plot (Fig. 4.14)showed that while the NADH binding site concentration was unchanged, the dissociation constant had increased to 1.8 μM and the fluorescence enhancement factor had decreased to 2.8. EDTA (6.6 mM) caused a decrease in the fluorescence of bound NADH, but the dissociation constant and NADH binding site concentration were unchanged.

4.4.11 NAD^+ Titrations

When NAD^+ is added to a cell in the fluorimeter containing enzyme, a smooth titration curve is obtained

FIG. 4.13 **TITRATION OF NADH BINDING SITES BY FLUORESCENCE**

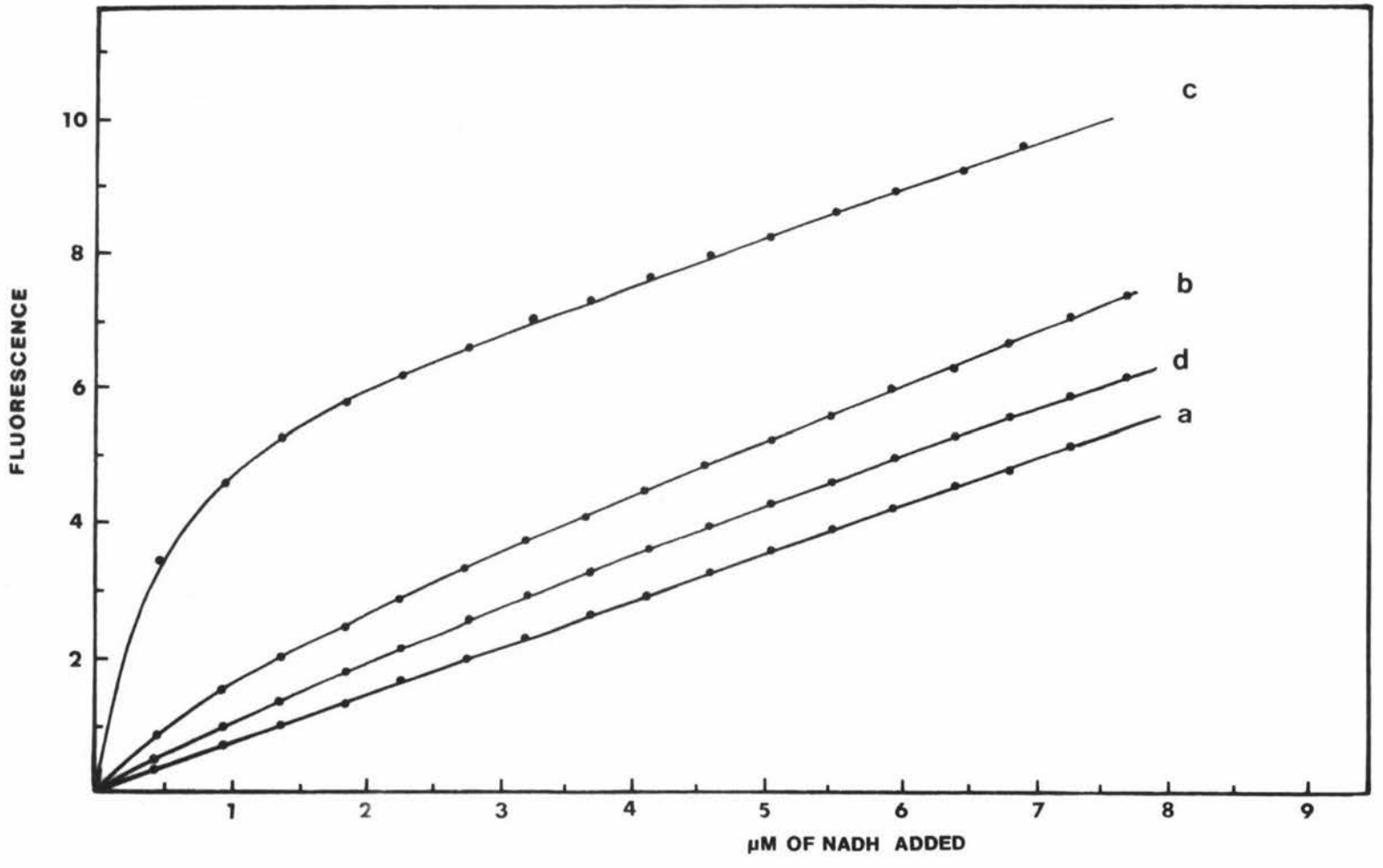

Line **a** shows the fluorescence of NADH only, **b** with enzyme added, **c** with enzyme and $MgCl_2$ (1.6 mM) added and **d** with enzyme and citrate (6.6 mM) added.

FIG. 4.14 Replots of NADH Titration Data

4.14a Plot of equation 3.20

The enzyme concentration calculated from the plot was 0.8 μM and the K_D value was 1.1 μM. ΔF_{max} was 2.1.

4.14b Scatchard Plot

Line a is enzyme and NADH only, ΔF_{max} was 2.0 and K_D equalled 1.1 μM. Line b is with $MgCl_2$ (1.6 mM) added, ΔF_{max} was 4.65 and K_D equalled 0.09 M. Line c is with citrate (6.6 mM) added, ΔF_{max} was 1.0 and K_D equalled 2 μM. The enzyme concentration was 0.8 μM.

FIG. 4.14 **REPLOTS OF NADH TITRATION DATA**

(a) Plot of equation 3.20

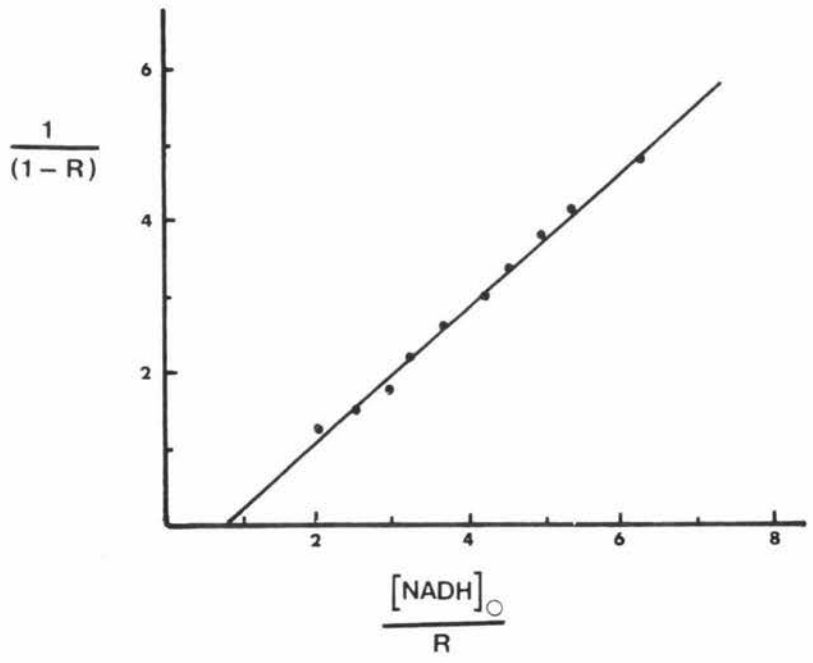

(b) SCATCHARD PLOT

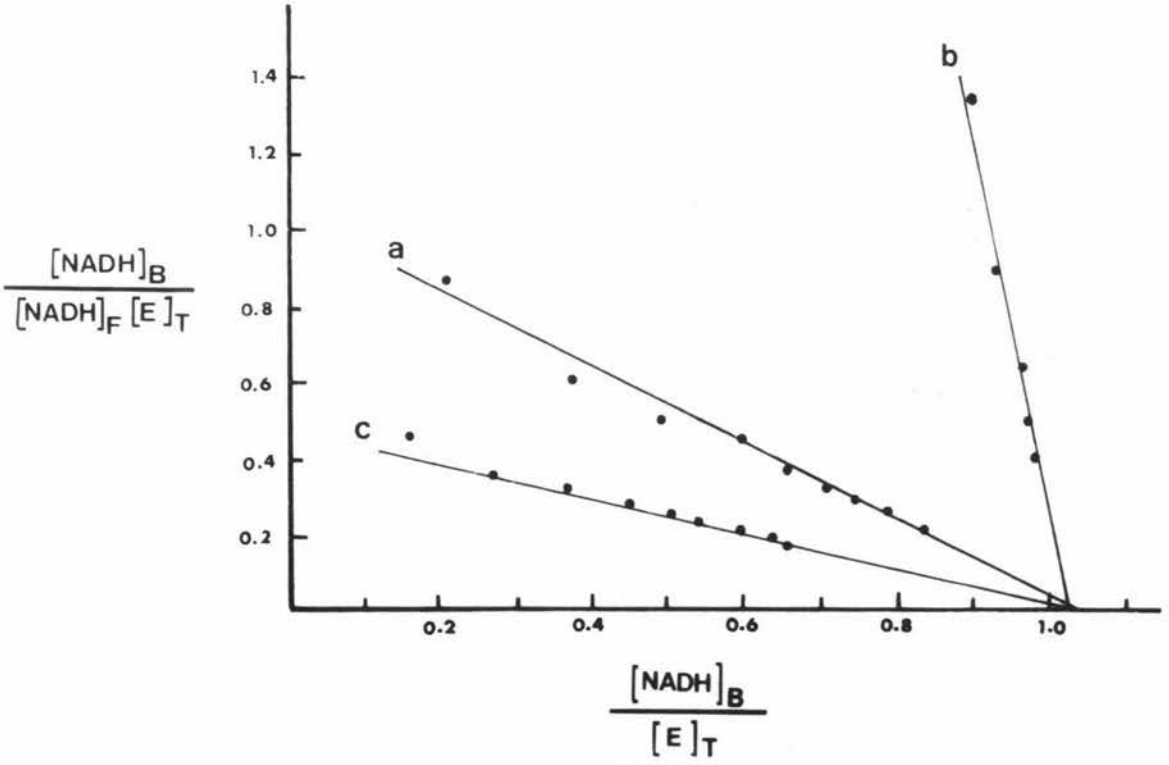

(Fig. 4.15), and when the data is replotted as a Scatchard plot, a straight line is obtained (Fig. 4.16). The dissociation constant was equal to 3.2 μM, a value somewhat lower than the value of 8 μM obtained from steady-state kinetic studies by MacGibbon et al. (1977a) The concentration of NAD^+ binding sites was found to be equal to the concentration of NADH binding sites, however the number of binding sites per tetramer for both NAD^+ and NADH varied from one enzyme sample to another. Values were obtained ranging from 1 binding site to 3 binding sites per tetramer, where the concentration of tetramers was determined from absorbance measurements at 280 nm.

When $MgCl_2$ (3.3 mM) was added to the titration mixture, the maximum quenching of protein fluorescence obtained, was twice that obtained in the absence of $MgCl_2$ (Fig.4.15). The scatchard plot of the data (Fig. 4.16) however, shows that the dissociation constant was decreased by a factor of 10 to 0.31 μM, but that the concentration of NAD^+ binding sites is unchanged in the presence of $MgCl_2$.

4.4.12 The Effect of $MgCl_2$ on the Enzyme Subunit Composition

4.4.12.1 Polyacrylamide gel electrophoresis

Attempts were made to determine whether $MgCl_2$ affected subunit composition by using polyacrylamide gel electrophoresis. If $MgCl_2$ caused a change in the number of subunits present in each enzyme molecule, this would be detectable using an electrophoresis gel which does not denature the enzymes, since dissociation of an enzyme tetramer into smaller units would result in a molecule which is smaller than the undissociated molecule but has the same charge. Such a dissociated molecule would move further down the gel compared to the original molecule. The reverse happens if association of subunits occurs, the larger molecule not moving as far as the original.

FIG. 4.15 TITRATION OF NAD^+ BINDING SITES BY PROTEIN FLUORESCENCE QUENCHING

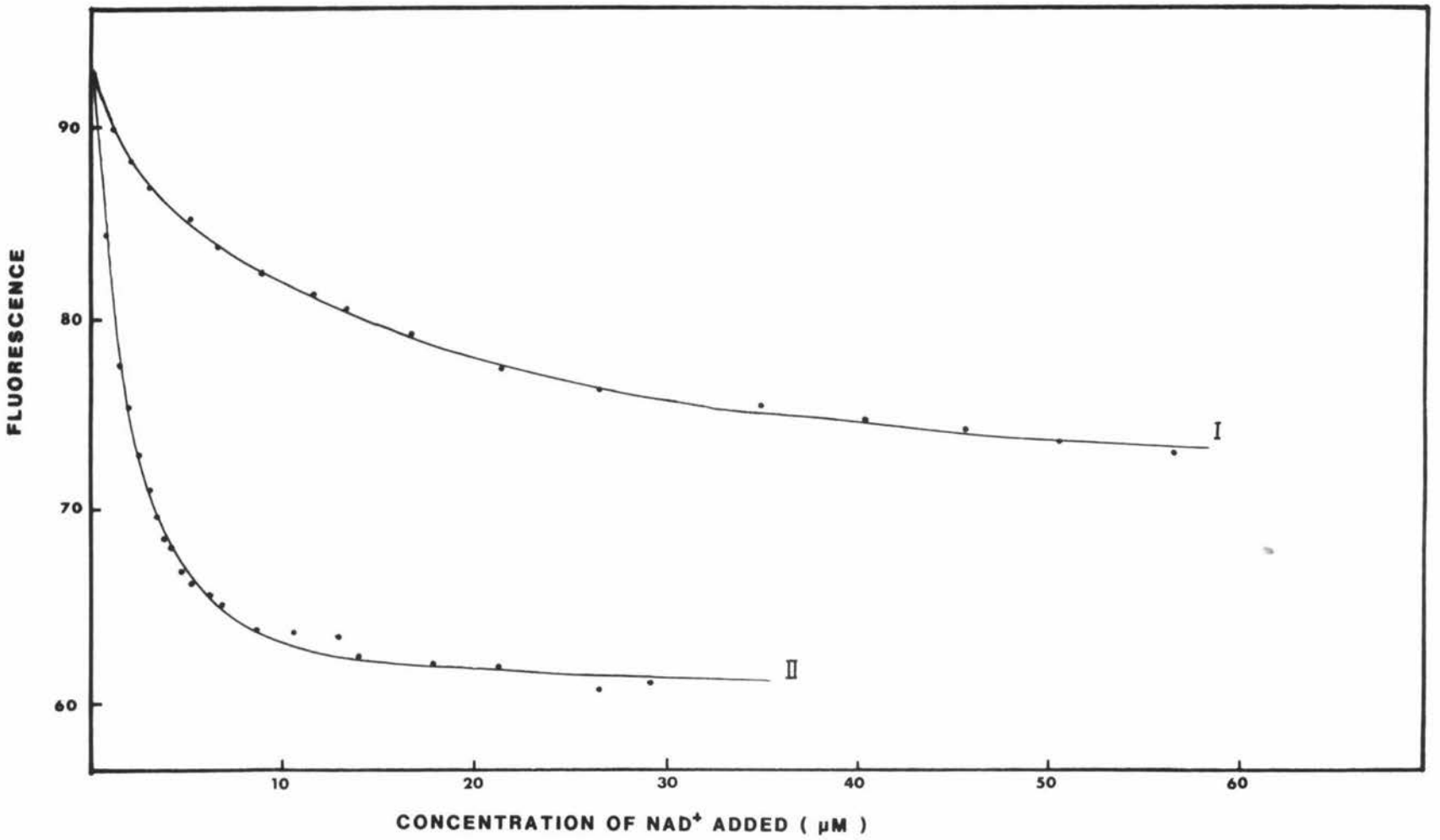

Line I shows the fluorescence quenching when NAD^+ is added to enzyme , and II when NAD^+ is added to enzyme and $MgCl_2$ (3.3 mM) .

FIG. 4.16 **SCATCHARD PLOT OF NAD^+ TITRATION DATA**

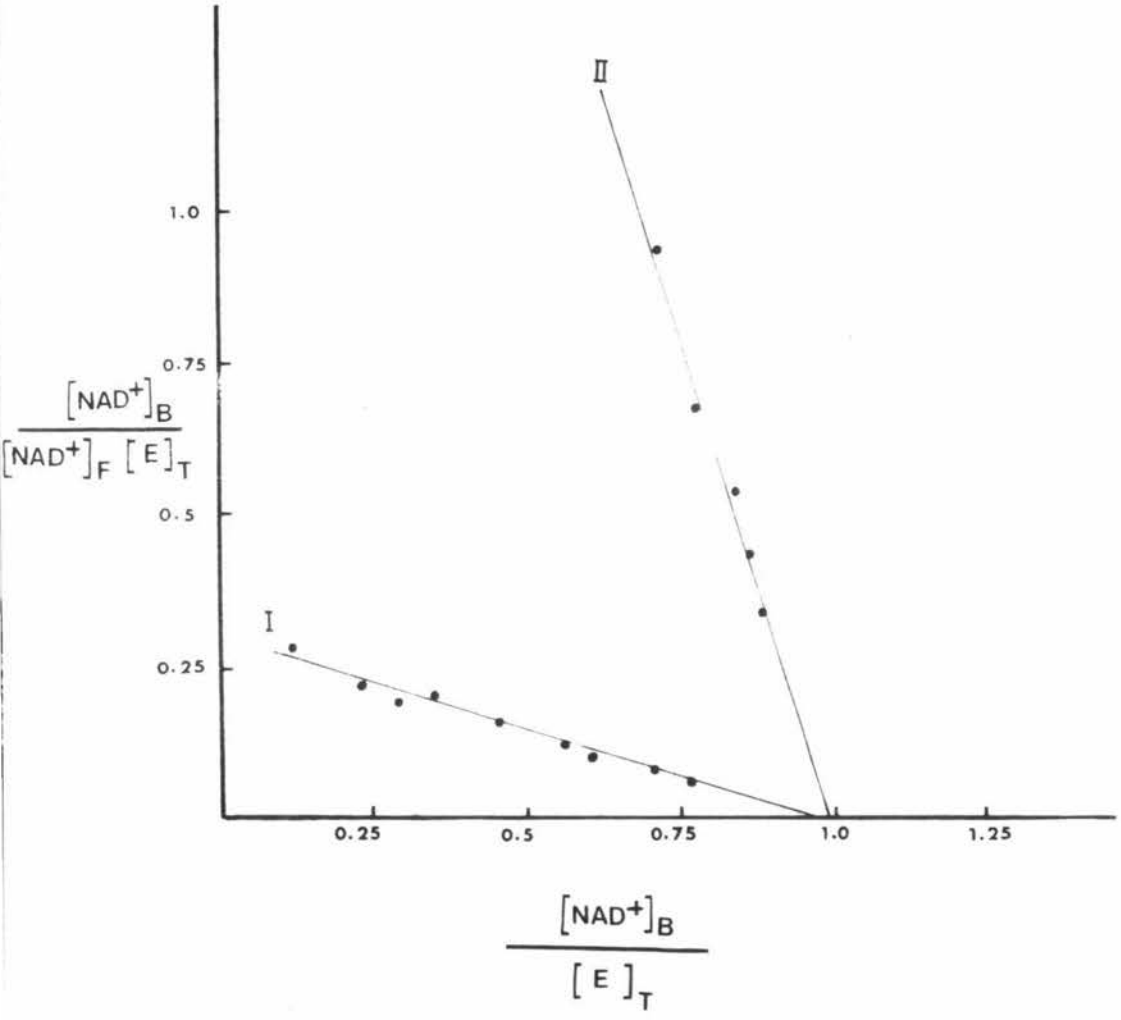

Line I is enzyme.NAD^+ only, K_D equals 3.2 μM. Line II is with 3.3 mM $MgCl_2$ added. ,the K_D equals 0.31 μM. △F max for enzyme.NAD^+ only was 12.6 and for enzyme.NAD^+.MgCl was 27.4 .

Initially an electrophoresis run was carried out in the absence of $MgCl_2$ with three standards of known molecular weight name; bovine catalase, yeast alcohol dehydrogenase and rabbit muscle aldolase. However when the experiment was repeated with 5 mM $MgCl_2$ present, application of the electric current resulted in the precipitation of both the aldehyde dehydrogenase samples and the standards in the loading wells. When the gel was stained for protein after the electrophoresis run only the catalase showed any movement down the gel.

4.4.12.2 Gel filtration experiments

Aldehyde dehydrogenase was eluted off the Sephacryl S 300 column in approximately 58 hours with an elution volume of 454 ± 2 cm^3. When the column was equilibrated with $MgCl_2$ (5 mM) and the aldehyde dehydrogenase sample (containing 5 mM $MgCl_2$) was run, the elapsed time was again about 58 hours and the elution volume 456 ± 2 cm^3. The standard, yeast alcohol dehydrogenase, was eluted in 59 hours with an elution volume of 463 ± 2 cm^3. Utilizing the fact that there is a linear relationship between elution volume and the logarithm of the molecular weight, an approximate elution volume of 471 cm^3 can be estimated for a protein with a molecular weight of 106 000 (half the tetramer molecular weight, MacGibbon et al., 1979). From these results it can be concluded that unlike the F_2 horse liver aldehyde dehydrogenase, the enzyme is not dissociating from tetramers to dimers in the presence of $MgCl_2$.

4.4.12.3 Laser light scattering experiments

The plot of ln (NIAF-1) against $(\sin\frac{\theta}{2})^2$ for enzyme (70 µM) in 35 mM pH 7.6 phosphate buffer is shown in Fig. 4.17. The slope of the line (i.e. $D_o \frac{1}{2}(\frac{4 n_o \pi}{\lambda_o})^2$) is equal to 28 000. When the experiment was repeated with 10 mM $MgCl_2$ added, there was a small decrease in the slope of the line to 24 500. As λ_o is a constant and n_o was unchanged in the presence of $MgCl_2$, the decrease in the slope corresponds to a decrease in D_o. Using equation 4.17 the effect on D_o of

FIG. 4.17 EFFECT OF $MgCl_2$ ON THE DIFFUSION COEFFICIENT

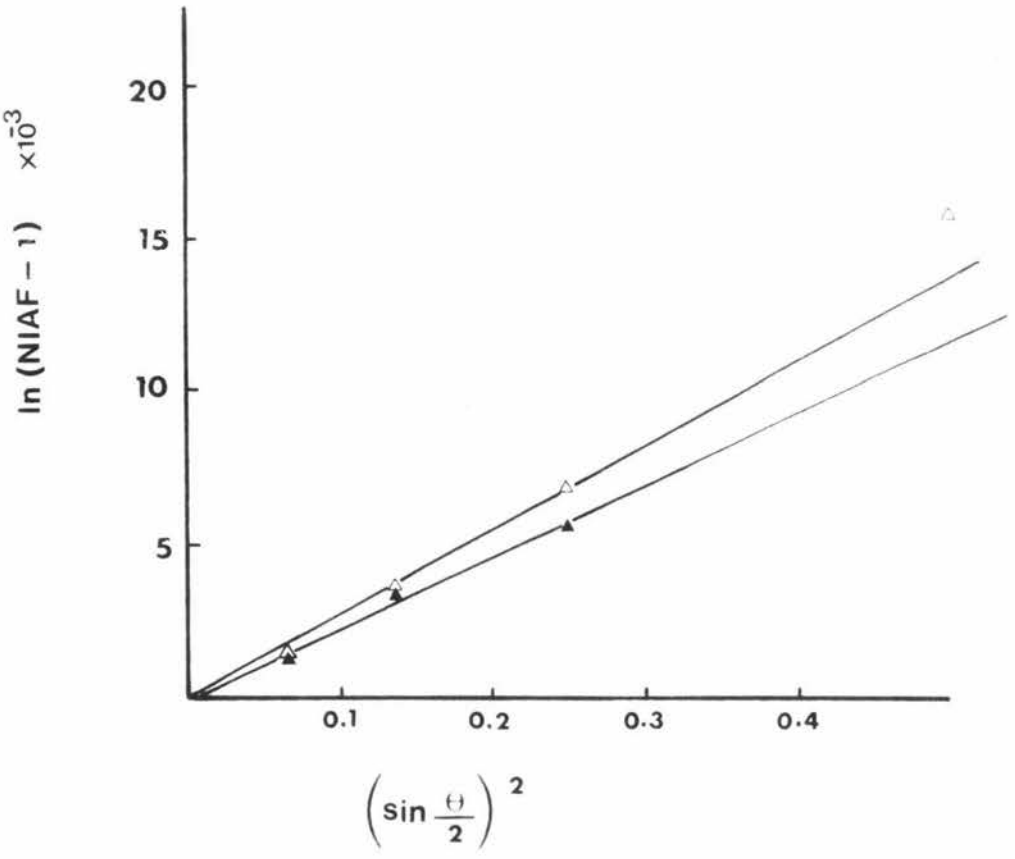

The upper line is enzyme (70 um) and buffer only, the slope equals 28 000. The lower line contains enzyme (70 uM) and $MgCl_2$ (3.3 mM), the slope equals 24 500.

of halving the molecular weight of the macromolecule under study can be calculated.

$$D_o \alpha \frac{1}{n^{\frac{1}{3}}} \qquad (4.17)$$

If the mass is halved the ratio of the diffusion coefficients for the unaltered macromolecule to the halved macromolecule would be:

$$D \alpha \frac{1}{0.7937}$$

which is 1:1.26, that is a 26% increase in D_o would be expected in the enzyme dissociated from tetramers to dimers. The fact that a decrease in D_o, rather than an increase, was observed supports the conclusion that the number of subunits per enzyme molecule does not decrease in the presence of $MgCl_2$, and in fact may increase. However the sensitivity of the light scattering technique is reliant on eliminating all dust particles from the sample, and for an enzyme solution it is extremely difficult to remove the charged dust particles without denaturing or precipitating the enzyme.

4.5 DISCUSSION

The physical properties and kinetic behaviour of the cytoplasmic sheep liver aldehyde dehydrogenase in the presence of $MgCl_2$ show some similarities to the two isoenzymes from horse liver, including inhibition of enzyme activity at high concentrations of $MgCl_2$ and enhancement of nucleotide fluorescence (Venteicher *et al.*, 1977). However there are also significant differences. Venteicher *et al.* (1977) have reported that both of the horse liver isoenzymes go through a region of activation at low concentrations of $MgCl_2$, but no such region was detected for the sheep liver

cytoplasmic enzyme used in this study. Instead inhibition was observed with $MgCl_2$ concentrations above about 20 μM and no effect on the enzyme activity was observed at concentrations below this value. Weiner et al., (1974) have shown that the pI 5.0 horse liver enzyme binds four NAD^+ molecules per tetramer, but only two NADH molecules under equilibrium conditions, and that the enzyme exhibits a phenomenon known as **half-site** reactivity in the steady-state and pre-steady-state since only two molecules of NADH are produced per tetramer (Weiner et al., 1976; Seydoux et al., 1974). The activation induced in the pI 5.0 horse liver enzyme by $MgCl_2$ has been explained by Takahashi and Weiner (1980) as resulting from a change to full-site reactivity, caused by the dissociation of enzyme from tetramers into dimers, with each dimer binding two NADH molecules. Using the concentration of tetramers determined for absorbance measurements at 280 nm (assuming an absorbance of 1.13 corresponds to 1.0 mg cm^{-3} of protein, Dickinson et al. (1981)) the number of NADH sites per tetramer in this study varied from 1.2 to 3.0 (with considerable variation being found in fractions from the same preparation (Motion, Personal Communication)). Erroneous values for binding site concentrations can be obtained if the enzyme sample contains contaminating proteins or inactive enzyme, since obviously in both of these cases the number of NADH binding sites per tetramer obtained will be lower than the actual value. Values higher than the true one may be obtained if the sample contains any contaminant enzyme which binds NADH with a resulting enhancement of fluorescence, however in this case unless the dissociation constant for the contaminant enzyme.NADH complex is identical to that of the aldehyde dehydrogenase-NADH complex, deviations from linearity in the Scatchard plots would be expected. The lack of any significant contamination of the enzyme sample by extraneous protein has been demonstrated by Agnew et al., (1981) indicating that dead or inactive aldehyde dehydrogenase is the only major problem in the NADH titration experiments. One possibility which can

account for the number of active sites per tetramer ranging between 2 and 3 is that the enzyme sample contains two isoenzymes, one of which binds two NADH molecules per tetramer, and the other four molecules per tetramer. However while there is evidence for two isoenzymes in the enzyme preparation (Agnew et al., 1981), there is no evidence that the isoenzymes behave differently with respect to NADH binding. Although difficulties were encountered in determining the exact number of NADH binding sites per tetramer, it was established that the number of NADH and NAD^+ binding sites were the same. It was also clear that the addition of $MgCl_2$ did not affect the number of binding sites per tetramer for either NADH or NAD^+. A change in the number of coenzyme binding sites would have been expected if the enzyme (like the horse liver F_2 isoenzyme) had dissociated from a tetramer into two dimers each of which binds two NADH molecules. However it appears that not only is there no increase in the number of NADH binding sites per tetramer in the presence of $MgCl_2$, but also the molecular weight determination experiments show that there is no evidence for any dissociation of the enzyme from a tetramer into dimers. The elution volumes on a Sephacryl S300 gel filtration column showed no difference within experimental error whether $MgCl_2$ was present or not, and the laser light scattering experiments also showed no decrease in molecular weight. These results indicate that the effect of $MgCl_2$ on the cytoplasmic sheep liver aldehyde dehydrogenase is completely different to that reported by Takahashi and Weiner (1980) for the F_2 (or mitochondrial) isoenzyme of horse liver.

In the presence of $MgCl_2$ there is a large increase in the fluorescence of NADH when it is bound to the enzyme, and both NADH and NAD^+ bind more tightly when $MgCl_2$ is present, with a resulting lowering of the dissociation constant. To cause these effects the magnesium ion must be able to bind to the enzyme.NADH and enzyme.NAD^+ complexes. If it is assumed that Mg^{2+} does not bind until

coenzyme binds as shown in scheme 4.2 , an expression may be derived relating the observed dissociation constant

$$E + NAD^+ \underset{K_D}{\rightleftharpoons} E.NAD^+ + Mg^{2+} \underset{K_i}{\rightleftharpoons} E.NAD^+.Mg^{2+} \qquad \text{(Scheme 4.2)}$$

$K_{D(obs)}$ to the dissociation constant (K_D) for the $E.NAD^+$ binary complex and the dissociation constant (K_i) for the $E.NAD^+.Mg^{2+}$ complex (equation 4.18).

$$\frac{1}{K_{D(obs)}} = \frac{1}{K_D}\left(1 + \frac{1}{\frac{K_i}{[Mg^{2+}]}}\right) \qquad (4.18)$$

From the experimental data K_D = 3 μM and $K_{D(obs)}$ = 0.33 μM for an $MgCl_2$ concentration of 3.3 mM, thus a K_i value can be calculated for Mg^{2+} binding. From the NAD^+ titration data K_i equals 320 μM and from the NADH titration data K_i equals 280 μM.

The double reciprocal plot of initial velocity versus NAD^+ concentration at various $MgCl_2$ concentrations resulted in a pattern of apparently parallel lines, indicating that $MgCl_2$ is an uncompetitive inhibitor with respect to NAD^+. Such a pattern is not consistent with the formation of an $NAD^+.Mg^{2+}$ inhibitor complex in some pre-equilibration step before the inhibitor complex binds as this would result in a competitive inhibition pattern with increasing concentrations of NAD^+ competing with the coenzyme binding site. While NAD^+ can complex Mg^{2+} the presence of 25 mM phosphate will result in most of the Mg^{2+} being present as phosphate complexes. Using a K_D value of 20 mM for the $NAD^+.Mg^{2+}$ complex (Apps, 1973) and a K_D of 3.16 mM for $Mg^{2+}HPO_4^{2-}$ complex (Dawson *et al.*, 1969) it can be calculated that less than 1% of the NAD^+ will be present as an $NAD^+.Mg^{2+}$ complex at the Mg^{2+} concentrations used in this study.

At concentrations of propionaldehyde below 2 mM the inhibition pattern observed with propionaldehyde as the varied substrate also appeared uncompetitive with a linear replot. From the double reciprocal plot (Fig. 4.6) it can be seen that both the Km for propionaldehyde (in this concentration range) and V_{max} are reduced with increasing $MgCl_2$ concentrations. Thus in the presence of $MgCl_2$ propionaldehyde binds more tightly, but the inhibitory effect appears to be caused by decreasing the rate constants for the steps which determine the magnitude of V_{max}.

A different inhibition pattern is seen at high concentrations of propionaldehyde (greater than 1 mM), here both the primary and secondary plots show downward curvature making the determination of a K_i value extremely difficult. Non-linear double reciprocal plots have been reported by MacGibbon et al. (1977) for the initial velocity versus aldehyde concentration plots for propionaldehyde and acetaldehyde. These workers suggested that the non-linearity may be due to the presence of different types of aldehyde binding sites, a situation which could arise if the enzyme contains two isoenzymes with different kinetic behaviour. Agnew et al. (1981) have shown the existence of two isoenzymes in cytoplasmic enzyme preparations, however in view of the almost identical isoelectric points of the isoenzymes and the fact that there are no deviations from linearity in the replots of the NAD^+ and NADH titrations, it seems unlikely that the two isoenzymes show different kinetic behaviour. A more likely situation is that there are two aldehyde binding sites on the enzyme.

In order to account for the above data, it was assumed that there were two different binding sites for propionaldehyde on the enzyme. A low Km binding site (designated P_1) and a high Km binding site (designated P_2). It was also assumed that only the low Km site was catalytically active, as there was no increase in the NADH burst amplitude between 100 μM propionaldehyde (where only the low Km site is occupied) and 20 mM propionaldehyde (where both sites are

occupied) (L.F. Blackwell, personal communication).

Calculations were made assuming that rapid equilibration conditions prevailed to all steps except the catalytic steps. Model 4.1 shows the mechanism assumed to be operating at low propionaldehyde concentrations. A

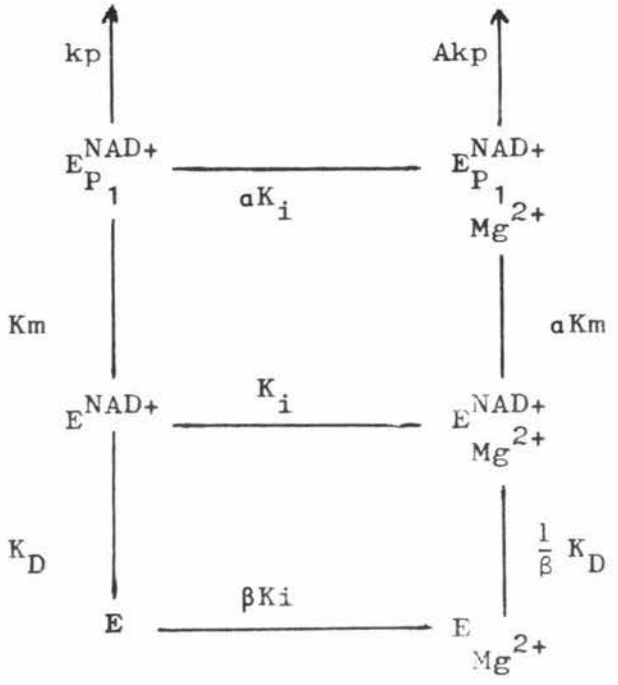

Model 4.1

value of 8.0 μM was assigned to K_D, since this was the average of the results obtained from NAD^+ titrations, and in the absence of a value for the propionaldehyde dissociation constant the Km value of 1.2 μM reported by MacGibbon et al. (1977a) was used. K_i was 320 μM as determined from NAD^+ titration, kp was set equal to 1.0 and A to 0.075 as the steady-state rate is approximately 93% inhibited by high $MgCl_2$ concentrations.

Initially simulations were carried out with $\alpha = \beta = 1$, that is assuming that the affinity of the enzyme for NAD^+ and propionaldehyde was unchanged in the presence of $MgCl_2$ and that a K_i value of 320 μM applied for Mg^{2+} binding to E, E^{NAD+} and $E^{NAD+}_{P_1}$. However it was found that with these values the results of the simulations differed from the experimental data. The simulations predicted a noncompetitive

inhibition pattern when the reciprocals of initial velocity and propionaldehyde concentration are plotted, whereas an uncompetitive pattern is observed experimentally. An uncompetitive pattern was obtained from simulations of 4.1 if it was assumed that Mg^{2+} bound more tightly to $E_{P_1}^{NAD+}$ than to either E^{NAD+} or E and thus (by the principle of microscopic reversibility) propionaldehyde binds more tightly to E^{NAD+} (i.e. $\alpha < 1$). The best fit resulted when α was 0.25 and B was 1.0, in this case the double reciprocal plots of initial velocity versus both propionaldehyde and NAD^+ concentrations appeared to be uncompetitive, and the replots were non-linear although in the $MgCl_2$ concentration range used in experiments the non-linearity was hard to detect (Figs. 4.18 and 4.19). The K_i values obtained from replots of the simulated double reciprocal plots were relatively insensitive to the values assigned to α and β, and a K_i value of 250 to 300 μM could be obtained from replots of the data obtained with both NAD^+ and propionaldehyde as the varied substrate when α was varied from 1 to 0.25 and β from 1 to 1000.

Model 4.2 shows the mechanism assumed to be operating at high propionaldehyde concentrations, and although the mechanism appears complex, the rapid equilibrium equations can be derived without knowing all the equilibrium constants. The values for K_D, K_{m1}, K_i, α, β and A were those used in the simulation of model 4.1. K_{m2} was the Km value reported for the low affinity propionaldehyde binding site (MacGibbon *et al.*, 1977a) and B was set to 3.0 since the k_{cat} value for the steady-state reaction increases by a factor of 3 going from a propionaldehyde concentration of 100 μM to 20 mM. C was determined by trial and error. The results of simulations of model 4.2 using these parameters showed non-linear double reciprocal plots of initial velocity versus propionaldehyde concentration, similar to that observed experimentally, indicating that the model is a good approximation to the actual experimental mechanism (Fig. 4.20).

FIG. 4.18 SIMULATED DOUBLE RECIPROCAL PLOT OF v VERSUS [ALDEHYDE] AT LOW LEVELS OF PROPIONALDEHYDE WITH ADDED $MgCl_2$

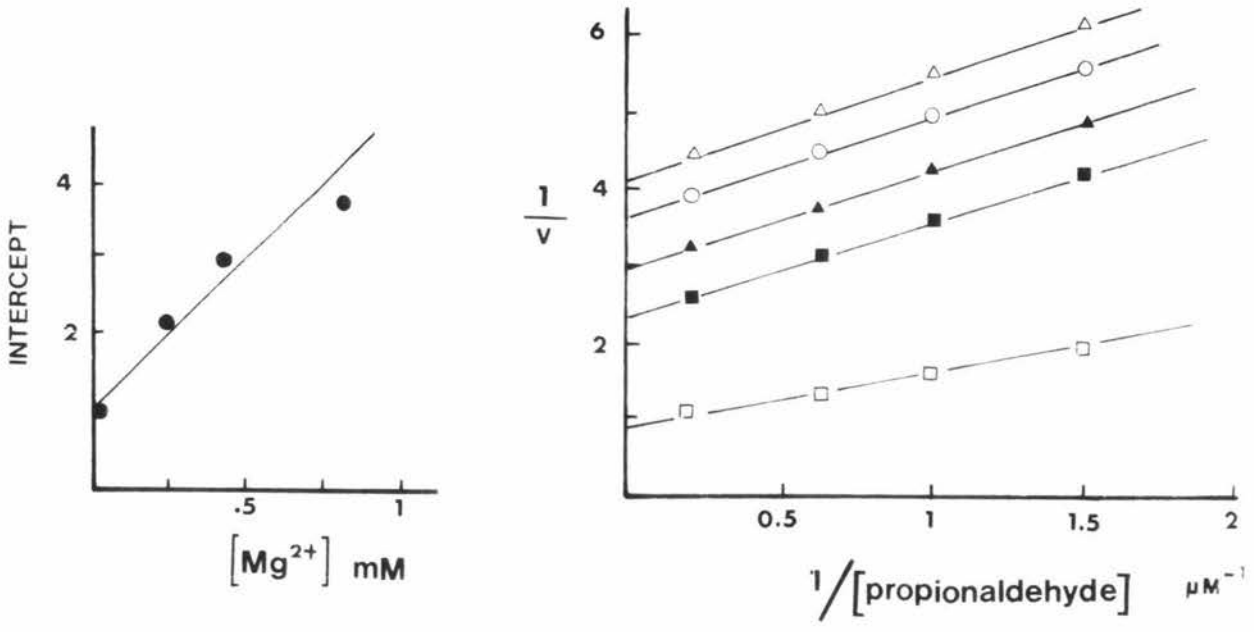

The NAD concentration was 444 μM and the $MgCl_2$ concentration varied as follows, △ 1.0 mM, ○ 0.8 mM, ▲ 0.4 mM, ■ 0.2 mM and □ no $MgCl_2$

FIG. 4.19 SIMULATED DOUBLE RECIPROCAL PLOT OF v VERSUS $[NAD^+]$ WITH ADDED $MgCl_2$

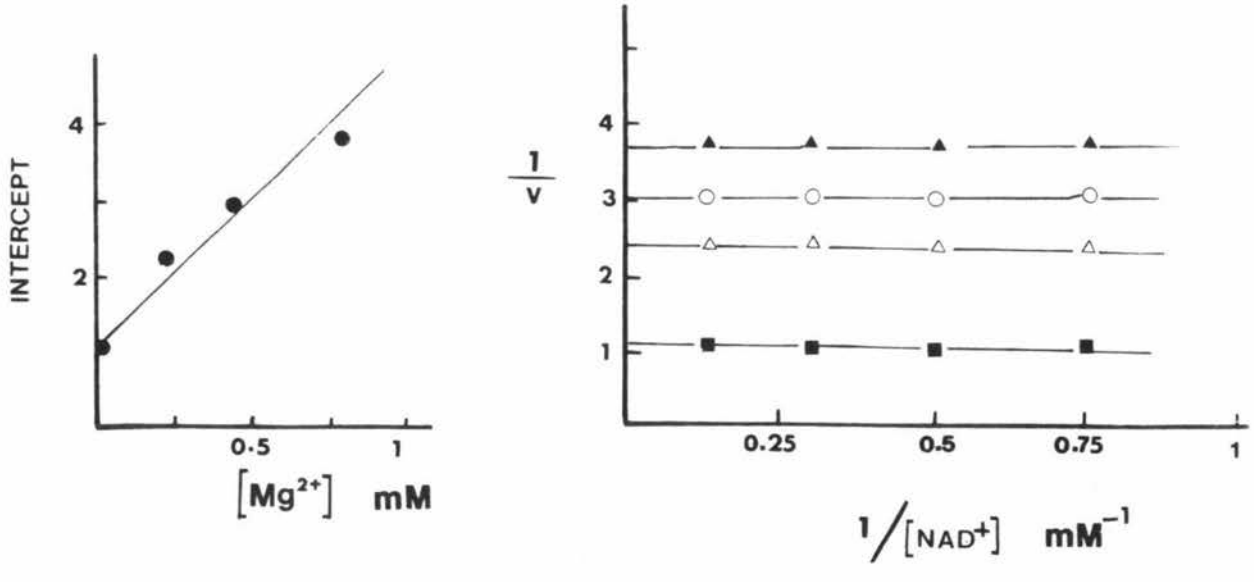

The propionaldehyde concentration was 60 μM and the $MgCl_2$ concentration varied as follows, ▲ 0.8 mM, ○ 0.4 mM, △ 0.2 mM and ■ no $MgCl_2$.

FIG. 4.20 SIMULATED DOUBLE RECIPROCAL PLOT OF v VERSUS [ALDEHYDE] AT HIGH LEVELS OF PROPIONALDEHYE WITH ADDED $MgCl_2$

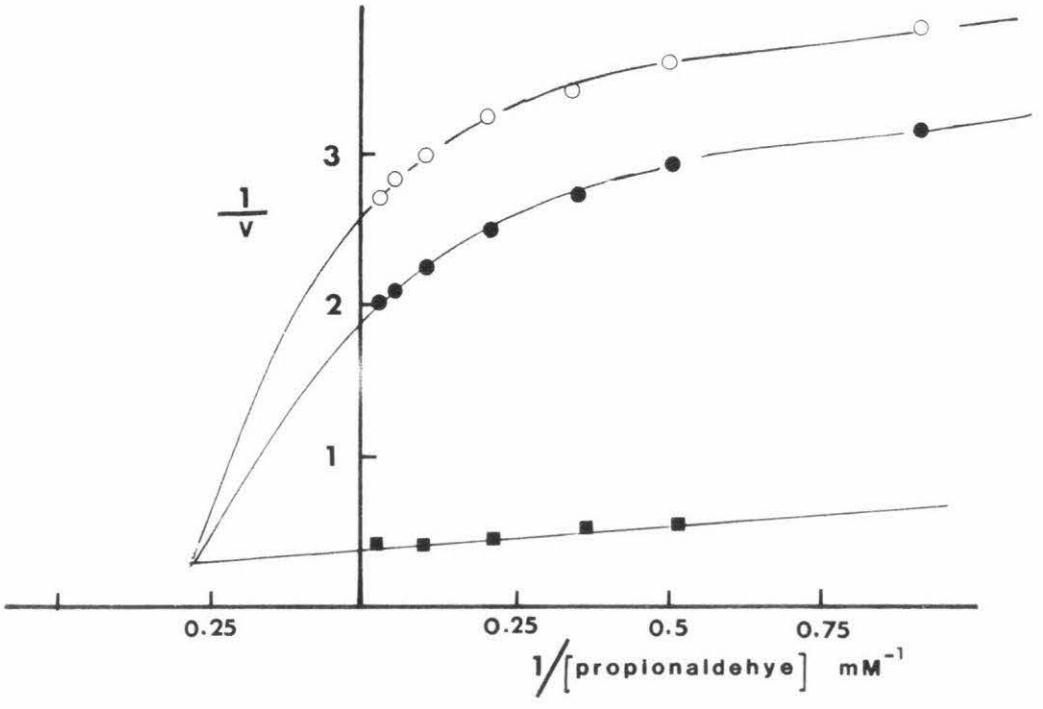

The NAD^+ concentration was 444 µM and the $MgCl_2$ concentration varied as follows, ○ 1.6 mM, ● 0.8 mM and ■ no $MgCl_2$.

FIG. 4.21 SIMULATED DOUBLE RECIPROCAL PLOT OF v VERSUS [PNPA] WITH ADDED NAD^+ AND $MgCl_2$

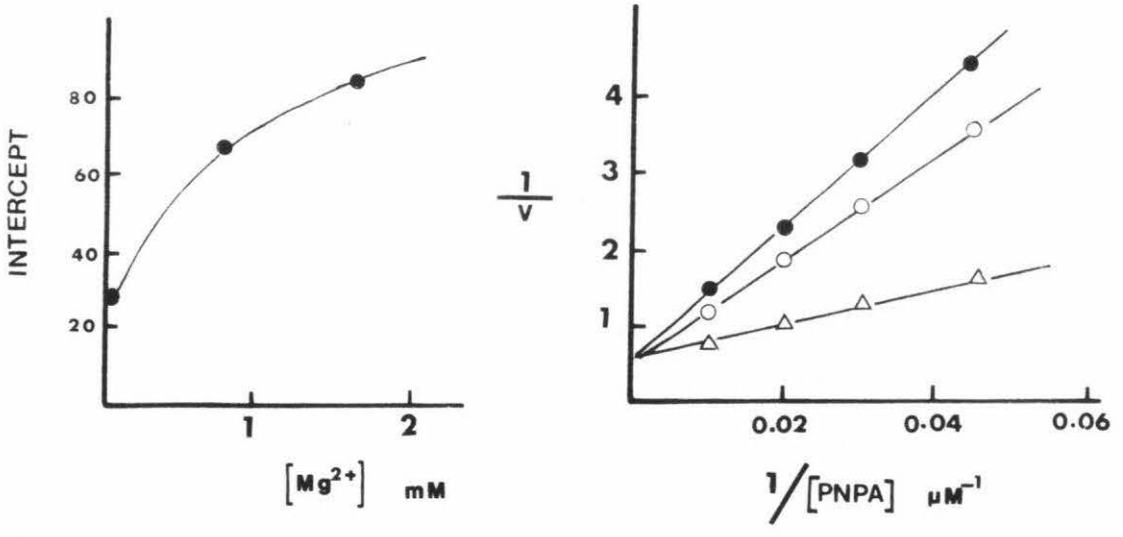

The NAD^+ concentration was 100 µM and the $MgCl_2$ concentration varied as follows, ● 1.6 mM, ○ 0.8 mM and △ no $MgCl_2$.

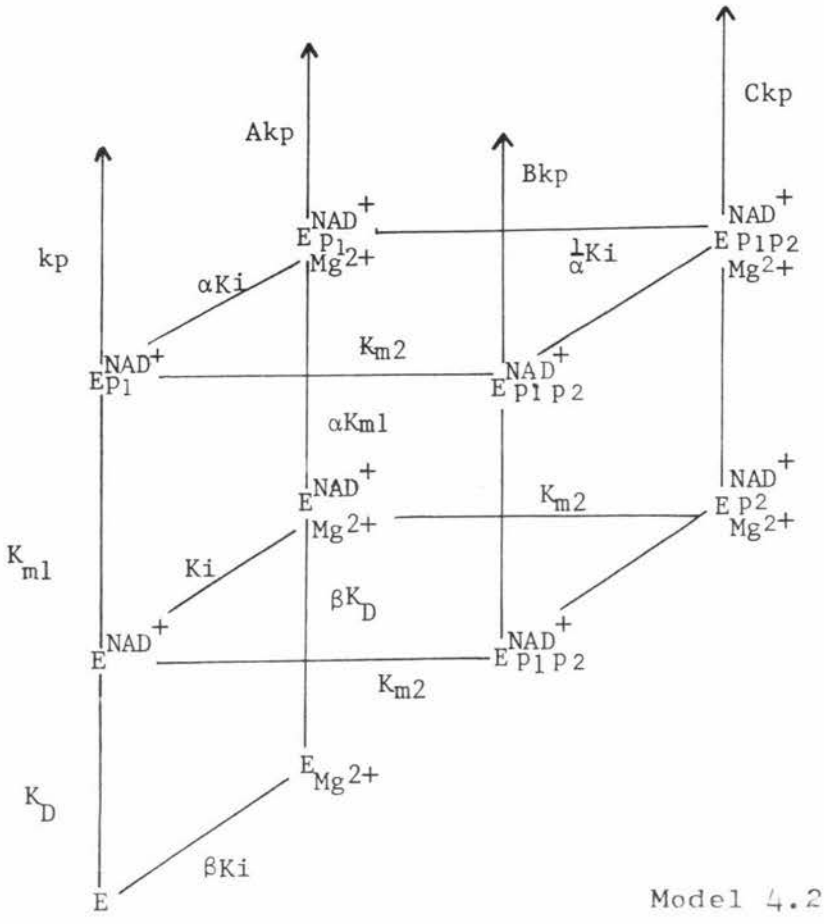

Model 4.2

The effect of Mg^{2+} on the esterase reaction also appears to be complex. The absence of any effect by $MgCl_2$ in the absence of NAD^+ can be explained in two ways;

(1) Mg^{2+} does not bind to the enzyme in the absence of NAD^+
(2) Mg^{2+} binds to the enzyme but does not exert any effect until NAD^+ binds.

Both explanations however assume that the binding of NAD^+ to the enzyme results in some change in the enzyme structure. A change, such as a conformational change, would also explain the activation observed when NAD^+ is added to an assay containing 4-nitrophenylacetate and enzyme (MacGibbon et al., (1978a) and the quenching of protein fluorescence when NAD^+ binds to the enzyme (MacGibbon et al., 1977c). This conclusion is further supported by the observation that NAD^+ analogues, with the exception of deamino NAD^+ which acts as substrate, have an entirely different effect in the presence

of $MgCl_2$. The NAD^+ analogues 3-acetyl pyridine adenine dinucleotide, 3-pyridine-aldehyde adenine dinucleotide and ADP^{3-} when added to esterase assays, resulted in inhibition rather than activation as observed for NAD^+, and when $MgCl_2$ was added to assays containing these analogues, activation, rather than further inhibition resulted. It can be seen that only coenzymes which act as substrates cause $MgCl_2$ to inhibit the esterase reaction.

Any change in the enzyme induced by NAD^+ must be different to that induced by NADH since the presence of $MgCl_2$ and NADH does not result in any significant inhibition. As Kitson (1981) has observed non-linear reaction rate versus time plots for the esterase reaction in the presence of NAD^+, it is not altogether surprising that the addition of $MgCl_2$ results in even more non-linearity. However it is interesting to note that the degree of inhibition caused by the addition of $MgCl_2$ to an assay containing enzyme and NAD^+ is the same at time Δt whether $MgCl_2$ is added before the reaction is initiated, or added at time Δt. This result indicates that one of the reaction products may be involved in the mechanism of $MgCl_2$ inhibition.

Model 4.3 was proposed in order to attempt to simulate the experimentally observed data. In this model it is assumed Mg^{2+} does not bind to enzyme in the absence of NAD^+, or that if it does, the subsequent binding and hydrolysis of the ester is not affected. The value used

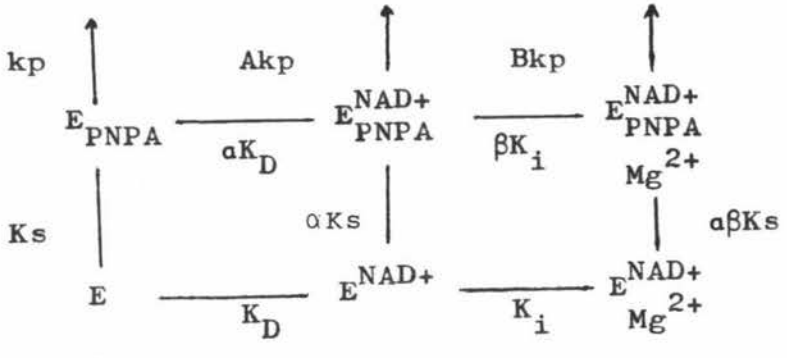

(Model 4.3)

for K_s was 5 μM, this being the Km value reported for PNPA binding to the enzyme reported by (MacGibbon et al., 1978a). α was set to 12.6 as these workers have also reported that the Km value for PNPA binding to the E^{NAD+} complex is 63 μM. K_i and K_1 were 320 μM and 8 μM as determined for the preceding simulations, and β was estimated by trial and error. A value of two assigned to A as a two-fold increase in the rate of the esterase reaction has been observed in the presence of NAD^+ (MacGibbon et al, 1978a)and B was also determined by trial and error.

It was observed that model 4.3 could reproduce the experimental data in the situation where the presence of NAD^+ and Mg^{2+} lowered the affinity of the enzyme for PNPA, but did not affect the rate of the hydrolysis reaction ($B = 2$, $\beta > 1$). The best fit was obtained when β was equal to 3.2 (Fig. 4.21).

The simulations of both the esterase and the dehydrogenase models indicate that substrate binding is affected by $MgCl_2$. The affinity of the enzyme for propionaldehyde at low concentrations is increased by $MgCl_2$, whereas for 4-nitrophenylacetate and propionaldehyde at high concentrations the affinity is decreased. This result is consistent with the suggestion that there may be two distinct substrate binding sites on the enzyme. Thus although the possibility of other kinetically equivalent models cannot be entirely excluded, the rapid equilibrium models (4.1, 4.2 and 4.3) proposed here, are excellent models which fit a wide range of the observed experimental results obtained in this study.

4.6 CONCLUSION

The mechanism of inhibition of the dehydrogenase reaction by $MgCl_2$ appears to be a slowing of the rate determining step and not a change in the number active sites per enzyme tetramer, as is the case for the F_2 horse liver aldehyde

enzyme. The experimental data suggests that cytoplasmic sheep liver dehydrogenase may contain a metal binding site which either, is only exposed when NAD^+ is bound to the enzyme, or can only exert an effect at the active site when NAD^+ is bound.

The results of this study show that cytoplasmic aldehyde dehydrogenase is greatly inhibited by concentrations of Mg^{2+} similar to those found in cells. However the concentration of free Mg^{2+} in the cell is extremely small as most of the ion is complexed by nucleotides and protein molecules. Therefore it is extremely unlikely that the enzyme is inhibited to any significant extent in vivo by intracellular Mg^{2+}.

SECTION 5

PRE-STEADY-STATE STUDIES ON THE EFFECTS OF $MgCl_2$ ON CYTOPLASMIC ALDEHYDE DEHYDROGENASE

5.1 INTRODUCTION

Steady-state studies on the effects of $MgCl_2$ on aldehyde dehydrogenase are not sufficient to identify which rate constants or intermediates are affected by $MgCl_2$. Equilibrium studies revealed changes in the dissociation constants for NAD^+ and NADH, however it was not possible to determine whether the decrease in K_D was caused by an increase in the coenzyme binding step or a decrease in the dissociation step. Pre-steady-state studies can provide more information about the individual rate constants, such as those involved in the binding and dissociation processes, and the effect $MgCl_2$ has on these rate constants.

5.1.1 NADH Displacement Experiments

If a solution contains an enzyme and quantities of NAD^+ and NADH (which both bind at the same site on the enzyme) according to equations 6.1 and 6.2, then there will be competition between the two species for the binding site.

$$E + NADH \underset{k_{-1}}{\overset{k_{+1}}{\rightleftharpoons}} E^{NADH} \qquad (6.1)$$

$$E + NAD^+ \underset{k_{-2}}{\overset{k_{+2}}{\rightleftharpoons}} E^{NAD+} \qquad (6.2)$$

When a solution containing enzyme and NADH is pushed against a solution of NAD^+ in the stopped-flow apparatus then some of the bound NADH will be displaced. If the concentration of NAD^+ is high so that $k_{+2}[NADH^+] >> k_{+1}[NADH]$, then the transient decrease in nucleotide

fluorescence due to the dissociation of NADH can be related to k_{-1} (Gutfreund, 1972).

MacGibbon et al. (1977c) have reported that the transient due to the displacement of enzyme bound NADH by NAD^+ is biphasic with rates of 0.85 s^{-1} and 0.2 s^{-1}. By using simulation and established deduction methods (Conan Doyle, 1890) they concluded that the biphasic trace was due to the mechanism shown in scheme 6.1. The process involving k_{+1} and k_{-1} was postulated as a conformational change.

$$*E^{NADH} \underset{k_{-1}}{\overset{k_{+1}}{\rightleftharpoons}} E^{NADH} \underset{k_{-2}}{\overset{k_{+2}}{\rightleftharpoons}} E + NADH$$

(Scheme 6.1)

A similar mechanism is assumed to operate in the reverse direction for the binding experiments which MacGibbon et al. (1977b) reported as also being biphasic.

5.2. METHODS

5.2.1 Apparatus

The apparatus used for the pre-steady-state experiments was that described in section 3.2.1. For experiments where fluorescence emission or quenching was monitored, the photomultiplier tube was mounted at 90° to the incident light path. Nucleotide fluorescence was exited with radiation at 340 nm and observed through wratten 47B and 2B filters which together have a maximum transmittance at 435 nM. Protein fluorescence was exited with radiation at 290 nm and observed through a wratten 18A filter which has a maximum transmittance at 340 nm.

5.2.2 Standardisation of Fluorescence Signal

The fluorescence was standardised by measuring the fluorescence of solutions containing known concentrations of NADH. The voltage reading was recorded with the buffer only in the observation chamber, then the voltage change when a solution of NADH of known concentration was forced into the observation chamber was recorded. For nucleotide fluorescence the photomultiplier was set to 825 V for the xenon lamp and 950 V for the tungsten lamp.

5.2.3 Preparation of Solutions

Solutions were made up in 35 mM pH 7.6 phosphate buffer which had been degassed on a water pump for 30 minutes prior to use. The concentration of NADH was determined by absorbance measurements at 340 nm and the enzyme concentration by assay as described in Section 3.2.1.1 or NADH titration as described in Section 3.2.1.2. Where 4-nitrophenylacetate was used as a substrate, a stock solution was prepared in acetonitrile then diluted with phosphate buffer so that the final concentration of acetonitrile was less than 3% v/v.

5.3 TREATMENT OF DATA

5.3.1 Burst Experiments

The data from burst experiments was collected and analysed as described in section 3.3.2.2.

5.3.2 Displacement Experiments

NADH displacement experiments, and other experiments such as NADH association experiments which resulted in biphasic reaction traces, were treated by either of two methods. If the rates of the two processes were sufficiently different (a difference of 10X or greater), a sweep time was selected which caused the faster exponential to appear as a single exponential followed by a steady-state process. The faster process could then be treated

as for a burst experiment (Section 3.3.2.2). By selecting a slower sweep time the slower process could also be treated as a burst experiment if the first 20% or so of the transient was discarded. The amplitude of the slower process was calculated by extrapolating the log difference plot back to time zero, and the amplitude of the faster process calculated by subtracting the amplitude of the slower process from the total transient amplitude.

Where the rates of the two processes were much closer together, but still separated by a factor of 3 or more, a method described by Gutfreund (1972) was used. The slower process was treated as a single exponential, with a baseline being drawn through the steady-state process to time zero. Then the log of the fluorescence difference between the transient and the baseline was plotted against time (Fig. 5.1.a) and the rate constant was obtained by multiplying the slope by -2.303. The rate constant for the faster process could then be obtained by plotting the log of the difference between the line obtained from the first log difference plot and the residue of the first plot (Fig. 5.1.b), then multiplying the slope of the line by -2.303. In this study the computer program described in Section 3.3.2.2 was used to perform these calculations (Fig. 5.2).

5.3.3 Calculation of Nucleotide Fluorescence Amplitudes

Voltage changes associated with the production, binding or dissociation of NADH were equated with the fluorescence of a known quantity of NADH by the calibration procedures described in Section 5.2.3. The amplitude of the process being observed could then be calculated using the enhancement factors calculated in section 4.4.10.

5.4 RESULTS

5.4.1 The effect of $MgCl_2$ on NADH Displacement

When NAD^+ (3 mM) was pushed against enzyme (3 μM) and NADH (18 μM) in the stopped-flow apparatus, a

FIG. 5.1 GRAPHICAL DERIVATION OF THE RATE CONSTANTS FOR A PROCESS INVOLVING TWO FIRST ORDER REACTIONS

(a) The slower process

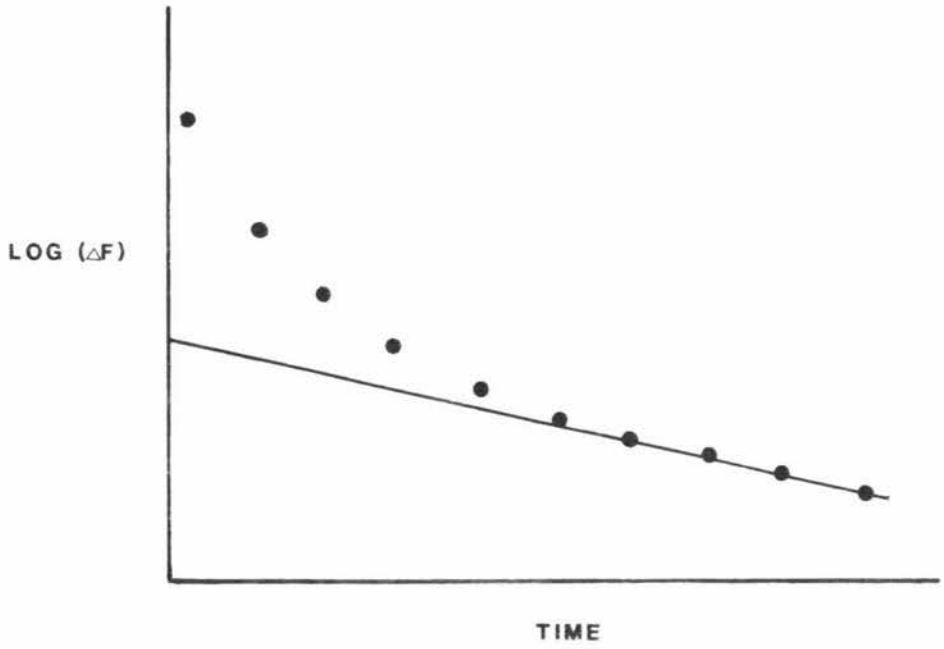

The plot shows the result of the log of the difference between the transient and the baseline, the rate of the slower process equals -2.303 x the slope of the line.

(b) The faster process

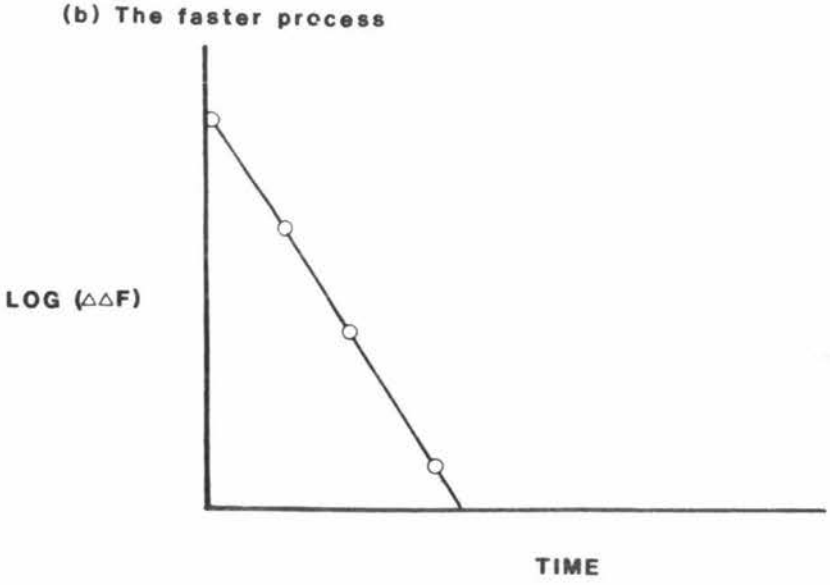

The plot shows the result of the log of the difference between the first log difference plot and the residue in (a), the rate of the faster process equals -2.303 x the slope of the line.

FIG. 5.2 Analysis of a Biphasic Transient By Computer

The trace shows the biphasic change in nucleotide fluorescence when NADH is displaced from the enzyme by NAD^+. Line A is a horizontal line fitted by least squares analysis through the last 10% of the trace, line B is a log difference plot between the baseline (A) and the transient and line C is a least squares line through the lower half of the log difference plot. The inset shows the log difference plot between line C and line B with a least squares line through it.

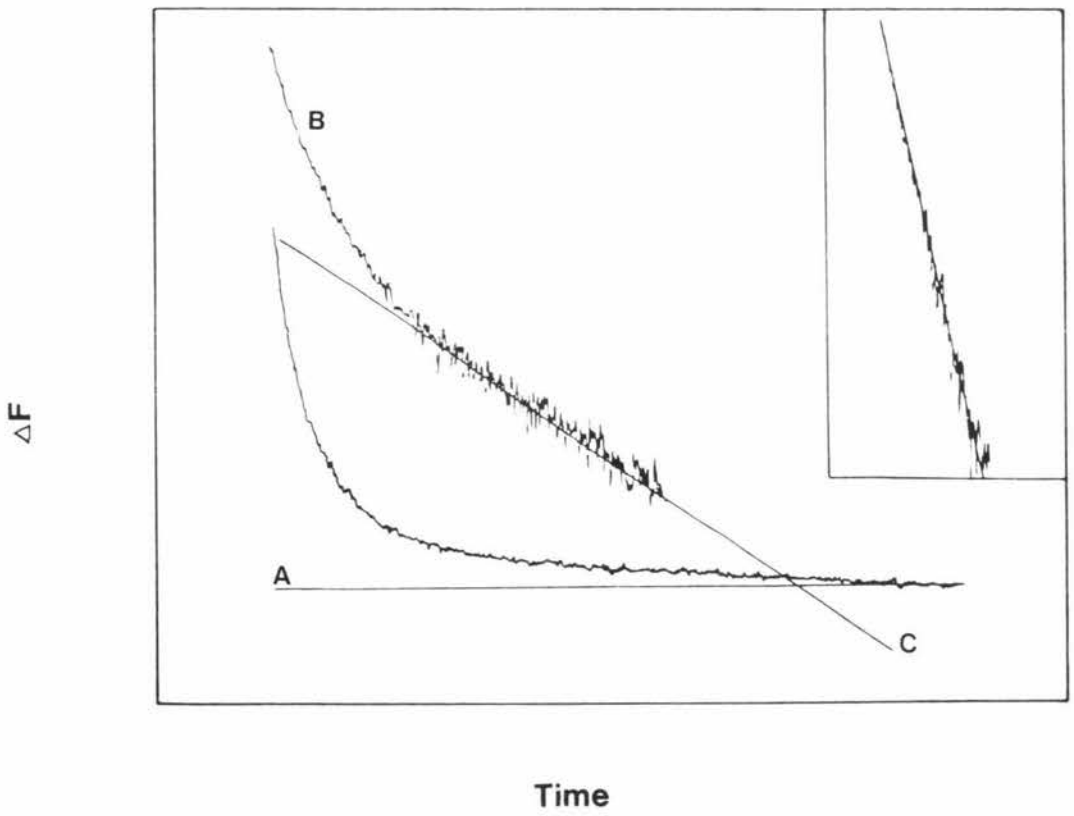
B
A
C
ΔF
Time

biphasic displacement curve was observed when the fluorescence at 435 nm was monitored (Fig. 5.3a). The rates of the two exponentials, 0.8 s^{-1} and 0.23 s^{-1}, are in good agreement with those reported by MacGibbon et al. (1977b) of 0.85 s^{-1} and 0.20 s^{-1}. The amplitude of the displacement was equal to 85% to 100% of the enzyme active site concentration as determined by NADH titration, also in good agreement with the value reported by these workers.

The addition of $MgCl_2$ in millimolar concentrations to either the NAD^+ or the enzyme syringe resulted in marked changes to the displacement curve (Fig. 5.3b). There was a considerable decrease in the rates of both of the displacement processes, the slower now having a rate of 0.025 s^{-1} and the faster 0.3 s^{-1}. Due to the very slow rate of the second process it was necessary to follow the reaction for more than 250 seconds to obtain the fluorescence at infinite time. At sweep times of this length it was difficult to distinguish the displacement signal from machine drift. The fluorescence change observed on NADH displacement in the presence of $MgCl_2$ was greater than that in the absence of $MgCl_2$, on average the absolute voltage change was 1.5X larger in the presence of $MgCl_2$, however when the enhancement factor of 18 (Section 4.4.10) is used the amplitude of the displacement process is approximately 50% of the enzyme active site concentration.

5.4.2 NADH Displacement in Absorbance

By utilizing the difference in absorption between free and enzyme bound at 328 nm (MacGibbon et al., 1979), it was possible to follow the displacement reaction in absorbance. The displacement in the absence of $MgCl_2$ resulted in a biphasic trace with rates of 0.65 s^{-1} and 0.2 s^{-1}, similar to those observed in nucleotide fluorescence. When $MgCl_2$ (5 mM) was added, a decrease in the displacement rates to 0.2 s^{-1} and 0.02 s^{-1} was observed. The amplitude of the displacement with

FIG. 5.3 NADH Displacement in Nucleotide Fluorescence

5.3a In the Absence of $MgCl_2$

A solution of enzyme (4.0 μM) and NADH(12.8μM) was pushed against NAD^+ (3 mM). The rate for the faster process was 0.8 s^{-1} and for the slower process 0.2 s^{-1}, the amplitude was 1.7 μM. 1 volt corresponded to the fluorescence of 13.7 μM NADH.

5.3b With Added $MgCl_2$

A solution of enzyme (3.0 μM), NADH (12.8 μM) and $MgCl_2$ (3.5 mM) was pushed against NAD^+ (3 mM). The rate for faster process was 0.097 s^{-1} and the rate for the slower process was 0.024 s^{-1}. The amplitude was 0.67 μM (assuming an enhancement factor of 18). 1 volt corresponded to the fluorescence of 15.7 μM of NADH.

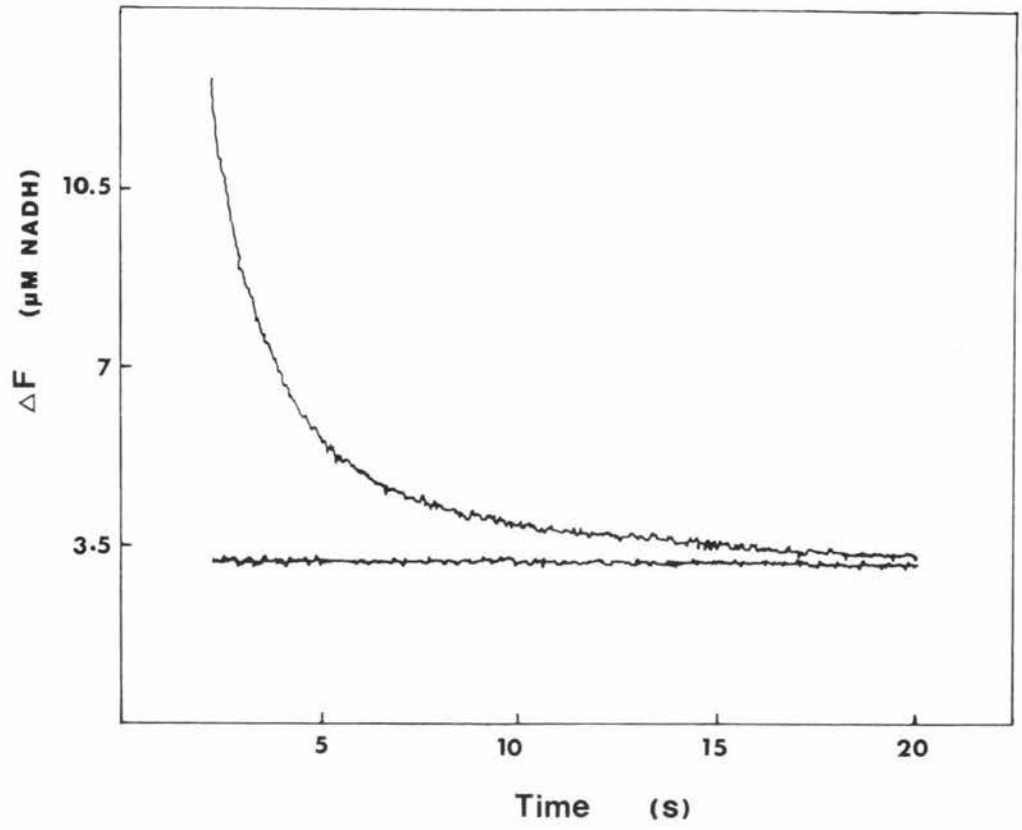
ΔF (μM NADH)
10.5
7
3.5
5
10
15
20
Time (s)

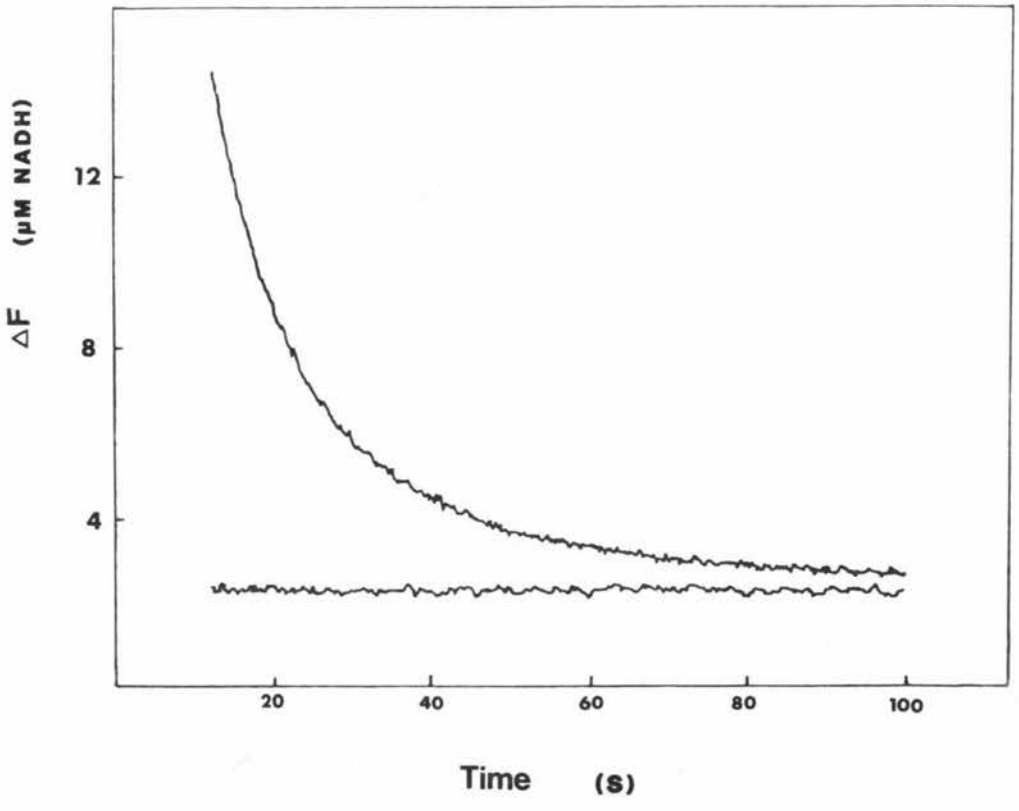
ΔF (μM NADH)
12
8
4
20
40
60
80
100
Time (s)

$MgCl_2$ (3.3 mM) added was larger than the displacement in the absence of $MgCl_2$, consistent with the results of the UV difference spectra experiments (Section 4.4.9) where the difference in absorption between free and enzyme-bound NADH was greater at 328 nm in the presence of $MgCl_2$. The change in extinction coefficient at 328 nm calculated from the displacement experiments was 481 l $mol^{-1}cm^{-1}$ in the absence of $MgCl_2$ and 813 l $mol^{-1}cm^{-1}$ with $MgCl_2$ added.

5.4.3 The Effect of Trisodium Citrate on NADH Displacement

When trisodium citrate was added to the NAD^+ syringe in NADH displacement experiments, a small increase in the displacement rates was observed. With 60 mM citrate present the rate of the faster process was 2.9 s^{-1} and that of the slower 0.5 s^{-1}.

The addition of citrate to the syringe containing NAD^+ in displacement experiments, where the enzyme-NADH containing syringe contained added $MgCl_2$, resulted in the removal of the inhibitory effect of $MgCl_2$ on the displacement rates, until at citrate concentrations tenfold greater than the $MgCl_2$ concentration, the effects of $MgCl_2$ were completely removed.

5.4.4 The Effect of $MgCl_2$ on NADH Association

5.4.4.1 Association experiments utilizing nucleotide fluorescence

When enzyme (3 μM) is pushed against NADH (18 μM) in the stopped-flow apparatus a biphasic binding curve was observed with the faster process having a rate of 5 ± 2 s^{-1} and the slower a rate of 1 ± 0.2 s^{-1} (Fig. 5.4.a). The amplitude of the binding process was greater than 90% of the NADH binding site concentration. These results are in good agreement with those published by MacGibbon *et al.* (1977b) of 7 ± 2 s^{-1} for the faster process 1.2 ± 0.3 s^{-1} for the slower at the same NADH concentration.

FIG. 5.4 NADH Association in the Presence and Absence of $MgCl_2$ Utilizing Nucleotide Fluorescence

5.4a NADH Association in the absence of $MgCl_2$

A solution of enzyme (3 μM) was pushed against NADH (18 μM). The rate of the slower process was 2.5 s^{-1} and that of the faster 0.9 s^{-1}. The amplitude was 1.5 μM and 1 volt corresponds to the fluorescence of 13.3 μM NADH.

5.4b NADH Association with $MgCl_2$ Present

A solution of enzyme (3 μM) was pushed against NADH (18 μM) and $MgCl_2$ (7 mM). The rate of the faster process was 10.3 s^{-1} and the slower process 1.15 s^{-1}. The amplitude was 1.46 μM (assuming an enhancement factor of 18), 1 volt corresponds to 13.28 μM NADH.

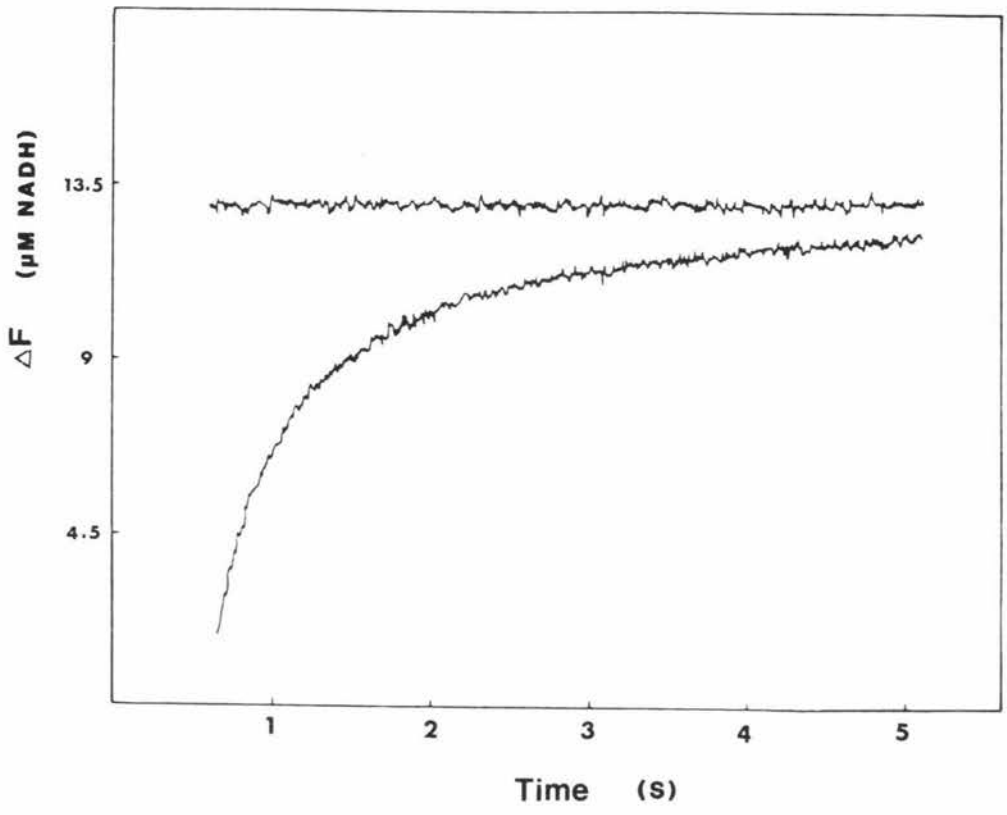
ΔF (μM NADH)
13.5
9
4.5
1
2
3
4
5
Time (s)

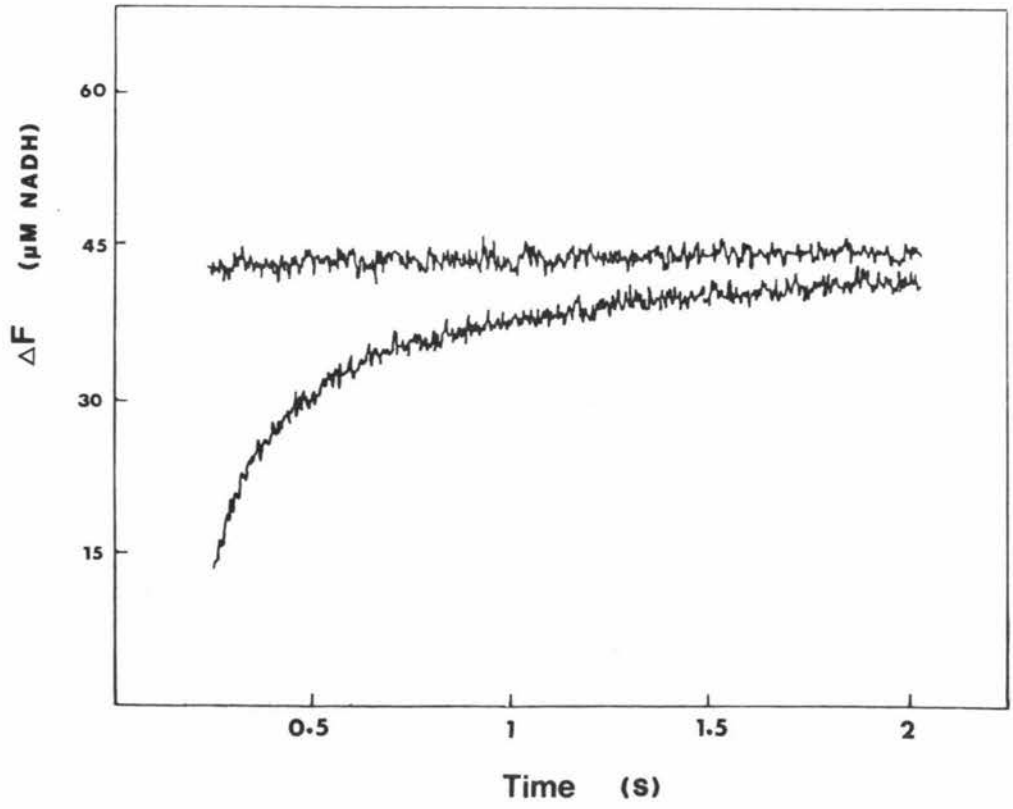
ΔF (μM NADH)
60
45
30
15
0.5
1
1.5
2
Time (s)

The addition of $MgCl_2$ (3.5 mM) to either the enzyme or NADH syringes resulted in a slight increase in the rates of both the fast and slow processes to 8 $\pm$ 2 s^{-1} and 1.3 $\pm$ 0.25 s^{-1} respectively (Fig. 5.4.b). The amplitude of the fluorescence change on NADH binding in the presence of $MgCl_2$ was several times larger than that observed in the absence of $MgCl_2$, however when the fluorescence enhancement factor of 18 is used, the amplitude of the binding process was calculated to be equal to the NADH binding site concentration.

5.4.4.2 Association experiments utilizing protein fluorescence quenching

The binding of NADH to the enzyme can also be observed by monitoring the quenching of protein fluroescence which occurs on NADH binding. When enzyme (3 μM) is pushed against NADH (18 μM), a biphasic quenching curve was observed with rates of 4 $\pm$ 1 s^{-1} and 0.8 $\pm$ 0.2 s^{-1} (Fig. 5.5.a). The addition of $MgCl_2$ (3.3 mM) to the enzyme solution resulted in a slight increase in the rates of the two processes to 8 $\pm$ 2 s^{-1} and 1.15 $\pm$ 0.2 s^{-1} (Fig. 5.5.b). The amplitude of the quenching process was also observed to increase in the presence of $MgCl_2$ to twice that in the absence of $MgCl_2$.

5.4.5 The Effect of $MgCl_2$ on NAD^+ Binding

The rate of NAD^+ binding can also be monitored by protein fluorescence quenching techniques (MacGibbon *et al.*, 1977c). The addition of $MgCl_2$ (3.3 mM) to the enzyme solution did not result in any change in the rate of NAD^+ binding.

5.4.6 The Effect of $MgCl_2$ on the NADH Burst

When enzyme is pushed against saturating concentrations of NAD^+ (> 400 μM) and propionaldehyde (> 1 mM), a burst in the production of NADH is observed when the fluorescence at 435 nm is monitored (MacGibbon *et al.*, 1977c). The burst has a rate of 11 s^{-1} and an

FIG. 5.5 NADH Association Utilizing Protein Fluorescence Quenching

5.5a NADH Associating in the Absence of $MgCl_2$

A solution of enzyme (3 μM) was pushed against NADH (18 μM). The rate of the faster process was 2.01 s^{-1} and the rate of the slower is 0.25^{-1}. The amplitude was 0.6 v.

5.5b NADH Association in the Presence of $MgCl_2$

A solution of enzyme (3.9 μM) was pushed against NADH (18 μM) and $MgCl_2$ (3.5 mM). The rate of the faster process was 3.45 s^{-1} and the slower 0.4 s^{-1}. The amplitude was 0.98 v.

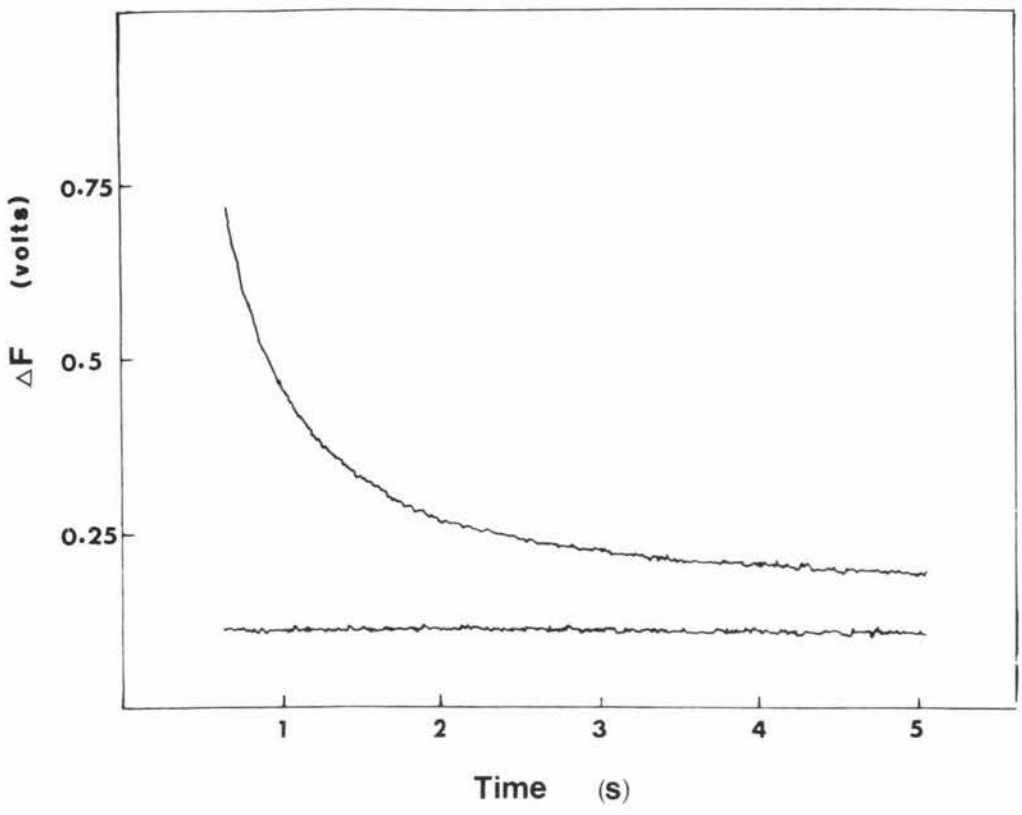
0.75
0.5
0.25
ΔF (volts)
1
2
3
4
5
Time (s)

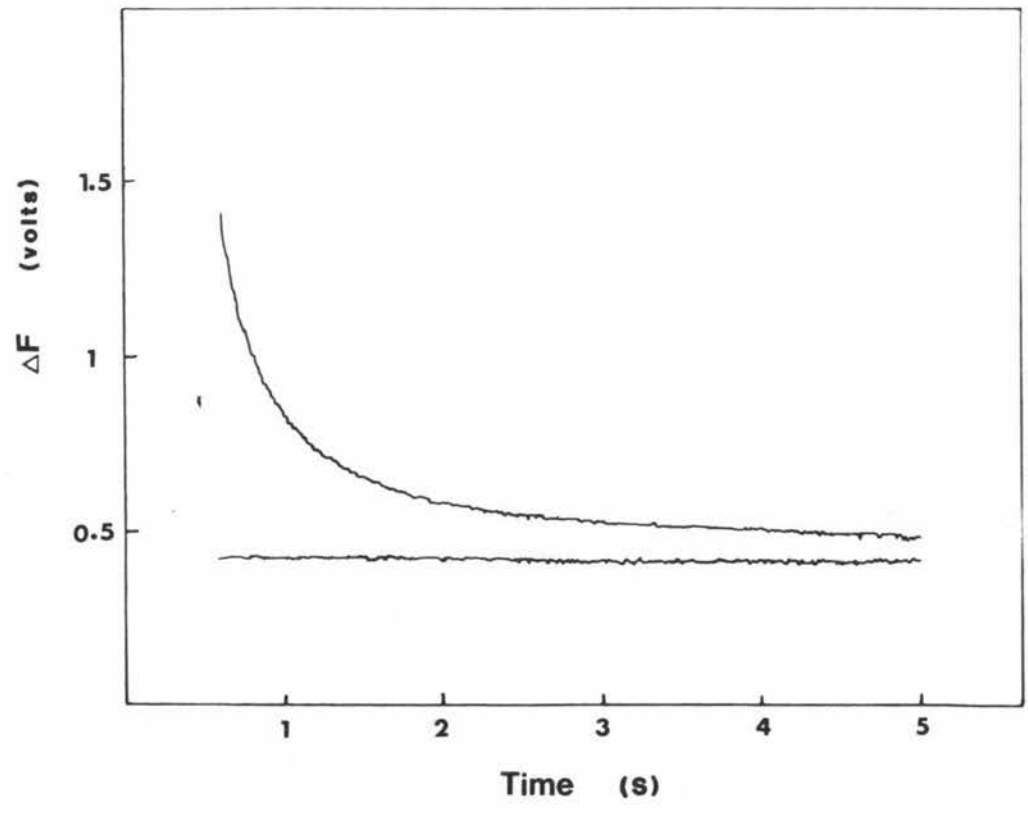
1.5
1
0.5
ΔF (volts)
1
2
3
4
5
Time (s)

amplitude equal to the enzyme active site concentration (Fig. 5.6a). When the experiment was repeated with $MgCl_2$ (3.3 mM) added to the enzyme solution, an approximately 25% increase in the burst rate to 15 s^{-1} was observed (Fig. 5.6.b). The relative fluorescence change of the burst with $MgCl_2$ added was very similar to the amplitude of the burst in the absence of $MgCl_2$, however when the enhancement factor of 18 (Section 4.4.10) was used, the amplitude of the burst was only about 30% of the active site concentration.

5.4.7 The Effect of $MgCl_2$ on the Proton Burst

When the proton burst experiment was carried out as described in Section 3.3.1.3 with $MgCl_2$ (1.6 mM) added, a proton burst was observed with an amplitude equal to 90% of the enzyme active site concentration and a rate constant of 11 s^{-1}.

5.4.8 Effect of $MgCl_2$ on the Esterase burst

When enzyme is pushed against saturating conditions of 4-nitrophenylacetate in the stopped-flow apparatus, a burst in the production of 4-nitrophenoxide ions is observed at 400 nm (MacGibbon *et al.*, 1978a) The rate of the burst was 12 $\pm$ 2 s^{-1} and the amplitude corresponded to 30% of the enzyme active site concentration. When the burst experiment was repeated with $MgCl_2$ (1.0 mM) added there was no observable change in either the burst rate constant or the burst amplitude.

Since it has been reported by MacGibbon *et al.*, (1978a)that NAD^+ activates the esterase activity, and it has been shown in this study (Section 4.4.5) that $MgCl_2$ inhibits the esterase reaction in the presence of NAD^+, it was decided to repeat the burst experiments with both NAD^+ and $NAD^+.MgCl_2$ added. The burst with 100 µM NAD^+ added had the same rate constant and amplitude as the burst in the absence of NAD^+, however the steady-state reaction following the transient process was several times

FIG. 5.6 NADH Burst in the Presence and Absence of $MgCl_2$

5.6a NADH Burst in the Absence of $MgCl_2$

The reaction mixture contained enzyme (1.5 μM), NAD^+ (1.5 mM) and propionaldehyde (20 mM). The burst rate is 9.3 s^{-1} and the amplitude was 1.48 μM. 1 volt corresponds to the fluorescence of 10.3 μM NADH.

5.6b NADH Burst in the Presence of $MgCl_2$

The reaction mixture contained enzyme (1.5 μM), NAD^+ (1.5 mM), propionaldehyde (20 mM) and $MgCl_2$ (3.7 mM). The burst rate was 12.3 s^{-1} and the amplitude was 0.41 μM (assuming an enhancement factor of 18). 1 volt corresponds to the fluorescence of 10.3 μM NADH.

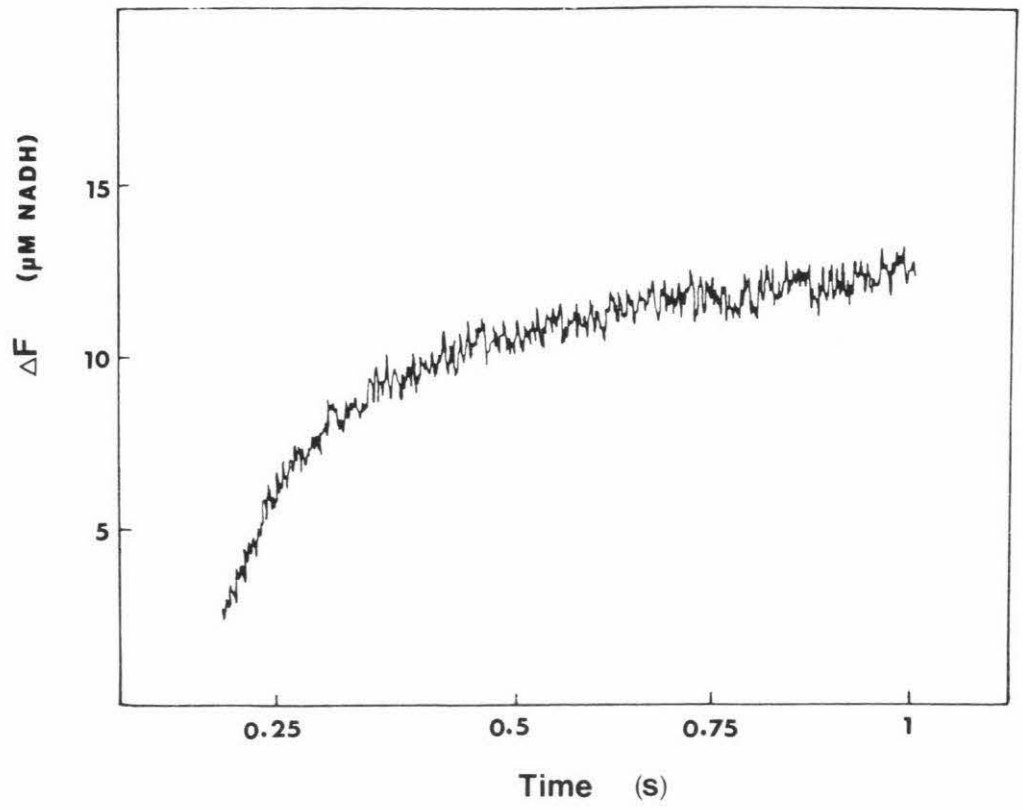
ΔF (μM NADH)
15
10
5
0.25
0.5
0.75
1
Time (s)

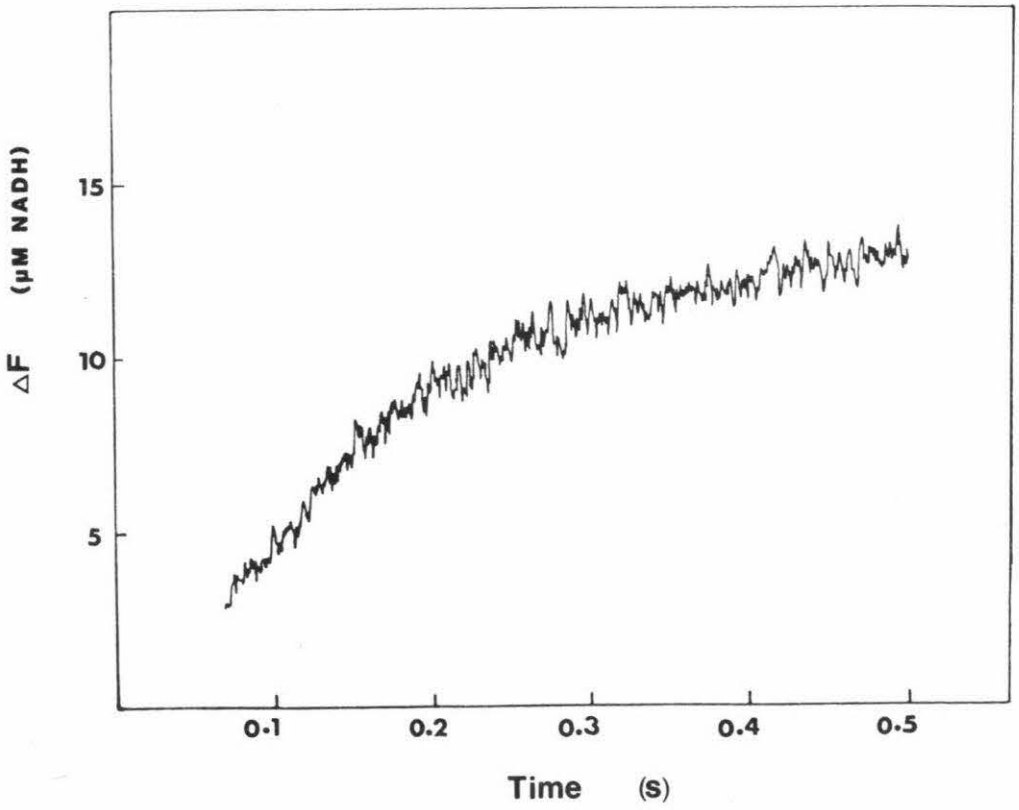
ΔF (μM NADH)
15
10
5
0.1
0.2
0.3
0.4
0.5
Time (s)

faster than the rate in the absence of NAD^+ (Fig. 5.7a). $MgCl_2$ (1.0 mM) added with NAD^+ (100 μM) to the enzyme solution also had no effect on the burst rate constant and amplitude (Fig. 5.7b), but did affect the steady-state reaction rate. The steady-state rate with added $MgCl_2$ and NAD^+ was initially faster than in the absence of both substances but slower than the rate with added NAD^+. However after about 10 seconds the rate was observed to decrease to below the rate of hydrolysis with enzyme and ester only.

5.4.9 Attempts to Determine the Rate of Nucleotide Fluorescence Enhancement

Attempts were made to determine the rate of enhancement of nucleotide fluorescence by $MgCl_2$ in the stopped-flow apparatus. If $MgCl_2$ is mixed with enzyme-NADH an enhancement of fluorescent occurs, if the rate of this process is less than about 500 s^{-1} it should be observable with a stopped-flow apparatus. When a mixture of enzyme (4 μM) and NADH (18 μM) is pushed against a mixture of NADH (14 μM) and $MgCl_2$ (1.6 mM) an increase in nucleotide fluorescence is observed (Fig. 5.8). The transient is biphasic with rates of 5.1 s^{-1} and 1.1 s^{-1}. A control experiment in which enzyme-NADH was pushed against NADH only resulted in no fluorescence change. The amplitude of the fluorescence change in the presence of $MgCl_2$ was considerably less than that expected if the process being observed was the fluorescence enhancement observed in the NADH titration experiments (Section 4). The rates of the two processes observed are in fact very similar to the rates of NADH binding (Section 5.4.5) and when the enhancement factor 18 determined in section 4.4.10 is used the amplitude corresponds to the binding of about 10% more NADH to the enzyme, a result which is consistent with the observation that the K_D value for NADH decreases in the presence of $MgCl_2$ (Section 4.4.10). When comparisons were made with NADH and enzyme-NADH only it was found that the fluorescence of the enzyme-NADH-Mg^{2+} complex was not significantly greater than that of the enzyme-NADH complex, indicating

FIG. 5.7 Esterase Burst in the Presence of NAD^+ and $NAD^+.MgCl_2$

5.7a Esterase Burst with Added NAD^+

The reaction mixture contained enzyme (4 μM), PNPA (200 μM) and NAD^+ (113 μM premixed with the enzyme). The burst rate was 10.8 s^{-1} and the amplitude was 0.7 μM.

5.7b Esterase Burst with Added NAD^+ and $MgCl_2$

The reaction mixture contained enzyme (4 μM), PNPA (200 μM), NAD^+ (113 μM) and $MgCl_2$ (0.2 mM). Both the NAD^+ and $MgCl_2$ premixed with the enzyme. The burst rate was 11.3 s^{-1} and the amplitude 0.71 μM.

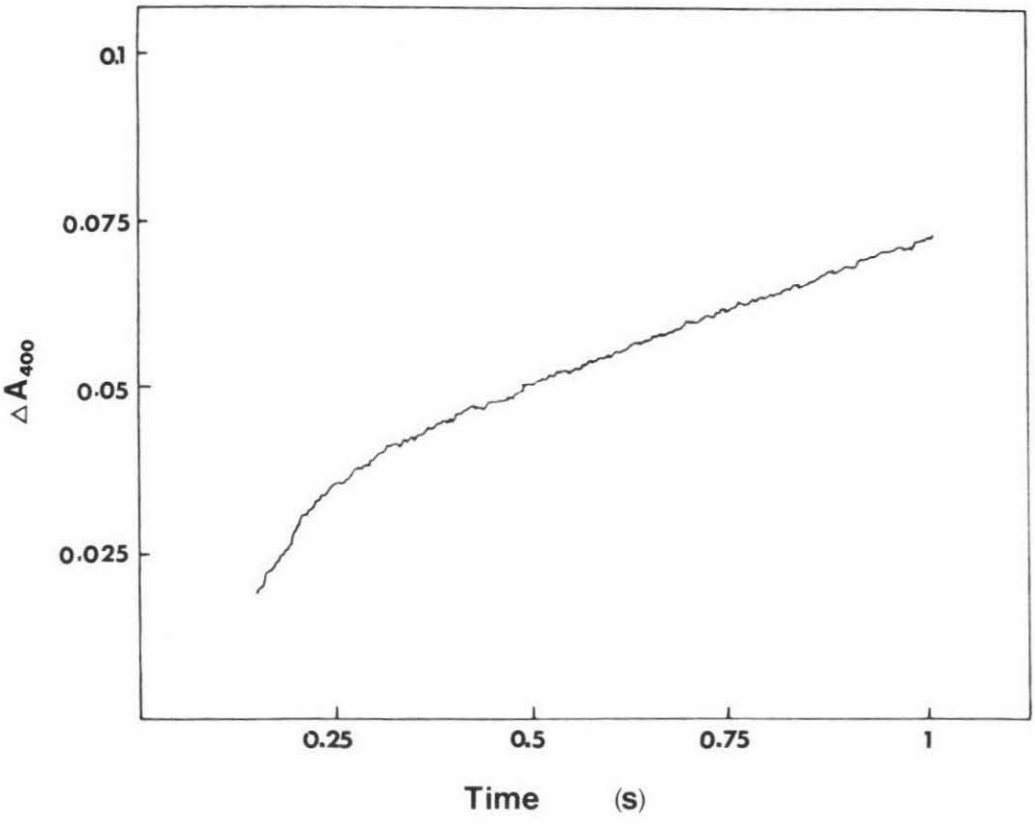
0.1
0.075
0.05
0.025
ΔA400
0.25
0.5
0.75
1
Time (s)

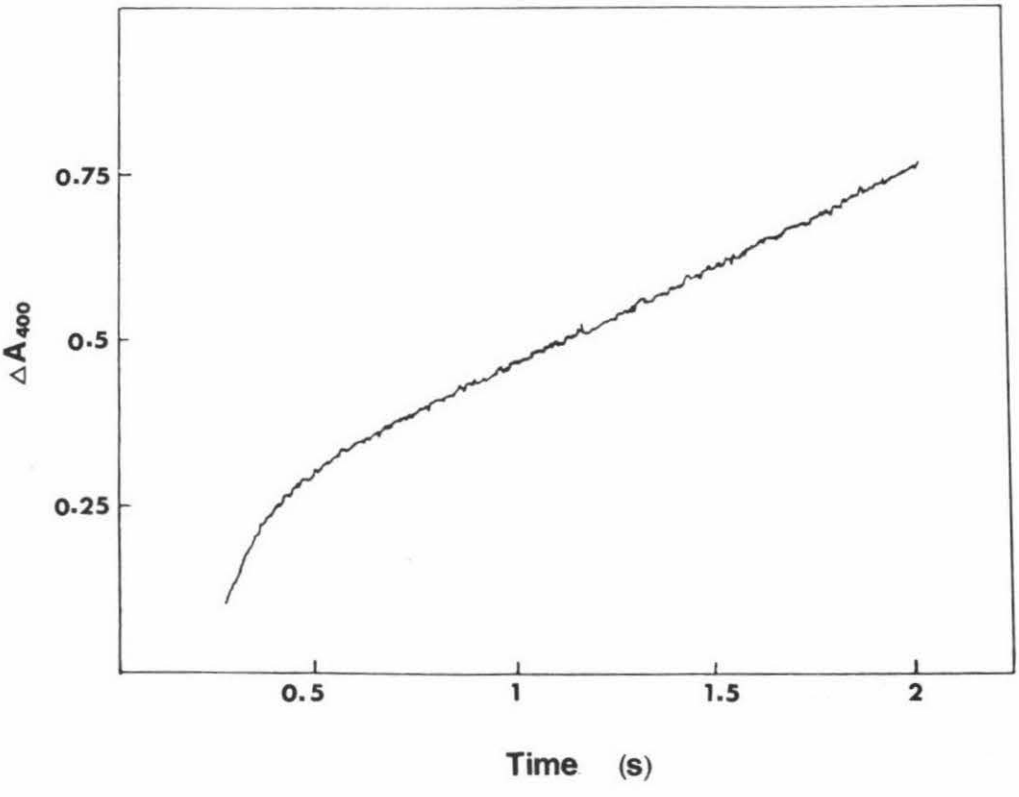
0.75
0.5
0.25
ΔA400
0.5
1
1.5
2
Time (s)

FIG. 5.8 E.NADH Versus NADH.$MgCl_2$

A solution of enzyme (3 μM) and NADH (12.8 μM) was pushed against a solution of NADH (9.8 μM) and $MgCl_2$ (3.5 mM). The rate of the faster process was 3.3 s^{-1} and that of the slower process 0.25 s^{-1}. The amplitude was 0.32 μM (assuming an enhancement factor of 18) and 1 volt equalled the fluorescence of 15.7 μM NADH.

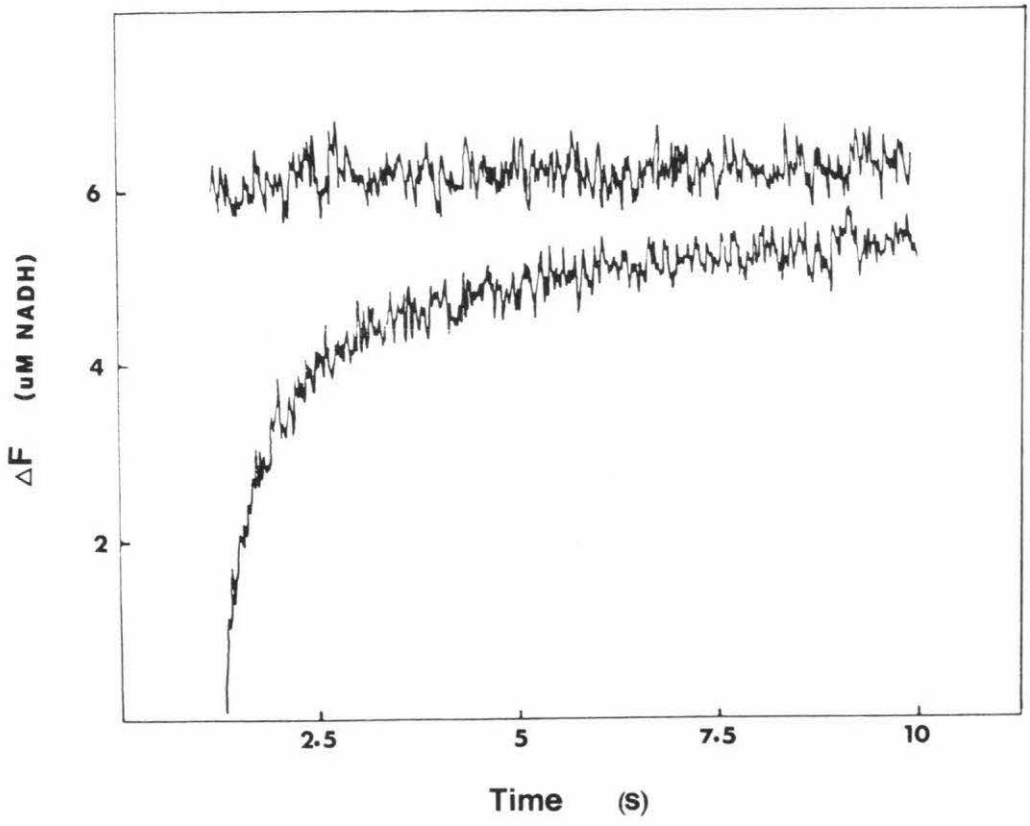
ΔF (uM NADH)
6
4
2
2.5
5
7.5
10
Time (S)

the absence of a rapid fluorescence enhancement during the mixing time of the apparatus.

5.5. DISCUSSION

The pre-steady-state experiments carried out with added $MgCl_2$ show that the major effect of $MgCl_2$ on the aldehyde dehydrogenase mechanism is to slow the steady-state rate determining step. Previous steady-state and pre-steady-state studies (MacGibbon *et al.*, 1977a,b,c) have shown that NADH dissociation is rate determining in the steady-state reaction at saturating levels of aldehyde (> 20 mM). Any slowing of this step would be expected to result in a corresponding decrease in the steady-state reaction rate. The results of displacement experiments with added $MgCl_2$ show that a considerable decrease in the displacement rates occurs, with the decrease (expressed as a percentage of the uninhibited displacement rates) being approximately equal to the percentage inhibition obtained for the steady-state reaction with the same concentration of $MgCl_2$ present. The close correlation between the decrease in the displacement rates and the inhibition of the steady-state rate indicates that at saturating aldehyde levels the inhibition by $MgCl_2$ may be due entirely to a decrease in the displacement rates. Evidence to support this conclusion comes from the observation that $MgCl_2$ does not decrease either the rates of the proton and NADH bursts, or the rate of NAD^+ binding.

At low aldehyde concentrations (< 100 μM) however the inhibition by $MgCl_2$ appears more complex. MacGibbon *et al.* (1977a,b) have reported that at propionaldehyde concentrations in this range, NADH dissociation is no longer rate limiting, the k_{cat} value now being about 30% of the rate of the slow displacement process (0.20 s^{-1}). Here the high degree of inhibition (< 90%) of the steady-state rate cannot be entirely accounted for by the effect of $MgCl_2$ on the displacement rates. A similar situation arises with aromatic aldehydes, for which the k_{cat} values are of

the order of 0.02 to 0.04 s^{-1} (MacGibbon 1976), again considerably slower than the slower NADH displacement rate of 0.2 s^{-1}. To cause the observed steady-state inhibition (approx. 88% at 1.6 mM $MgCl_2$) $MgCl_2$ must be affecting another step in the reaction mechanism, as the displacement rates in the presence of this concentration of $MgCl_2$ will be 0.25 s^{-1} and 0.02 s^{-1}, both of which are still faster than the inhibited turnover number of approximately 0.002 s^{-1} for the aromatic aldehydes. The position of the step $MgCl_2$ is affecting must be after hydride transfer, as the NADH burst rate is unaffected by the presence of $MgCl_2$, and most likely involves a slowing of either the acid product release step, or the nucleophilic attack by H_2O on the supposed acyl-enzyme-NADH intermediate.

While there was no observable effect on the proton burst by $MgCl_2$, the NADH burst amplitude observed in nucleotide fluorescence was only about 30% of the enzyme active site concentration when enhancement factor of 18 was used. Since it has been seen in Section 3.3.4 that under most conditions the proton and NADH bursts are closely coupled, it is unlikely that there is any change in the concentration of intermediates in the presence of $MgCl_2$. Therefore the fluorescence enhancement factor of 18 obviously does not apply in the NADH burst experiments. This situation may arise because of the different intermediates being observed in the titration and burst experiments. In the titration the fluorescence of an Enzyme-NADH complex is monitored, whereas the fluorescence observed in tne NADH burst may in fact result from an enzyme-Acyl-NADH intermediate rather than the enzyme-NADH complex. This intermediate could have different fluorescent properties in the presence of $MgCl_2$ than the enzyme-NADH complex observed in the **NADH** titrations, and therefore not slow any enhancement. In this case the amplitude of the NADH burst, like the proton burst, will be unaffected by the presence of $MgCl_2$.

The enhancement of nucleotide fluorescence in the presence of $MgCl_2$ observed during the NADH titrations was also observed in binding and dissociation experiments.

The fluorescence enhancement calculated from the binding experiments (18) was found to be equal to that calculated in Section 4.4.10. However when the amplitude of the displacement in the presence of $MgCl_2$ was calculated using the same fluorescence enhancement factor of 18, the resulting value was only about 60% of NADH binding site concentration. This value may be an underestimate since as the rate of the slow dissociation step was so low, the reaction may not have gone to completion when the amplitude measurements were made (typically 250 s after mixing). The absence of any significant nucleotide fluorescence enhancement when a mixture of enzyme and NADH is pushed against a solution of NADH and $MgCl_2$ is not understood. This experiment is essentially the same as adding $MgCl_2$ to a mixture of enzyme and NADH in the fluorimeter, which results in a similar fluorescence enhancement to an NADH titration. A strict comparison between the fluorescence obtained in the fluorimeter and the stopped-flow apparatus is not possible however, due to the presence of different optical systems in the two instruments. In the fluorimeter the wavelength of both the exciting and emitted radiation is controlled by a monochromator, whereas in the stopped-flow apparatus only the wavelength of the exciting radiation is controlled by a monochromator. The wavelength of the emitted radiation is controlled by two filters which have a maximum transmission at 435 nm and negligible transmission above 470 nm and below 400 nm. Thus any change in either the shape of the fluorescence profile or the wavelength at which maximum fluorescence occurs, induced by $MgCl_2$, may result in different fluorescence intensities being observed in the fluorimeter and the stopped flow apparatus. The likelihood of such a change is indicated by the significant changes in the absorption spectrum of enzyme bound NADH when $MgCl_2$ is present (Section 4.4.9).

The results of the esterase burst experiments are consistent with model 4.3 proposed in Section 4. This model predicts that $MgCl_2$ will not affect the esterase burst

in the absence of NAD^+ as was observed experimentally. With NAD^+ present a reduction in the burst amplitude would be expected at low ester concentrations, as in the presence of Mg^{2+} and NAD^+ an enzyme complex is formed which has a lower affinity for the ester, thus effectively lowering the enzyme concentration. However from Fig. 4.9 it can be seen that at an $MgCl_2$ concentration of 1.6 mM and a PNPA concentration of 200 μM (the concentrations used in the burst experiments) even the enzyme-NAD^+-Mg^{2+} complex will be saturated with ester. In this case very little, if any, reduction in the esterase burst amplitude would be expected, as was observed experimentally.

5.5 CONCLUSION

The results of the pre-steady-state studies support the conclusion reached from the steady-state data, that is that the major effect of $MgCl_2$ on the aldehyde dehydrogenase mechanism involves a slowing of the steady-state rate-determining step or steps. There is no evidence for any change in the number of active sites per enzyme tetramer, or for any increase in the steady-state rate or the ampltidue of the burst phase. Clearly the behaviour of the cytoplasmic sheep liver aldehyde dehydrogenase in the presence of $MgCl_2$ differs markedly from the F_2 horse liver aldehyde dehydrogenase. In view of the close similarities in the kinetic behaviour of most mammalian aldehyde dehydrogenases, more similar behaviour of the two enzymes in the presence of $MgCl_2$ would be expected. One possibility which can account for the large differences in the observed behaviour of the two enzymes is that the F_2 horse liver enzyme is mitochondrial in origin, whereas the sheep liver enzyme used in this study is cytoplasmic in origin. Venteicher *et al.* (1977) reported that the F_1 or cytoplasmic horse liver aldehyde dehydrogenase was more sensitive to the presence of metal ions than was the F_2 or mitochondrial enzyme, a similar pattern has been observed for the sheep liver

isoenzymes with the mitochondrial enzyme being less sensitive to the presence of $MgCl_2$ than the cytoplasmic (P.D. Buckley, personal communication). While further work is required to determine whether the mitochondrial sheep liver aldehyde dehydrogenase is affected by $MgCl_2$ in a similar fashion to the mitochondrial horse liver enzyme, the subunit dissociation and subsequent increase in activity reported by Takahashi and Weiner (1980) for the F_2 horse liver enzyme may be a characteristic only of mitochondrial mammalian aldehyde dehydrogenases.

SECTION 6

KINETIC STUDIES ON MITOCHONDRIAL ALDEHYDE DEHYDROGENASE FROM SHEEP LIVER

6.1 INTRODUCTION

The existence of isoenzymes of aldehyde dehydrogenase localised in both the cytoplasmic and mitochondrial fractions of the liver of a number of mammalian species is well documented. Horse liver (Eckfeldt et al., 1976), bovine liver (Sugimoto et al., 1976), rat liver (Shum and Blair, 1972), human liver (Greenfield and Pietruszko, 1977) and sheep liver (Crow et al., 1974) isoenzymes have all been purified and characterised. There are a number of similarities between the cytoplasmic and mitochondrial isoenzymes which are common to all species. Both isoenzymes are composed of four subunits and both have similar molecular weights of about 200 000. A similar amino acid content has been found for both isoenzymes as has a low specificity towards different aldehydes. However there are significant differences in the behaviour of the isoenzymes in the presence of the drug disulfiram with the cytoplasmic isoenzymes showing a markedly greater sensitivity and loss of activity than do the mitochondrial isoenzymes. A general trend in isoelectric points is also noticeable, with the cytoplasmic enzyme generally having a lower pI value than the mitochondrial one. An exception to this are the horse liver enzymes, for which the mitochondrial isoenzyme is reported to have a lower pI than the cytoplasmic (Sanny and Weiner, 1977) isoenzyme.

Two reports on the kinetic behaviour of the sheep liver mitochondrial isoenzyme have been published. MacGibbon et al. (1978b) have reported the results of steady-state and pre-steady-state experiments during which they observed that the mitochondrial isoenzyme behaved in many respects like the cytoplasmic isoenzyme. The behavioural similarities include non-linear Lineweaver-Burk plots with acetaldehyde as the varied substrate, an enhancement of nucleotide fluorescence on

NADH binding to the enzyme and the quenching of protein fluorescence on NAD^+ binding. Both isoenzymes also exhibit a burst in NADH production with the same maximum rate constant with propionaldehyde as the substrate, however the amplitude of the burst for the mitochondrial isoenzyme is only 50% of the active site concentration whereas for the cytoplasmic enzyme it is equal to the active site concentration. Further differences were observed in the kinetic parameters determined in the study. The K_m value obtained at low acetaldehyde concentrations was 0.2 μM compared to 0.67 μM for the cytoplasmic isoenzyme and the rate constants for NADH dissociation were somewhat slower than those for the cytoplasmic isoenzyme being 0.6 s^{-1} and 0.093 s^{-1} for the mitochondrial isoenzyme and 0.8 s^{-1} and 0.2 s^{-1} for the cytoplasmic isoenzyme.

On the basis of these results MacGibbon *et al.* (1978b) suggested that the mechanism of the mitochondrial isoenzyme is an ordered Bi Bi mechanism (Scheme 6.1) similar to that proposed for the cytoplasmic isoenzyme (MacGibbon *et al.*, 1977c).

$$E \underset{k_{-1}}{\overset{k_{+1}[NAD^+]}{\rightleftharpoons}} E^{NAD+} \underset{k_{-2}}{\overset{k_{+2}[Ald]}{\rightleftharpoons}} E^{NAD^+}_{Ald} \xrightarrow{k_{+3}} E^{NADH} \underset{k_{-4}}{\overset{k_{+4}}{\rightleftharpoons}} E + NADH$$

(Scheme 6.1)

Hart and Dickinson (1977, 1978) have also reported the results of a study on the kinetics of the mitochondrial isoenzyme. These workers observed apparently parallel Lineweaver-Burk plots with both propionaldehyde and NAD^+ as the varied substrate, a result not expected from an ordered mechanism, and were unable to detect a burst in the production of NADH. The lack of an isotope effect on the steady-state rate indicated that hydride transfer was not rate-limiting. Hart and Dickinson have suggested Scheme 6.2 as a possible mechanism for the

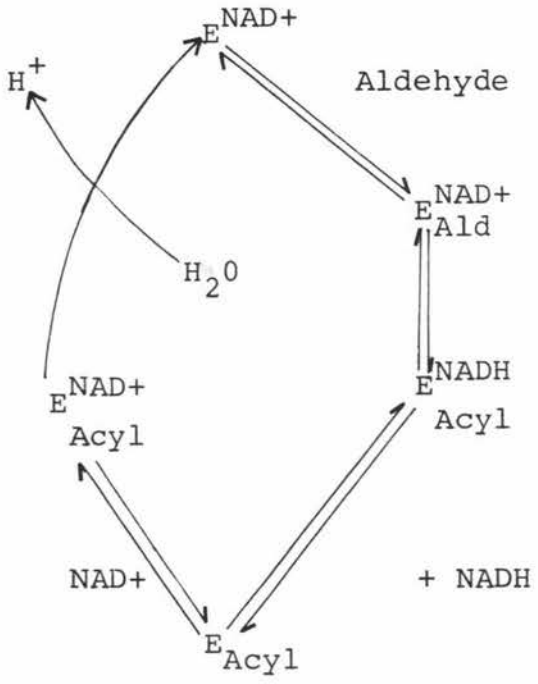

(Scheme 6.2)

mitochondrial enzyme. The essential feature of this mechanism are that the enzyme oscillates between a binary enzyme-NAD^+ and an acyl-enzyme intermediate with alternating substrate addition and product release and that free enzyme does not appear in the catalytic cycle.

While both of the postulated mechanisms can explain some of the data, neither can satisfactorarily explain all of it, so it was decided to carry out further pre-steady-state studies in order to gain more information about the reaction mechanism and decide which if either of the two mechanisms is the better model. It was also of interest to determine whether the mitochondrial isoenzyme exhibits an esterase burst, as it has been suggested that the low amplitude esterase burst exhibited by the cytoplasmic enzyme may be due to mitochondrial contamination (Duncan, 1979) of the cytoplasmic preparation.

6.2 METHODS

6.2.1 Spectrophotometric Assays

6.2.1.1 Assays at pH 7.6

Assays at pH 7.6 were carried out as described in Section 3.2.1.1a using the apparatus described in Section 3.2.1.1.

6.2.1.2 Assays at pH 7.0

Assays were carried out as above, using pH 7.0 phosphate buffer prepared by adjusting 35 mM pH 7.6 phosphate buffer to pH 7.0 with 0.1 M NaOH using a radiometer pH meter 28.

6.2.1.3 Assays at low buffer concentrations

Assays were carried out as described in Section 3.2.1.1.b.

6.2.1.4 Esterase activity assays

Assays for esterase activity were carried out as described in Section 4.2.1.2.

6.2.2 Pre-steady-state Experiments

6.2.2.1 Apparatus

Pre-steady-state experiments were carried out using the apparatus described in Section 3.3.1.1. For NADH dissociation and nucleotide fluorescence burst experiments the apparatus was set up as described in Section 5.2.1.

6.2.2.2 Preparation of solutions

6.2.2.2a Proton burst experiments

The enzyme solution was dialysed and the solutions for the stopped-flow experiments were prepared as described in Section 3.3.1.3.

6.2.2.2b Nucleotide fluorescence experiments

Solutions used in the nucleotide fluorescence experiments were prepared as described in Section 5.2.3.

6.2.2.2c Esterase experiments

Solutions used in the esterase burst experiments were prepared as described in Section 5.2.3.

6.3 TREATMENT OF DATA

6.3.1 Determination of the Enzyme Active Site Concentration

The concentration of NADH binding sites was estimated from NADH displacement experiments. It was assumed that in the displacement reaction more than 90% of the bound NADH was displaced by NAD^+. The enzyme active site concentration could then be calculated by dividing the fluorescence change resulting from the NADH dissociation by the fluorescence enhancement factor of 6.5 reported by Hart and Dickinson (1977).

6.3.2 Calibration of Activity at 560 nM and 340 nM

The rate of the reaction, as determined by monitoring proton release at 560 nm with phenol red, was related to the rate of reaction determined by monitoring NADH production of 340 nM as described in Section 3.3.2.1.

6.3.3 Analysis of Transients

Burst experiments were treated as described in Section 3.3.2.2 and biphasic transients were treated as described in Section 5.3.2.

6.4 RESULTS

6.4.1 Calibration of Activity at 560 nm and 340 nm

Due to the presence of a small quantity of buffer in the stopped-flow solutions the initial velocity as determined from measuring the proton release with phenol red indicator at 560 nm was less than the initial velocity determined by monitoring the production of NADH at 340 nm. Assuming a stoichiometry of 2 protons per NADH molecule produced in the steady-state reaction, the difference between the observed activity at 560 nm and that at 340 nm was found to be 70 $\pm$ 10. This value was used to determine an apparent molar extinction coefficient of 1.29×10^3 $\ell mol^{-1} cm^{-1}$ for phenol red under these conditions. This value was used to calculate proton burst amplitudes from measurements made at 560 nm.

6.4.2 Proton Burst

When enzyme (13.8 μM) was mixed with saturating concentrations of NAD^+ (2 mM) and propionaldehyde (40 mM) in the presence of phenol red (24 μM), Na_2SO_4 (0.21 mM) and $NaNO_3$ (0.15 mM) in the stopped-flow apparatus a burst in the production of protons was observed followed by a slow steady-state proton release (Fig. 6.1). The transient was a single first order process with a rate constant of 6 s^{-1} and an amplitude (calculated as in Section 6.4.1) equal to half the concentration of NADH binding sites.

6.4.3 NADH Displacement Experiments

When NAD^+ (3 mM) was pushed against a solution of enzyme (3 μM) and NADH (18 μM), a biphasic displacement curve was observed. The faster process had a rate of 0.25 s^{-1} and the slower a rate of 0.03 s^{-1}, while the amplitude of the displacement was composed of 70% of the fast process and 30% of the slow. The displacement rates are somewhat slower than those reported by MacGibbon

FIG. 6.1 Mitochondrial Proton Burst

The reaction mixture contained enzyme (7.9 μM), phenol red (12 μM), $NaNO_3$ (0.21 mM), Na_2SO_4 (0.21 mM), NAD^+ (6.5 mM) and propionaldehyde (20 mM). The rate constant of the burst was 6 s^{-1}, and the amplitude was 3.68 μM.

FIG. 6.2 Mitochondrial Esterase Burst

The reaction mixture contained enzyme (2.7 μM) and 4-nitrophenylacetate (117 μM), the burst rate constant was 7.3 s^{-1} and the amplitude was 0.3 μM .

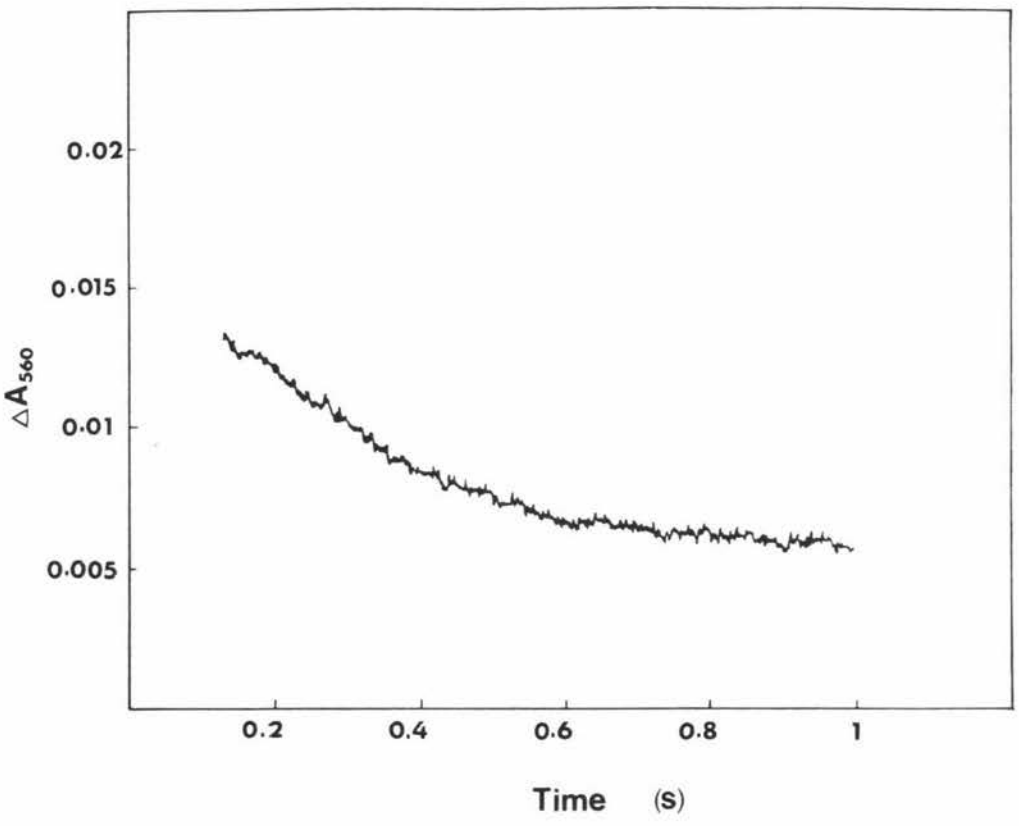
0.02
0.015
0.01
0.005
$\triangle A_{560}$
0.2
0.4
0.6
0.8
1
Time (s)

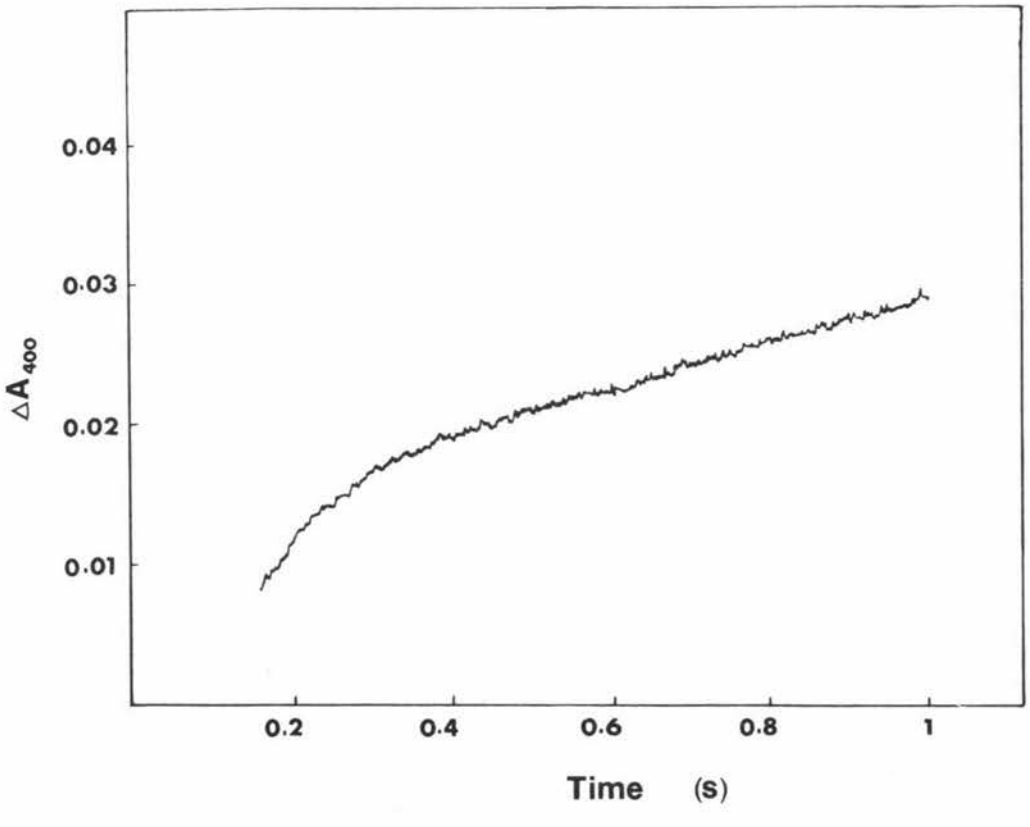
0.04
0.03
0.02
0.01
$\triangle A_{400}$
0.2
0.4
0.6
0.8
1
Time (s)

et al. (1978) of 0.6 s^{-1} and 0.09 s^{-1} but the amplitude contributions (69% fast and 31% slow) are in excellent agreement with those determined in this study.

6.4.4 NADH Burst Experiments

When enzyme (3 μM) was mixed with NAD^+ (2 mM) and propionaldehyde in the stopped-flow apparatus a burst in the production of NADH was observed. The burst was a single first order process with a rate constant of 17 ± 3 s^{-1} and an amplitude equal to half the formal enzyme concentration (as calculated from displacement experiments). These results are in good agreement with those reported by MacGibbon et al. (1978b) who observed a burst in NADH production with a rate constant of 11 s^{-1} and an amplitude equal to half the enzyme concentration at saturating propionaldehyde concentrations.

6.4.5 Esterase Burst

When enzyme (5.4 μM) was mixed in the stopped-flow apparatus with 4-nitrophenylacetate (315 μM) a burst in the production of 4-nitrophenoxide ion was observed (Fig. 6.2) followed by a slow steady-state production of 4-nitrophenoxide ions. The rate constant for the burst was 7.3 s^{-1} and the amplitude corresponded to 22% of the NADH binding site concentration. The solution used in the burst experiment contained 1.6 mM β-mercaptoethanol, however (MacGibbon et al, 1978 a) shown that mixing β-mercaptoethanol and 4-nitrophenylacetate does not result in a burst in 4-nitrophenoxide ion production.

6.4.6 Comparison of k_{cat} for the Dehydrogenase and Esterase Reactions

The turnover numbers (k_{cat}) for the dehydrogenase and esterase reactions have not been published, due to difficulties in determining the enzyme active site concentration. k_{cat} is defined as the maximum rate of reaction (V_{max}) divided by the enzyme active site

concentration, so a comparison can be made of the k_{cat} values for the esterase and dehydrogenase reactions, even if the active site concentration is unknown, by using the same quantity of enzyme solution in each assay.

The V_{max} value for an assay of the dehydrogenase activity as described in Section 3.2.1.1a was 1.54×10^{-7} mol$\ell^{-1}s^{-1}$ of NADH and using an equal quantity of the same enzyme solution the V_{max} value obtained from an esterase assay was 1.46×10^{-7} mol$\ell^{-1}s^{-1}$ of 4-nitrophenoxide ion. The ratio of V_{max}(ester):V_{max} (dehydrogenase) is 0.95 and is equal to the ratio of the two k_{cat} values. The closeness of the ratio of the two k_{cat} values to 1.0 indicates (as was found for the cytoplasmic enzyme, MacGibbon et al., 1977a; MacGibbon et al., 1978b) that the k_{cat} values for the two reactions are the same.

6.5 DISCUSSION

The group transfer mechanism proposed by Hart and Dickinson (1978) for the sheep liver mitochondrial aldehyde dehydrogenase, differs from the ordered Bi Bi mechanism which is commonly found for most aldehyde dehydrogenases. In the former mechanism there is no accumulation of an enzyme-NADH complex as NADH dissociation occurs before the hydrolysis of the assumed acyl-enzyme intermediate. As a result of this, free enzyme does not appear in the mechanism shown in Scheme 6.2. This scheme was postulated by Hart and Dickinson (1978) because of their observation of apparent parallel Lineweaver-Burk plots and their failure to observe a burst in the production of NADH, both facts being inconsistent with an ordered Bi Bi or ternary complex mechanism. The group transfer mechanism does explain the observation of parallel double reciprocal plots (Dalziel 1957), and if the equilibrium for the step $E^{NAD+}_{Ald} \rightleftharpoons E^{NADH}_{Acyl}$ lies well to the left, a burst in the production of NADH would not be expected.

However Hart and Dickinson have noted that the mechanism does not satisfactorarily explain a number of observed kinetic results. The invariance of V_{max} and K_m for NAD^+ with different aldehydes are features expected in ordered ternary complex and Theorell-Chance type mechanisms rather than group transfer mechanisms like Scheme 6.2.

MacGibbon et al. (1978b) have also suggested a possible mechanism for the mitochondrial enzyme, these workers using a sensitive fluorescence method were able to detect a burst in NADH production equal to 50% of the active site concentration and this result was confirmed in the present study. On the basis of their observation of an NADH burst and the similarity of the rates of NADH dissociation to those of the cytoplasmic enzyme, these workers concluded that an ordered Bi Bi mechanism was operating as shown for the cytoplasmic enzyme (MacGibbon et al., 1977c).

The observation of a proton burst with a rate nearly identical within experimental error to that of the NADH burst indicates that a proton is released prior to the steady-state rate limiting step. The position of the proton release in the reaction mechanism cannot be positively identified without further work, however the following possibilities can be considered. The proton may be released as a result of NAD^+ binding, aldehyde binding, the hydrolysis of the acyl-enzyme intermediate, a conformational change, the ionization of a functional group, or a combination of several of these events. The hydrolysis of the acyl-enzyme appears unlikely to be the origin of the protons due to the observation of a burst in the production of 4-nitrophenol for the esterase reaction. The observation of a burst implies that deacylation is rate-determining for the esterase reaction and is likely to be considerably slower than 7 s^{-1}. As it has been claimed that the esterase and dehydrogenase reactions both have the hydrolysis of an acyl-enzyme intermediate as a common step (Feldman and Weiner, 1972b) the rate of proton release resulting from the hydrolysis of an acyl-enzyme intermediate would be expected to be considerably slower than the burst rate constant observed experimentally. Proton release most probably results

from an ionisation reaction, but since chemical steps are seldom rate-limiting (Laidler, 1973) the ionisation more than likely follows a conformational change as is thought for the cytoplasmic enzyme (Section 3.5).

The magnitude of the esterase burst observed (22% of the enzyme active site concentration) proves that the cytoplasmic esterase burst reported by MacGibbon et al., (1978a) cannot be due to contamination of the cytoplasmic enzyme solution by the mitochondrial enzyme, as the mitochondrial burst would have to have had an amplitude at least equal to the enzyme concentration to cause an observable burst in a contaminated cytoplasmic preparation.

The observation of a proton burst does not rule out either of the suggested mechanisms for the mitochondrial enzyme as both can accommodate a transient release of protons, however objections to the group transfer mechanism can be raised from the published data. A value of 9×10^3 $\ell mol^{-1} s^{-1}$ can be calculated for the ratio $V_{max}/K_{m.NAD^+}$, using values of 36 μM for $K_{m.NAD^+}$ and 77 min^{-1} for V_{max}/e (Hart and Dickinson, 1978) and a value of 4 NADH binding sites per tetramer (Hart and Dickinson, 1977). This value is identical within experimental error to the second order rate constant of 2×10^4 $\ell mol^{-1} s^{-1}$ for NAD^+ binding reported by MacGibbon et al., (1978b) using protein fluorescence quenching techniques. The equivalence of these two values is indicative of an ordered Bi Bi mechanism with NAD^+ binding first (Hart and Dickinson, 1978).

Both the proton and NADH bursts observed for the mitochondrial enzyme differ from those observed for the cytoplasmic enzyme in that the former exhibited bursts equal to half the NADH binding site concentration, whereas for the latter the amplitude of the bursts was 100% of the enzyme concentration. There are a number of possible exaplanations for this observation. MacGibbon et al. (1978b) have suggested that the presence of non-fluorescent enzyme containing intermediates may be causing the reduction in amplitude observed for the NADH burst. A reduction in the proton burst amplitude might also be expected in these circumstances if the equilibrium for the proton release step favours the

reverse direction. The half bursts could also arise as a result of the enzyme containing two different types of active site or two distinct isoenzymes. Hart and Dickinson (1978) have reported evidence suggesting that there may be two distinct types of active site. When they modified the enzyme with disulfiram or iodoacetamide so that 50% of the activity remained, different kinetic behaviour was observed, the double reciprocal plots now being linear rather than curved as observed prior to thiol modification. If only one type of active site exhibits proton and NADH bursts, then bursts equal to half the enzyme active site concentration will be observed. Agnew et al. (1981) have reported the existence of five isoenzymes of the mitochondrial sheep liver aldehyde dehydrogenase. If the isoenzymes show different kinetic behaviour then this may account for the observed half-bursts.

It is not known which if any of the above explanations is the correct one, however it is of interest to note that it has been recently reported that the mitochondrial horse liver aldehyde dehydrogenase exhibits half-site reactivity (Weiner et al., 1976, Takahashi and Weiner, 1980). The enzyme binds four molecules of NAD^+ under equilibrium conditions but in the pre-steady-state and steady-state only two NADH molecules per enzyme are produced. If a similar situation exists for the sheep liver mitochondrial aldehyde dehydrogenase then the observed half proton and NADH bursts would be expected.

6.6 CONCLUSION

Neither of the postulated models for the mitochondrial aldehyde dehydrogenase (Schemes 6.1 and 6.2) can explain all of the experimental observations completely, but the ordered Bi Bi mechanism is a better model in that it explains more of the data than the group transfer model. The presence of five isoenzymes on isoelectric focussing complicates the interpretation of any experimental data obtained, and further work needs to be done on separating

and characterising the isoenzymes to determine whether they exhibit different kinetic behaviour.

The origin of the proton observed during the proton burst has not been identified, but it appears likely that a conformational change on aldehyde binding (as was suggested in Section 4.5 for the cytoplasmic enzyme) is the rate limiting step in the pre-steady-state and is also the cause of the proton release.

APPENDIX I

ABBREVIATIONS

A	Concentration of species A
acyl	$-C(=O)-R$
ADP-ribose	adenosine 5'-diphosphoribose
DEA	diethylamino
Deamino-NAD^+	deamino diphosphopyridine nucleotide (Nicotinamide Hypoxanthine dinucleotide)
D_o	diffusion coefficient
E	enzyme
$E.NAD^+$	enzyme with NAD^+ bound
E.NADH	enzyme with NADH bound
E^{Ald}_{NADH}	enzyme with NAD^+ and aldehyde bound
EDTA	ethylendiaminetetraacetic acid
ε	molar extinction coefficent
F	fluorescence
ΔF	fluorescence difference
ΔF_{max}	maximum fluoresence difference
g	gram
$\underline{g}$	unit of gravitation field
I	concentration of inhibitor
Ka, Kb	Michaelis constants for A,B
k_{cat}	turnover number
K_D	dissociation constant
K_{ia}	dissociation constant for A
λ	observed decay constant
η_o	solvent viscosity
n_o	refractive index
NAD^+	nicotinamide adenine dinucleotide
NADH	dihydronicotinamide adenine dinucleotide
NIAF	normalised intensity autocorrelation function
PNPA	4-nitrophenylacetate

PEG	polyethylene glycol
ρ	Hammet rho value
Q	fluorescence enhancement
Δq	fluorescence quenching
Δq	maxium fluoresence quenching
R	fractional saturation of NADH binding sites
s	seconds
SDS	sodium dodecyl sulfate
θ	scattering angle (laser expt)
v	velocity
V_{max}	maximum velocity

APPENDIX II

CHEMICALS

Acetaldehyde	British Drug Houses (B.D.H.) Poole, England
Acetonitrile	J. T. Baker Chemical Company, Philipsburg, New Jersey
1,2,2,2-^{2}H Acetaldehyde	Bio-Rad Laboratories, Richmond, California
ADP-Ribose	Sigma Chemical Company, Saint Louis, Missouri
Ammonium Sulphate	May and Baker (M&B), Dagenham, England
Benzaldehyde	M&B
Chlorophenol red	B.D.H.
Cyclohexane	B.D.H.
DEA Cellulose	Whatman Biochemicals Ltd.,
Deamino-NAD^{+}	Sigma
EDTA	B.D.H.
2-Hydroxybenzaldehyde	Koch Light Laboratories, Colnbrook, Buoks, England
Magnesium Chloride	Prolabo, Paris, France
β-Mercaptoethanol	J. T. Baker
4-Methoxybenzaldehyde	B.D.H.
NAD^{+}	Grade III, Sigma
NADH	Grade III, Sigma
4-Nitrobenzaldehyde	B.D.H.
1-Nitropropane	B.D.H.

REFERENCES

Agnew, K.E.M., Bennett, A.F., Crow, K.E., Greenway, R.M., Blackwell, L.F. and Buckley, P.D. (1981) Eur. J. Biochem. 119, 79-84

Apps, D.K. (1973) Biochim. Biophys. Acta 320, 379-387

Bernhard, S.A., Dunn, M.F., Luisi, P.L., and Schack, P. (1970) Biochemistry, 9, 185-192

Bland, J.H. (1963) Clinical Metabolism of Body Water and Electrolytes, W.B. Saunders, London, Philadelphia

Brandon, C.I. and Eklund, H. (1980) in Dehydrogenases Requiring Nicotinamide Coenzymes (Jeffrey, J. ed.) Birkhauser, Boston

Briggs, G.E. and Haldane, J.B.S. (1925) Biochem. J. 19, 338

Brooks, R.L. and Shore, J.D. (1971) Biochemistry 10, 3855-3858

Brown, A.J. (1902) ibid, 81, 373

Buttner, H. (1965) Biochem. Z. 341, 300-314

Cleland, W.W. (1963a) Biochem. Biophys. Acta 67, 104-137

Cleland, W.W. (1963b) Biochem. Biophys. Acta 67, 173-187

Cleland, W.W. (1975) Accounts of Chemical Research 8, 145-151

Cohen, G. and Collins, M. (1970) Science 167, 1749-1751

Conan-Doyle, A. (1890) The Sign of Four

Crow, K.E., Kitson, T.M., MacGibbon, A.K.H., and Batt, R.D. (1974) Biochim. Biophys. Acta 350, 121-128

Crow, K.E. (1975) Thesis, Ph.D., Massey University.

Dalziel, K. (1957) Acta Chem. Scand. 11, 1706-1723

Davis, V.E. and Walsh, M.J. (1970) Science 167, 1005-1007

Dawson, R.M.C., Elliot, D.C., Elliot, W.H. and Jones, K.M. (1969) Data for Biochemical Research, Oxford University Press, London

Dickinson, F.M. and Dickenson, C.J. (1978) Biochem. J. 171, 613-627, 629-637

Dickinson, F.M. and Berrieman, S. (1979) Biochem. J. 179, 709-712

Dickinson, F.M., Hart, G.J. and Kitson, T.M. (1981) Biochem. J. 199, 573-579

Duncan, R.J.S. (1979) Biochem. J. 183, 459-462

Eckfeldt, J., Mope, L., Takio, K. and Yonetani, T. (1976) J. Biol. Chem. 251, 236-240

Eckfeldt, J.H. and Yonetani, T. (1976) Arch. Biochem. Biophys. 173, 273-281

Eklund, H., Nordstrom, B., Zeppezauer, E., Soderlund, G., Ohlsson, I., Bowie, T. and Brandon, C.-I. (1974) FEBS Letters 44, 200-204

Feldman, R.I. and Weiner, H. (1972a) J. Biol. Chem. 247, 260-266

Feldman, R.I. and Winer, H. (1972b) J. Biol. Chem. 247, 267-272

Frost, A.A., and Pearsons, R.G. (1961) Kinetics and Mechanism, 2nd edition John Wiley and Sons, New York

Geraci, G. and Gibson, Q.H. (1967) J. Biol. Chem. 242, 4275-4278

Gibson, Q.H. and Milnes, L. (1964) Biochem. J. 91, 161-171

Greenfield, N.J., and Pietruszko, R. (1977) Biochem. Biophys. 483, 35-45

Gutfreund, H. (1972) Enzymes: Physical Properties, Wiley Interscience, London

Hardman, M.J., Coater, J.H. and Gutfreund, H. (1978) 171, 215, 223

Hart, G.J. and Dickinson, F.M. (1977) Biochem. J. 163, 261-267

Hart, G.J. and Dickinson, F.M. (1978) Biochem. J. 175, 899-908

Hart, G.J. and Dickinson, F.M. (1978b) Biochem. J. 175, 753-756

Heck, H.d'A., McMurray, G.H. and Gutfreund, H. (1968) Biochem. J. 108, 793-796

Hiromi, K. (1979) Kinetics of Fast Enzyme Reactions: Theory and Practice, Halstead Press, New York

Holbrook, J.J. and Gutfreund, H. (1973) FEBS Letters 31, 158-169

Holbrook, J.J. and Ingram, V.A. (1973) Biochem. J. 131, 729-738

Horecker, B.L. and Kornberg, A. (1948) J. Biol. Chem. 175, 385

Iwatsubo, M. and Pantaloni, D. (1967) Bull. Soc. Chim. Biol. 49, 1563-1572

Jacoby, W.B. (1963) in The Enzymes Vol. 7 (Boyer, P.D., Lardy, H. and Myrback, K. eds.) Academic Press, New York

Jakeman, E. and Pike, E.R. (1969) J. Phys. A. 2, 411

Johnson, K. and Degering, E.F. (1943) J. Org. Chem. 8, 10-11

Kitson, T.K. (1975) Biochem. J. 151, 407-412

Kitson, T.M. (1978) 175, 83-90

Kitson, T.M. (1981) Biochem. J. Submitted for Publication

Kosower, E.M. (1968) An Introduction to Physical Organic Chemistry, pp. 48-60 John Wiley and Sons, New York

Kraemer, R.J. and Deitrich, R.A. (1968) J. Biol. Chem. 243, 6402-6408

Kvassman, J. and Pettersson, G. (1980a) Eur. J. Biochem. 103, 557-564

Kvassman, J. and Pettersson, G. (1980b) Eur. J. Biochem. 103, 565-575

Laidler, K.J. and Bunting, P.S. (1973) The Chemical Kinetics of Enzyme Action. 2nd Edition, Clarendon Press, Oxford

Leitch, L.C. (1955) Can. J. Chem. 33, 400-404

MacGibbon, A.K.H., Blackwell, L.F. and Buckley, P.D. (1977a) Eur. J. Biochem. 77, 93-100

MacGibbon, A.K.H., Blackwell, L.F. and Buckley, P.D. (1977b) Biochem. J. 165, 455-462

MacGibbon, A.K.H., Blackwell, L.F., Buckley, P.D. (1977c) Biochem. J. 167, 469-477

MacGibbon, A.K.H., Blackwell, L.F. and Buckley, P.D. (1978) Biochem. J. 171, 527-531

MacGibbon, A.K.H., (1976) Thesis: Massey University

MacGibbon, A.K.H., Haylock, S.J., Buckley, P.D. and Blackwell, L.F. (1978) Biochem J. 171, 533-538

MacGibbon, A.K.H., Motion, R.L., Crow, K.E., Buckley, P.D. and Blackwell, L.F. (1979) Eur. J. Biochem. 96, 585-595

Mackler, B., Mahler, H.R. and Green, D.E. (1954) J. Biol. Chem. 210, 149-164

Maguaire, R.J., Hijazi, N.H. and Laidler, K.J. (1974) Biochem. Biophys. Acta 341, 1-14

Michaelis, L. and Menten, M.L. (1913) Biochem. Z., 49, 333

O'Driscoll, R.C. and Pinder, D.N. (1980) J. Phys. E. 13, 192

Parker, D.M. and Holbrook, J.J. (1977) in Pyridine Nucleotide Dependant Dehydrogenases (Sund, H. ed.) pp. 485-501, Walter de Gruyter, Berlin and New York

Racker, E. (1949) J. Biol. Chem. 177, 883-892

Rajagopalan, K.V. and Handler, P. (1964) J. Biol. Chem. 239, 2027-2035

Sanny, C.G. and Winer, H. (1977) in Alcohol and Aldehyde Metabolizing Systems (Thurman, R.G., Williamson, J.R., Drott, H.R. and Chance, B. eds.). Vol. II pp. 167-174

Scatchard, G. (1949) Ann. N.Y. Acad. Sci. 51, 660

Segel, I.H. (1975) Enzyme Kinetics, John Wiley and Sons, New York

Seydoux, F., Malhotra, O.P. and Bernhard, S.A. (1974) CRC Crticial Reviews in Biochemistry 2, 227-257

Shore, J.D., and Gutfreund, H. (1970) Biochemistry 9, 4655-4659

Shore, J.D., Gtufreund, H., Brooks, R.L., Santiago, D. and Santiago, P. (1974) Biochemistry 13, 4185-4191

Shum, G.T. and Blair, A.H. (1972) Can. J. Biochem. 50, 741-748

Sidhu, R.S. and Blair, A.H. (1975) J. Biol. Chem. 250, 7894-7898

Soman, S.D., Joseph, K.T., Raut, S.J., Mulay, C.D., Parameshwaran, M. and Panday, V.K. (1970) Health Phys. 19, 641

Stoppani, A.O.M. and Milstein, C. (1959) Anales Asoc. Quim. Arg. 47, 11-18

Sugimoto, E., Takahashi, N., Kitagawa, Y. and Chiba, H. (1976) Agr. Biol. Chem. 40, 2063-2070

Takahashi, K. and Weiner, H. (1980) J. Biol. Chem. 255, 8206-8209

Takahashi, K., Weiner, H. and Hu, J.H. (1980) Arch. Biochem. Biophys. 205, 571-578

Theorell, H. and McKinely-McKee, J.S. (1961) Acta Chem. Scand. 15, 1797-1810

Theorell, H., Ehrenberg, A., and de Zalenski, C. (1967) Biochim. Biophys. Acta 27, 309-314

Tottmar, S.O.C., Petterson, H. and Kiessling, K.-H. (1973) Biochem. J. 135, 577-586

Trotter, C.M. (1980) Thesis, Ph.D., Massey University

Truitt, E.B. and Walsh, M.J. (1971) The Biology of Acoholism, Vol 1, edited by B. Kissin and H. Begleiter. Plenum Press N.Y. and London pp. 165-195.

Venteicher, R., Mope, L. and Yonetani, T. (1977) in Alcohol and Aldehyde Metabolizing Systems, Vol. II. (Thurman, R.G., Williamson, J.R., Drott, H.R. and Chance, B. eds.) pp. 157-166, Academic Press, New York

Weiner, H., King, P., Hu, J.H.J. and Bensch, W.R. (1974) in Alcohol and Aldehyde Metabolising Systems Vol. I. (Thurman, R., Yonetani, T., Williamson, J.R. and Chance, B. eds.). Academic Press, New York

Weiner, H., Hu, J.H.J. and Sanny, C.G. (1976) J. Biol. 251, 3853-3855

Whitaker, J.R., Yates, D.W., Bennett, N.G., Holbrook, J.J. and Gutfreund, H. (1974) Biochem. J. 139, 677-697

Wonacott, A.J. and Biesecker, G. (1977) in Pyridine Nucleotide Dependant Dehydrogenases (Sund, H. ed.) pp. 140-156. Walter de Gruyter, Berlin and New York